PHYSIOLOGICAL AND BIOLOGICAL MECHANISMS OF BISPHOSPHONATE ACTION

A DISSERTATION SUBMITTED TO THE UNIVERSITY OF OXFORD

IN PARTIAL FULFILMENT OF THE REQUIREMENTS FOR THE DEGREE OF

DOCTOR OF PHILOSOPHY

BY

XUCHEN DUAN

WADHAM COLLEGE
OXFORD
MICHAELMAS TERM 2010

I would like to dedicate my thesis to my beloved grandpa who will be in my heart, always!

ABSTRACT

Physiological and biological mechanisms of bisphosphonate action
Xuchen Duan **Doctor of Philosophy**
Wadham College **Michaelmas Term 2010**

Bisphosphonates (BPs) are stable analogues of pyrophosphate widely used for the treatment of bone diseases characterised by increased bone resorption. Studies over the years have shown that the pharmacological potencies of BPs are dependent both on their binding affinities for bone mineral and on their inhibitory actions on osteoclasts. In addition, potential effects on other cell types present locally in the environment of skeletal tissues have been reported.

The present study systematically evaluated the relative mineral-binding affinities of individual BPs of clinically relevance in mixtures of these compounds and the changes with elution pH by using column chromatography with ceramic hydroxyapatite and fluoroapatite combined with mass spectrometric identification and quantitation of the individual BPs. The results indicate that pH has a profound effect on the ionisation of the phosphonate and R2 functional groups, with BPs having greater affinities at lower pH as shown by increased retention times. Moreover, two other approaches, namely using Langmuir adsorption isotherms and competition assays based on fluorescent BP, have been developed to assess the mineral-binding capacities and dissociation constants of BPs. These results suggest that there are substantial differences among BPs in their binding to hydroxyapatite.

From the cellular aspect of my study, I present evidence for the anti-apoptotic effects of BPs in osteocytes and osteoblasts. However, the study of prosurvival signalling pathways involved in these cells needs to be optimised.

The work described in this thesis provides novel insights into the physiological and biological mechanisms of BP action. My project has provided a better knowledge of the physicochemical properties of BPs, which are highly relevant to their differential distributions within bone, their biological potencies, and their durations of action. Additionally, the cell culture studies may provide new information on the cellular effects of BPs on osteocytes and osteoblasts.

ACKNOWLEDGEMENTS

This is the most difficult section for me to write, and my thanks are expressed from the heart. When I look back, I realise that this thesis is not only my work but is the result of efforts and contributions by many people. I would like to convey my sincere gratitude to all of them who helped me accomplish this work.

Although I officially enrolled as a DPhil student at Nuffield Department of Orthopaedics, Rheumatology and Musculoskeletal Sciences, University of Oxford in 2008, my research experience in this department started one year earlier with Dr. Zhidao Xia on evaluations of the mineral-binding affinities of bisphosphonates. I offer my heartfelt regards to Dr. Xia as he not only guided me to the world of bisphosphonates, but also most importantly introduced me to Prof. Graham Russell and Prof. James Triffitt, who later became my supervisors for my DPhil study.

I have been very fortunate with my supervisors and mentors, Prof. Graham Russell and Prof. James Triffitt. I am deeply indebted to you both for your constant guidance, support and encouragement. It is a great privilege to have worked with two of the best scientists, and also two great and respected persons. I thank both of you for the time and efforts you have put into this work and for taking good care of me since three years ago.

I would like to acknowledge Dr. Rachel Locklin and Dr. Philippa Hulley for supervising my cell culture work. Many thanks for your continuous assistance in my experiments and for teaching me many techniques and sharing your research experiences. I also appreciate the continuous support of Dr. James Dunford and Dr. Aaron Kwaasi. You two not only gave me great input in my research, but also helped me in many other ways and made me feel at home in Oxford.

I am very thankful to Dr. F. Hal Ebetino at Warner Chilcott. Your immense knowledge and valuable remarks helped me greatly with my research project. Moreover, I am sincerely thankful for the precious opportunities you provided me to collaborate with experts around the world. Thank you for taking care of me during my visit to the USA last year and arranging a considerable amount of time for me to spend with collaborators at Procter & Gamble. I convey my special gratitude to Mr. Mike Quijano and Dr. Roy Dobson who conducted the mass spectrometry analysis of our studies, to Ms. Gwyn Jeans who works on the study of fluorescently labelled bisphosphonates and rat bisphosphonate/fluorescent

bisphosphonate urine excretion study, and Dr. Bobby Barnett who taught me new insights on the modelling of bisphosphonates. My sincere thanks go to Prof. Alan Boyde at the University of London who works on the imaging of fluorescent bisphosphonates by using confocal microscopy. With the above-mentioned experts, we had a great collaboration, out of which we produced so much in such a short time. I have learnt a great deal from their experience and insights. Thank you all for your contribution to my research.

During my visit to the USA, I was given a great opportunity to visit Indiana University to present our work and meet researchers including Dr. Teresita Bellido and Dr. Lilian Plotkin and others. With their expertise on the *in vitro* and *in vivo* studies of osteocytes and osteoblasts, I had fruitful discussions about my cell culture work and their vital comments and suggestions are very much appreciated. I also express my gratitude to Prof. Charles McKenna at the University of Southern California for kindly providing me stocks of fluorescent bisphosphonates for my fluorescent competitive binding assays and providing valuable comments and suggestions on my work.

In addition, I would like to thank Prof. Nick Athanasou for being my college advisor. I have enjoyed the formal halls at Wadham with you at the high table. Thank you for giving me the chance to meet individuals from all walks of life and all areas of academia at Wadham College. I really appreciate the advice you gave to me both on my scientific research and on my student life at Oxford.

Last but definitely not least, I would express my deepest thanks and regards to my dear parents, loving husband and friends who have provided me with support, friendship, love and encouragement. Thank you for being there for me for all my life. It's hard to find the words to appreciate all the love you give me. Without your support and drive, none of what follows would have been possible.

TABLE OF CONTENTS

FIGURES

TABLES

ABBREVIATIONS

ALN	Alendronate
5(6)-FAM-amino-RIS	5(6)-carboxylfluorescein-amino-risedronate
5(6)-FAMRIS	5(6)-carboxylfluorescein-risedronate
AF647-RIS	Alexa Fluor 647-risedronate
ANGELS	Activators of Non-Genomic Oestrogen Ligands
ANOVA	One-way Analysis of Variance
ATP	Adenosine Triphosphate
Bmax	Maximal number of binding sites
BMUs	Bone Multicellular Units
BPs	Bisphosphonates
CAP	Carbonated apatite
CLO	Clodronate
DAPI	4', 6-diamidino-2-phenylindole
DMP-1	Dentin Matrix Protein-1
ERKs	Extracellular Signal-Regulated Kinases
ETI	Etidronate
FAP	Fluoroapatite
FCS	Fetal Calf Serum
FDA	Food and Drug Administration
FGF	Fibroblast Growth Factor
FL-BP	Fluorescently Labelled BP
FPLC	Fast Performance Liquid Chromatography
FPPS	Farnesyl Pyrophosphate Synthase
HAP	Hydroxyapatite
HPLC	High-Performance Liquid Chromatography
HUVEC	Human Umbilical Vein Endothelial Cells
IBN	Ibandronate

IFN	Interferon
IGF	Insulin-like Growth Factor
IL-1	Interleukin 1
IS	Internal standard
ITC	Isothermal Titration Calorimetry
IV	Intravenous
Kd	Dissociation constant
Ki	Dissociation constant
MCSF	Macrophage Colony-Stimulating Factor
MEPE	Matrix Extracellular Phosphoglycoprotein
Mes	4-Morpholine ethanesulfonic acid
MIN	Minodronate
MRM	Multiple Reaction Monitoring
MS	Mass Spectrometry
N-BPs	Nitrogen-containing BPs
NER	Neridronate
NMR	Nuclear Magnetic Resonance
NT assay	Nick Translation assay
ONJ	Osteonecrosis of the Jaw
OPA	O-phthaldialdehyde
OPG	Osteoprotegerin
PAM	Pamidronate
PBS	Phosphate-Buffered Saline
PDB	Paget's Disease of Bone
PDGF	Platelet-Derived Growth Factor
PHEX	Phosphate-regulating gene with Homologies to Endopeptidases on the X chromosome
PPi	Inorganic Pyrophosphate
PTH	Parathyroid Hormone
PTHrP	PTH-related Protein

PVDF	Polyvinylidene Difluoride
RANKL	Receptor Activator of Nuclear Factor kappa-B Ligand
RCTs	Randomised Controlled Trials
RFU	Relative Fluorescent Units
Rho-RIS	Rhodamine-risedronate
Rho-RISPC	Rhodamine-phosphonocarboxylate-risedronate
RIS	Risedronate
RLX	Raloxifene
SD	Standard Deviation
SDS-PAGE	Sodium Dodecyl Sulfate-Polyacrylamide Gel Electrophoresis
SERM	Selective Oestrogen-Receptor Modulator
SREs	Skeletal-Related Events
TGF-β	Transforming Growth Factor β
TNF	Tumour Necrosis Factor
TUNEL	Terminal Deoxynucleotidyl Transferase-mediated Biotin-dUTP Nick End Labelling
UV	Ultraviolet
ZOL	Zoledronate
αMEM	Alpha Modified Minimum Essential Medium

CHAPTER 1 GENERAL INTRODUCTION

1.1 The skeletal system

1.1.1 The skeletal system

Function of the skeleton

The human skeletal system is composed of 206 bones and their cartilages, together with ligaments and tendons [1]. Bone is a specialised and mineralised connective tissue that is metabolically active throughout life [2–4]. The bones of the adult skeletal system are shown in Figure 1.

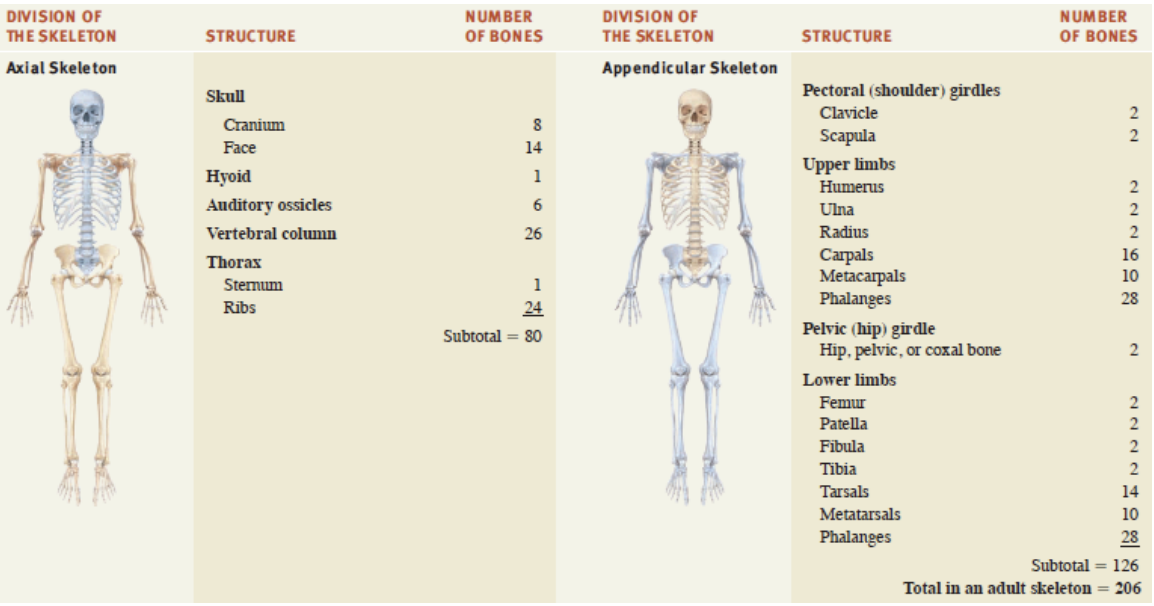

DIVISION OF THE SKELETON	STRUCTURE	NUMBER OF BONES
Axial Skeleton		
	Skull	
	Cranium	8
	Face	14
	Hyoid	1
	Auditory ossicles	6
	Vertebral column	26
	Thorax	
	Sternum	1
	Ribs	24
	Subtotal = 80	

DIVISION OF THE SKELETON	STRUCTURE	NUMBER OF BONES
Appendicular Skeleton		
	Pectoral (shoulder) girdles	
	Clavicle	2
	Scapula	2
	Upper limbs	
	Humerus	2
	Ulna	2
	Radius	2
	Carpals	16
	Metacarpals	10
	Phalanges	28
	Pelvic (hip) girdle	
	Hip, pelvic, or coxal bone	2
	Lower limbs	
	Femur	2
	Patella	2
	Fibula	2
	Tibia	2
	Tarsals	14
	Metatarsals	10
	Phalanges	28
	Subtotal = 126	
	Total in an adult skeleton = 206	

Figure 1 The bones of the adult skeletal system [1].

The skeleton serves a variety of functions, such as:

1. Mechanics: the skeleton maintains a body shape, supports the entire weight of the body and interacts with the muscular system to carry out body movement [5, 6].

2. Protection: bones offer a protective environment for vital internal organs. For instance, cranial bones protect the brain, vertebrae protect the spinal cord, and the ribs protect the heart and lungs [1, 5].
3. Production of blood: blood cells are produced by the red bone marrow in some bones. The yellow bone marrow stores fat, which can be converted to red bone marrow if the body needs additional blood production [4-6].
4. Storage and supply of minerals: bone matrix serves as a major reservoir of calcium and phosphate that may be drawn on as necessary for the maintenance of serum homeostasis, growth factors and cytokines [4-6]. In addition, along with the liver and spleen, bone marrow can store iron as ferritin that is involved in iron metabolism [6, 7].

Types of bone

The adult human skeleton is composed of 80% cortical or compact bone and 20% trabecular bone (also called spongy or cancellous bone) [6] (Figure 2). Cortical bone has a dense, ordered structure and forms the protective exterior portion of all bones [3, 6]. The components of cortical bone tissue are arranged into repeating structural units called osteons or Haversian systems [1]. Trabecular bone is a spongy interior bone tissue less dense than the outer layer [3, 6]. In contrast to cortical bone, trabecular bone does not contain osteons [1]. Microscopically, cortical

bone and trabecular bone are normally formed in a lamellar pattern, in which collagen fibrils are laid down in alternating orientations. The normal lamellar pattern is absent in woven bone, in which the collagen fibrils are laid down in a disorganised manner. Woven bone is mechanically weaker than lamellar bone. Woven bone is normally produced during formation of primary bone but is later replaced by lamellar bone. In adults, woven bone may be created when rapid new bone formation occurs after fractures or in Paget's disease [6, 8].

Figure 2 The structure of bone [9].

Composition of bone

Bone is composed of 50% – 70% mineral, 20% – 40% organic matrix, 5% – 10% water, and 3% lipids [6]. The mineral content of bone is mostly carbonated, calcium-deficient, poorly crystalline hydroxyapatite [$Ca_{10}(PO_4)_6(OH)_2$, HAP], with small amounts of carbonate, citrate, sodium, magnesium and a trace of fluoride [6, 7]. The physicochemical reactivity of the HAP mineral is essential for bone uptake of many substances [7]. The organic component of the bone matrix before mineralisation ensues is called osteoid, and contains mainly type I collagen fibrous and a number of non-collagenous materials such as proteoglycans, glycoproteins, phospholipids and phosphoproteins, osteocalcin, osteonectin and bone sialoprotein [4, 7, 8]. With mineralisation the proportion of the latter falls to leave a highly calcified matrix. The collagen network plays an important part in the integrity of bone. In bone, crystals are formed with HAP depositing within the collagen fibrils [7], the surface area of these crystals is up to 200 m^2/g and the possibilities for adsorption and surface exchange and interaction are remarkable. This unique adsorption-desorption property of HAP has been applied for decades in the chromatographic separation of proteins, nucleic acids and lipids, as discussed in Chapter 3 [7, 10]. Although the crystallised inorganic mineral salts provide mechanical rigidity and load-bearing strength to bone, the collagenous organic matrix provides elasticity and flexibility [6]. In addition, bone contributes to mineral

homeostasis by absorbing and releasing calcium and phosphate ions in the circulatory fluids. Furthermore, components of the organic matrix are thought to initiate the formation of the crystals in bone by a process of heterogeneous nucleation [7].

1.1.2 Modelling and remodelling

In the healthy human body, each bone constantly undergoes modelling and remodelling throughout life. Modelling is a process recognised as the deposition of mineralised tissue during growth and development and in response to physiologic influences or mechanical forces, leading to growth in size and changes in shape of bone [2, 6, 11] while remodelling process breaks down old, possibly microdamaged bone and builds back new bone to help preserve bone strength and ability to execute its metabolic functions [6, 11].

Skeletal remodelling can be triggered by the systemic hormones that regulate mineral metabolism and by mechanical loads and local damage, which act through local factors via multiple signalling pathways [2, 11]. The bone remodelling cycle follows an activation-resorption-reversal-formation sequence of event (Figure 3). These highly regulated phases depend on the interactions of the mesenchymal osteoblastic lineage cells and the hematopoietic osteoclastic lineage cells that structured in bone multicellular units (BMUs) [2, 6, 11]. Activation leads to the

differentiation, migration, and fusion of the large multinucleated osteoclasts that mediate bone resorption [6, 11]. These cells secrete hydrogen ions via H^+-ATPase proton pumps and chloride channels, as well as lysosomal enzymes into the resorbing compartment to lower the pH to as low as 4.5, which dissolve bone mineral and degrade the matrix components from mineralised bone and create small cavities or lacunae [6, 11-13]. The multinucleated osteoclasts, after they have completed their resorption cycle, undergo apoptosis and thus their work of bone removal is completed. Subsequently, a variety of mononuclear cells, including monocytes, and possibly osteocytes released from bone matrix, together with preosteoblasts fill in the resorption cavities [6]. The reversal phase is when bone resorption transitions to bone formation, where osteoblasts take over the process of rebuilding the resorbed bone tissue. Osteoblasts fill in the resorption cavity by production and maturation of osteoid matrix, and subsequent mineralisation of this matrix during the final formation phase of the remodelling cycle [5, 11]. Ongoing bone remodelling activity ensures a continuous supply of newly formed bone that has relatively low mineral content and thus has the potential to exchange ions more readily with the extracellular fluid [6]. In the normal adult skeleton, bone formation only occurs, for the most part, where bone resorption has already taken place. The end result of each bone remodelling cycle is production of a new osteon [6].

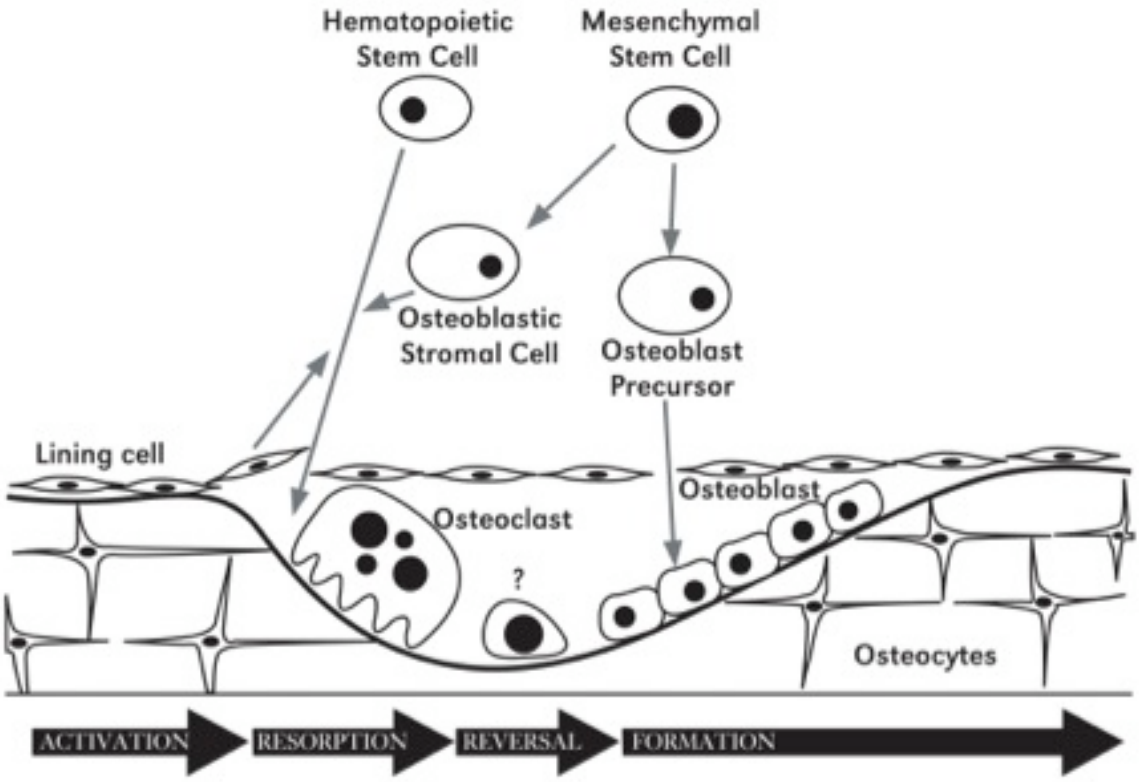

Figure 3 Bone remodelling sequence [14].

Bone is constantly being remodelled following the sequence of activation, resorption, reversal, and formation. The activation step depends on cells of the osteoblast lineage, interacting with hematopoietic cells to form bone-resorbing osteoclasts. The resorption phase may take place under a layer of lining cells as illustrated here. After a brief reversal phase, the osteoblasts begin to lay down new bone. The end result of each bone remodelling cycle is production of a new osteon.

The metabolic functions of the skeleton are controlled primarily by two major calcium-regulating hormones, parathyroid hormone (PTH) and 1, 25-dihydroxy vitamin D (calcitriol) [2, 15]. PTH regulates serum calcium concentration, and under conditions of low serum calcium, stimulates osteoclastic bone resorption. On the other hand, it also affects bone formation processes since osteoblasts have receptors for this hormone [15]. In addition, osteocytes have been shown recently to rapidly downregulate sclerostin, a key osteoblast inhibitory protein, in response

to intermittent PTH, which should allow formation of new bone on previously quiescent surfaces [15]. Therefore, it has become an area of interest to investigate the role played by osteocytes and bone-lining cells in coordinating surface anabolic activity. Due to the bone-building effect of PTH, it is used clinically as an anabolic agent that stimulates bone formation for the treatment of osteoporosis [4, 11, 16]. Calcitriol has its greatest effect on intestinal calcium and phosphate absorption, but it also has the potential effects on formation and mineralisation of bone and other tissues as well as regulating immune cell function [4, 11, 16]. A third hormone, calcitonin, acts to reduce blood calcium by inhibiting the activity of osteoclasts, which counters the effects of PTH. Even though its function is usually not significant in the regulation of normal calcium homeostasis, as a potent inhibitor of bone resorption, calcitonin has been used as a treatment for osteoporosis [16].

Along with calcium-regulating hormones, oestrogen is probably the most essential systemic hormone in maintaining normal bone turnover as well as the mass and strength of bone. Oestrogen treatment can achieve a decrease in both formation and resorption of bone with a net balance in favour of bone formation and this effect is thus associated with decreased remodelling but increased bone mass [11]. Growth hormone is another important regulator of skeletal growth, which stimulates bone formation and resorption. Glucocorticoids are required for bone cell

differentiation during development; nevertheless their greatest associated effect is to inhibit bone formation, which is regarded as the major pathogenetic mechanism of glucocorticoid-induced osteoporosis. Thyroid hormones stimulate bone resorption and formation by increasing the energy production of bone cells and are critical for maintenance of normal bone remodelling [11]. More recently leptin has been shown to be a regulator of bone mass by acting as a potent inhibitor of bone formation. It acts through the central nervous system in a hypothalamic relay [17].

Lastly, some factors of systemic origin may act on bone cells through local mediators. Local regulators include paracrine and autocrine factors specifically cytokines (e.g., interleukin 1 (IL-1), tumour necrosis factor (TNF), IL-6, IL-11 and receptor activator of nuclear factor kappa-B ligand (RANKL) that may cause bone loss, and IL-1, IL-13, IL-18, interferon (IFN), osteoprotegerin (OPG) and IL-1ra that may prevent bone loss), growth factors (e.g., insulin-like growth factor (IGF), transforming growth factor β (TGF-β), platelet-derived growth factor (PDGF), PTH-related protein (PTHrP), and fibroblast growth factor (FGF)) and prostaglandins, leukotrienes, and nitric oxide secreted by local cells and factors stored in bone matrix and released during bone resorption [4, 11].

Osteoclasts and osteoblasts regulate bone modelling that occurs during development and bone remodelling that occurs during development, maintenance, and repair of the skeleton [4, 5]. In a healthy adult, bone resorption and bone formation are in approximate balance, with matrix production and subsequent mineralisation proceeding at a constant rate [3]. However, conditions such as changing mechanical forces or metabolic and nutritional stress like that occurring during the menopause in females and with ageing in both genders, tend to disrupt this equilibrium [11]. Abnormalities of bone remodelling result in a variety of skeletal disorders [3, 11], such as osteoporosis and Paget's disease of bone and these conditions will be discussed in section 1.2.

1.1.3 Bone cells

The existence and the structure of the skeleton solely depends on the development, number, lifespan, and activities of four specific types of bone cells whose activities are controlled by a variety of factors [4]. These cells are osteoclasts, osteoblasts, bone lining cells, and osteocytes that permeate the interior of bone. They are also in contact with endothelial cells [4] (Figure 4).

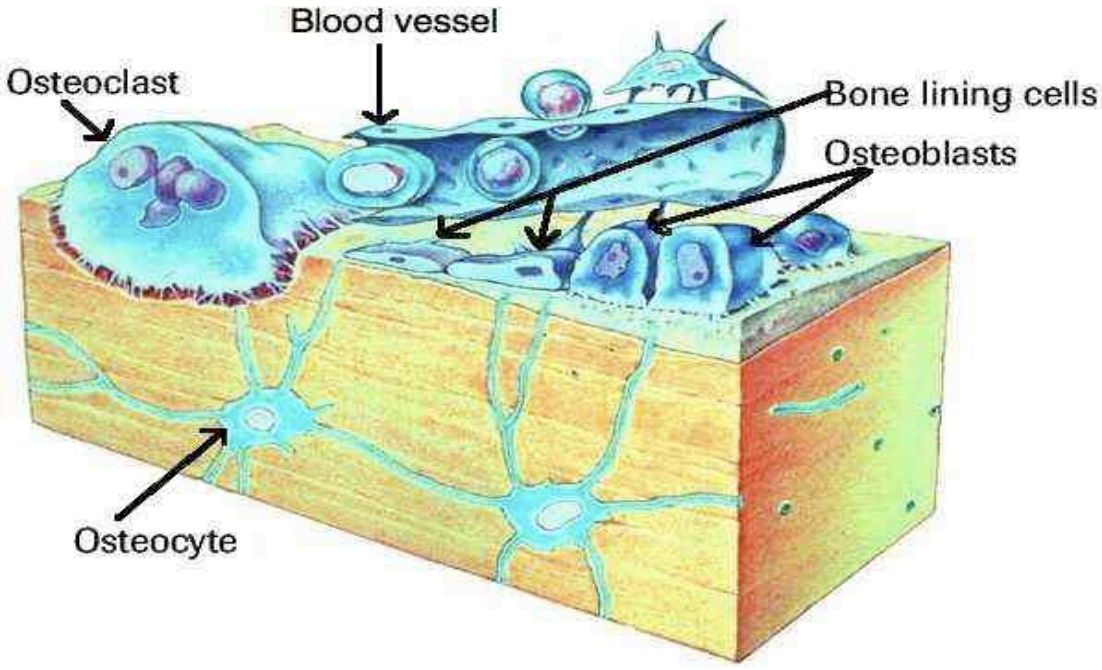

Figure 4 Diagram of bone cells, modified from [18].

Osteoclasts are large, multinucleated cells and are responsible for bone resorption. Osteoblasts synthesise new bone matrix on bone-forming surfaces. Some of the osteoblasts remain inside the bone and are converted to osteocytes, which are connected to each other and to the surface osteoblasts. Bone-lining cells are flat, thin, elongated cells that cover the surface of quiescent bone.

Osteoclasts are large, multinucleated cells and are responsible for bone resorption [4, 6]. Activated osteoclasts are derived from precursors of the hematopoietic mononuclear-phagocyte lineage and have two distinct plasma membrane specialisations with contact to bone surfaces, a clear zone and a ruffled border [4]. Bone resorption is accomplished by osteoclasts excavating a resorption cavity by secretion of hydrogen ions and lysosomal cathepsin K into the resorption compartment beneath their ruffled border (Figure 5). The acidic pH of this microenvironment dissolves bone mineral while cathepsin K digests the bone matrix into small peptides and amino acids such as hydroxyproline [2, 6].

The image originally presented here cannot be made freely available via ORA because of copyright. The image was sourced at Sevgi B. Rodan, L.T.D., *Cathepsin K – A new molecular target for osteoporosis.* IBMS BoneKEy, 2008. **5**: p. 16-24.

Figure 5 Mechanism of osteoclastic bone resorption [19].

Bone resorption is accomplished by osteoclasts excavating a resorption cavity by secretion of hydrogen ions and lysosomal cathepsin K into the resorption compartment beneath their ruffled border. The acidic pH of this microenvironment dissolves bone mineral while cathepsin K digests the bone matrix into small peptides and amino acids.

Osteoblasts come from the stromal cell lineage in the bone marrow, and manufacture a complex extracellular matrix, which subsequently mineralises [4]. Osteoblasts are in control of laying down new bone matrix constituents, collagen and ground substance. It combines the functions of a structural engineer, a message transformer, and a synthesiser of an exceedingly complex tissue. Two important cytokines secreted by the osteoblast, macrophage colony-stimulating factor (Csf1/MCSF) and receptor activator of nuclear factor kappa-B ligand (Tnfsf11/RANKL), are known to be critical for osteoclast development,

which suggests that osteoblasts may be responsible for affecting not only bone formation but also bone resorption [2, 6, 20]. Osteoblasts synthesise osteoid towards the bone surface, which later becomes mineralised under its influence. However, at regular intervals, an osteoblast will secrete matrix away from the bone surface, which will surround itself to become an osteocyte [4].

Osteocytes are the most abundant type of bone cell. The origin of osteocytes is from osteoblasts that have been trapped in the mineralised bone matrix they produced [2]. Osteocytes are linked to each other through gap junctions composed mainly of connexin 43 as an intercellular network via the canalicular system [6]. With the extensive canalicular network, osteocytes are connected to bone surface lining cells, osteoblasts and other osteocytes [6]. Gap junctions are essential for osteocyte maturation, activity, and survival [6]. The primary functions of osteocytes include mechanosensation in response to mechanical loading and maintaining bone structure. A recent discovery has been that osteocytes make sclerostin, the protein product of the SOST gene, which is an inhibitor of canonical Wnt signalling [21] (Figure 6). In addition, new evidence has suggested that sclerostin may be regulated by PTH, the key factor in the control of bone remodelling [22], which indicates that osteocytes might be able to initiate remodelling activity at specific sites within bone and regulate calcium homeostasis [2-4, 23]. Unexpectedly,

osteocytes appear to also regulate phosphate homeostasis that is essential for energy metabolism, cell signalling, bone matrix mineralisation and as a urinary buffer for acid-base homeostasis [24, 25]. There are four critical molecules expressed in osteocytes that play a role in phosphate homeostasis: phosphate-regulating gene with homologies to endopeptidases on the X chromosome (PHEX), dentin matrix protein 1 (DMP-1), matrix extracellular phosphoglycoprotein (MEPE), and fibroblast growth factor 23 (FGF-23) [24-26]. It has been suggested that FGF-23 is the key mediator to coordinate the actions of the other structures implicated in phosphate metabolism, such as the kidneys, intestines, parathyroids and bone, in order to maintain phosphate homeostasis [25]. Research into the role of osteocytes in regulating phosphate homeostasis could also have important implications for managing phosphate homeostatic disorders [25]. Furthermore, recent discoveries propose that osteocytes may employ these molecules to play an active role in paracrine regulation of bone mineralisation [25, 27]. Osteocyte apoptosis in response to oestrogen deficiency or glucocorticoid treatment seems to compromise these functions and is harmful to bone structure [28]. Recent evidence suggests that oestrogens, bisphosphonates (BPs), and physiologic mechanical loading of bone may help prevent osteoblast and osteocyte apoptosis [28, 29].

The image originally presented here cannot be made freely available via ORA because of copyright. The image was sourced at Robling, A.G., A.B. Castillo, and C.H. Turner, Biomechanical and molecular regulation of bone remodeling. Annu Rev Biomed Eng, 2006. 8: p. 455-98.

Figure 6 Inhibition of bone formation by sclerostin interfering with Wnt signalling [30].

Mechanical loading requires signalling through the Lrp5 receptor to initiate bone formation. This signal is initiated by Wnt, which binds to the receptor complex made up of Lrp5 and Frizzled. Sclerostin (Sclr) inhibits Wnt signalling and therefore blocks mechanotransduction and reduces bone formation.

Bone-lining cells are flat, thin, elongated cells that cover the surface of quiescent bone [4]. It is generally considered that these cells are quiescent osteoblasts that undergo neither formation nor resorption [6]. Their function is not well understood although it is suggested that they protect the bone by acting as a selective barrier between bone and other extracellular fluid compartments, participate the remodelling of the cortical bone and regulate crystal growth in bone [4, 5].

1.2 Metabolic bone disease

1.2.1 Introduction

Skeletal health is of paramount importance to ensure a good quality of life, particularly in ageing populations. One of the hallmarks of ageing is the loss of bone mass, which leads to an increase in the prevalence of metabolic bone diseases.

Metabolic bone disease is a term used to describe those generalised disorders of the skeleton often associated with and identified by the weakening of the bone or abnormalities of mineral metabolism [31]. Classic metabolic bone diseases include osteoporosis, Paget's disease of bone (PDB), osteomalacia/rickets and osteogenesis imperfecta. Finding more effective ways to prevent and treat these diseases in which bone mass and strength are compromised has become an important goal of long-term healthcare [32, 33]. In the next two sections, the pathogenesis and therapeutic management of the major skeletal diseases osteoporosis and Paget's disease of bone will be briefly reviewed.

1.2.2 Osteoporosis and its major treatments

Osteoporosis

Osteoporosis is by far the most common metabolic bone disease affecting the health of many adults in developed countries [33, 34]. It has

been defined as “a systemic skeletal disorder characterised by a decrease in bone mass and deterioration of the microarchitecture of the bones with a corresponding reduction in strength and an increase in bone fragility and fracture risk [34].” The most devastating consequence of osteoporosis is bone fracture, especially hip fracture, which adversely affects mortality and morbidity of the elderly [35]. In addition, other serious clinical consequences include chronic pain, loss of mobility and independence, and increased mortality [33, 37, 38]. Osteoporosis occurs in both sexes but particularly in postmenopausal women since the loss of oestrogen at the menopause leads to accelerated bone turnover and resorption [34]. Alternatively, the causes in men and premenopausal women often relate to particular hormonal disorders and other chronic diseases or as a result of smoking and medications, such as administration of glucocorticoids [33, 39].

Pathogenesis of osteoporosis

Bone homeostasis is under the influence of both endogenous hormonal changes and external mechanical loads caused by physical activity. These in turn regulate the relative activities of osteoblasts and osteoclasts that are in charge of bone deposition and resorption, respectively [11, 20]. It has been suggested that an imbalance in bone remodelling plays a key role in the pathogenesis of osteoporosis, that is, bone formation fails to keep pace with resorption [20]. At menopause, loss of oestrogen leads to

increased production of multiple cytokines essential for not only osteoclast proliferation and differentiation but also the inhibition of osteoclast apoptosis. In addition, any defect in osteoblast function results in insufficient replacement of bone loss at each remodelling site and hence bone mass is decreased [11, 36, 37]. Furthermore, use of certain medications used to control inflammatory conditions also lead to bone loss. Oral glucocorticoids are the most common inducers to drug-related osteoporosis [38, 39]. Glucocorticoids have direct and indirect effects on osteoblasts and osteocytes, they depress the replication, differentiation and function of osteoblasts and induce the apoptosis of mature osteoblasts and osteocytes, while on the other hand they favour osteoclastogenesis [38, 39]. Understanding the physiology of the skeleton and recent insights into the molecular basis of osteoporosis pathogenesis is of great importance in the management of this disease.

Management of osteoporosis

The successful management of osteoporosis includes identifying patients at risk, implementing lifestyle modifications, and a long-term compliance to non-pharmacological and pharmacological treatments [37, 40]. The goal of osteoporosis prevention is to increase peak bone mass, minimise subsequent bone loss, and ultimately prevent fractures [41, 42]. Lifestyles such as getting adequate intake of calcium and vitamin D, having appropriate exercise, reducing caffeine and alcohol intake,

avoidance of tobacco, precaution of fall, are all essential to bone health [43].

On the other hand, if osteoporosis is diagnosed, as well as consideration of calcium and vitamin D supplementation and lifestyle modification, pharmacologic management should be considered to stop further bone loss and to prevent fractures [37, 40]. Based on the pathophysiology of osteoporosis, current medications fall into three categories, drugs that inhibit bone resorption (anti-resorptive agents), drugs that stimulate bone formation (anabolic agents), and drugs that act by a combination of both mechanisms (dual-acting agents) [2]. Most forms of osteoporosis are due to an imbalance in bone remodelling such that bone resorption exceeds bone formation. Therefore, the majority of therapies for use in prevention or treatment of osteoporosis approved by the U.S. Food and Drug Administration (FDA) act by inhibiting osteoclast mediated bone resorption. Examples of this kind of pharmacologic agent are the BPs (alendronate, risedronate and ibandronate), the selective oestrogen-receptor modulator (SERM) raloxifene (RLX), calcitonin, and oestrogen [2]. In contrast, PTH 1-34 (teriparatide) is the only anabolic agent with FDA approval, and the intact hormone (PTH 1-84) is in clinical trials [15, 44]. The dual-acting strontium ranelate is used in some countries [45]. A detailed comparison of the anti-fracture efficacy of these agents is shown in Figure 7.

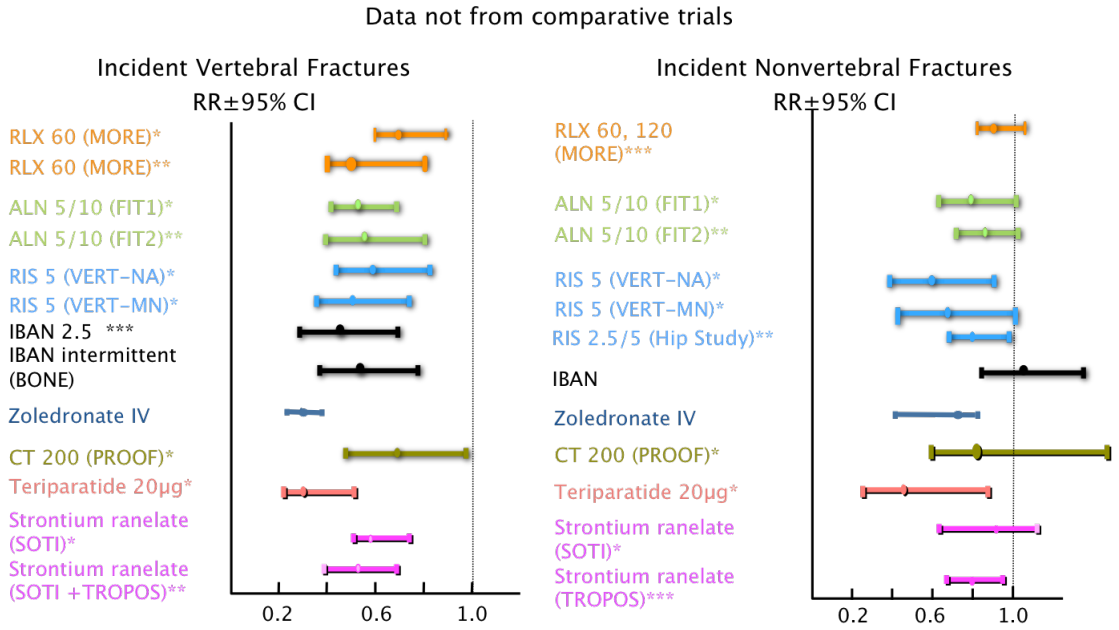

Figure 7 Anti-fracture efficacy of current osteoporosis agents [46].

Among the many anti-resorptive agents, BPs have been established as the leading group of drugs used for the prevention and treatment of osteoporosis and related metabolic bone diseases [47]. BPs have been shown to increase bone mass, and amongst them, alendronate and risedronate reduce all types of fracture when given in adequate doses and zoledronate is the first and only once-a-year osteoporosis medication approved to date [33]. BPs are nonhydrolysable analogues of inorganic pyrophosphate, which is a naturally occurring bone resorption inhibitor. BPs have a strong affinity for bone mineral, i.e., hydroxyapatite, which ensures that they achieve therapeutic concentrations in skeletal tissue fluids [48].

As our understanding of the mechanisms of action of the medications used for osteoporosis management increased rapidly, the discovery of the molecular pathways involved in bone cell differentiation and function has also been the centre of skeletal research. Several novel pharmacological interventions aimed at modifying some of the pathogenic processes, have recently been discovered and are currently under clinical observation [49, 50]. Examples of new anti-resorptive molecules are: osteoprotegerin, RANKL-antibodies (denosumab), and cathepsin K inhibitors (e.g., odanacatib), newer SERMs (lasofoxifen and bazedoxifene) and "ANGELS" (activators of non-genomic oestrogen ligands) [49, 50]. In addition, peptide sequences of PTH or PTH analogues with the capability of stimulating osteoblastic activity may also be introduced as potent anabolic agents [2, 44, 51].

1.2.3 Paget's disease of bone and its major treatments

PDB is another relatively common metabolic bone disease in the UK [32, 52]. PDB is a chronic metabolic disease of bone characterised by uncontrolled, increased bone resorption in focal areas followed by disorganised bone formation, with eventual replacement of the normal skeletal architecture [53]. PDB is associated with an increased risk of bone pain, fracture, deformity, premature arthritis and deafness [5, 54]. The majority of patients with PDB are older people of Western European descent, with an age of 55 years or older [53].

Pathogenesis of Paget's disease of bone

Both genetic and nongenetic factors have been investigated to be involved in the pathogenesis of PDB [52]. Genome-wide searches have suggested several genetic loci on chromosomes 2q36, 10p13, and 5q35 as potential loci for PDB [55]. Mutations in four genes, namely SQSTM1, TNFRSF11A, TNFRSF11B, and VCP that involved in the RANK-NF-κB signalling pathway have been identified to be associated with PDB [56, 57]. In addition, other studies suggest that PDB results from a chronic paramyxoviral infection [11, 52]. PDB is thought to be initiated by multinucleated, hyperactive and unregulated giant osteoclasts resorbing bone at local affected sites [53]. Resorption then stimulates osteoblasts to replace the resorbed bone, however, the new bone formed is often uncontrolled and structurally disorganised [11, 52].

Management of Paget's disease of bone

Based on the pathogenesis of PDB, anti-resorptive agents are considered as the direction for PDB treatment [58]. In the early 1970s two differing agents of this kind competed for the treatment of Paget's disease, namely calcitonin and the first BP, etidronate [59]. Both drugs are able to suppress osteoclast activity albeit with different mechanisms of action. In the end, calcitonin treatment has been revealed to be sometimes poorly tolerated and often inadequate to decrease the activity of the disease [53]. On the other hand, etidronate showed partial or complete

remissions in PDB patients. With the development of newer generations of aminobisphosphonates that are more powerful and specifically directed towards resorption inhibition, these agents are proven to suppress the symptoms effectively and may prevent the development of complications [53]. Therefore, today the aminobisphosphonates have become standard therapy for PDB, which includes oral therapy with alendronate and risedronate, and the most effective intravenous therapy with pamidronate and zoledronate [54].

1.3 Bisphosphonates

1.3.1 Introduction

Nowadays, there is a great demand for finding effective ways to prevent and treat metabolic bone diseases such as osteoporosis in which bone mass and strength are compromised. Studies over the past forty years have shown that the major class of pharmaceuticals known as BPs are particularly effective in preserving bone mass in this condition and also in limiting the resorptive consequences of metastatic bone disease in cancer patients [60]. In these aspects they are the most widely used drugs and are highly potent therapeutically.

1.3.2 Structure-activity relationships of bisphosphonates and their mechanisms of action

There are a number of BPs that are used clinically. Each BP has a distinctive property that is attributable to the unique molecular structure (Figure 8). BPs are stable analogues of pyrophosphate (PPi, P-O-P, Figure 8), a natural modulator of calcification, with carbon substituting for oxygen in the central moiety (P-C-P) [60]. The structure-function profile of BPs is determined by the phosphonate groups and also by the two side groups, R1 and R2, with R1 being mainly a hydroxyl (OH) [61]. The first biological studies of BPs started in the 1960s and demonstrated their properties including high affinity for bone mineral, the ability to inhibit dissolution and formation of hydroxyapatite crystals and to prevent calcification both *in vitro* and *in vivo* [62, 63]. Due to these promising physical-chemical properties, they were then developed as inhibitors of bone resorption for the treatment of diseases characterised by increased bone resorption [64].

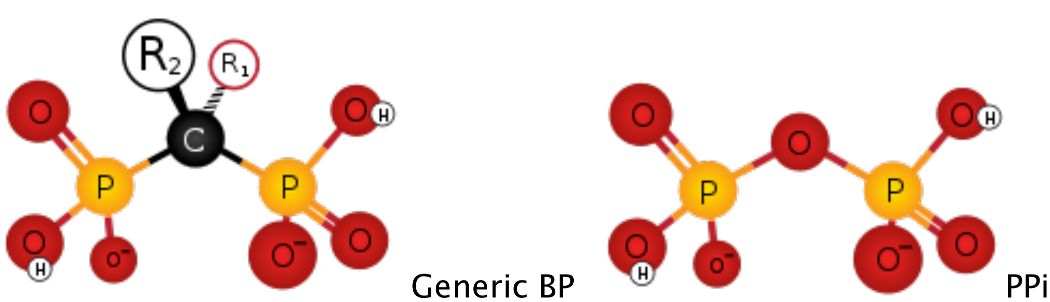

Figure 8 Chemical structures of bisphosphonate (left) and pyrophosphate (right) [65].

The capacity of BPs to inhibit bone resorption depends on two critical properties of the BP molecule (Figure 9) [66]. The first such property is the strong affinity for bone mineral, which allows the rapid and selective targeting of BPs to bone mineral surfaces [66]. The P-C-P moiety is responsible for this property because the negative charge of the oxygen atoms on the phosphonate groups can chelate the positively charged calcium ions on the surface of bone [66]. Both phosphonate groups are required for this tight binding and modifications to one or both reduce affinity for bone mineral [66]. It has been well characterised that the affinity for calcium is even greater if BPs contain a hydroxyl group at R1 position, as in most clinically used BPs, owing to the more effective tridentate binding to calcium [67].

The second important property of the BP molecule relies on the structure of the R2 side chain [66]. Once localised within bone, it is the structure of the R2 side chain that determines the anti-resorptive potency and influences the capability of specific targeting of the drugs [68]. The most potent anti-resorptive BPs, consist of a hydroxyl group in the R1 position and a nitrogen-containing R2 side chain, and therefore known as nitrogen-containing bisphosphonates (N-BPs) [69].

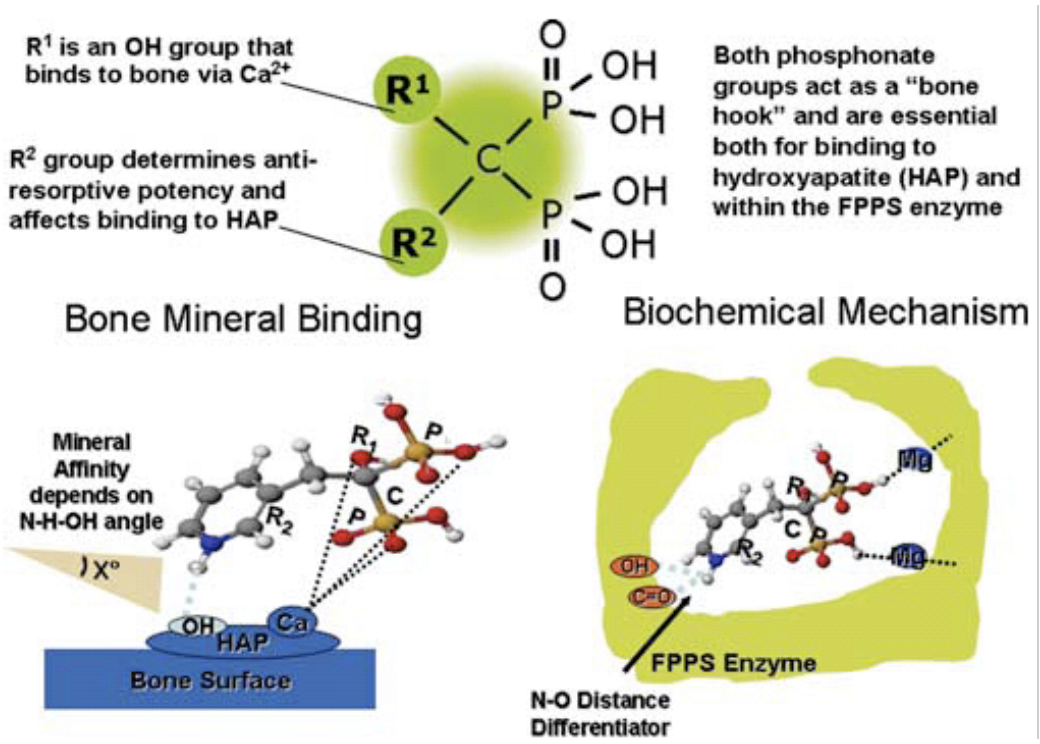

Figure 9 Functional domains within the BP structure and how these influence BP binding to HAP and to the farnesyl pyrophosphate synthase (FPPS) enzyme [70].

A large number of studies have demonstrated that the effects of BPs on bone resorption are mainly due to their effect on osteoclasts [71] (Figure 10). After administration, BPs are taken up by the skeleton, primarily at active remodelling sites, and bind strongly to bone mineral. During bone resorption, the acidic environment beneath the resorbing osteoclasts causes the dissolution of the bone mineral, which subsequently leads to the release of BPs from the bone surface. As a result, high local concentrations of BPs are present in the resorption space and are most likely to be taken up by osteoclasts through fluid-phase endocytosis [72], while non-resorbing cells take up only small amounts of BPs that become available due to natural desorption from the bone surface [73].

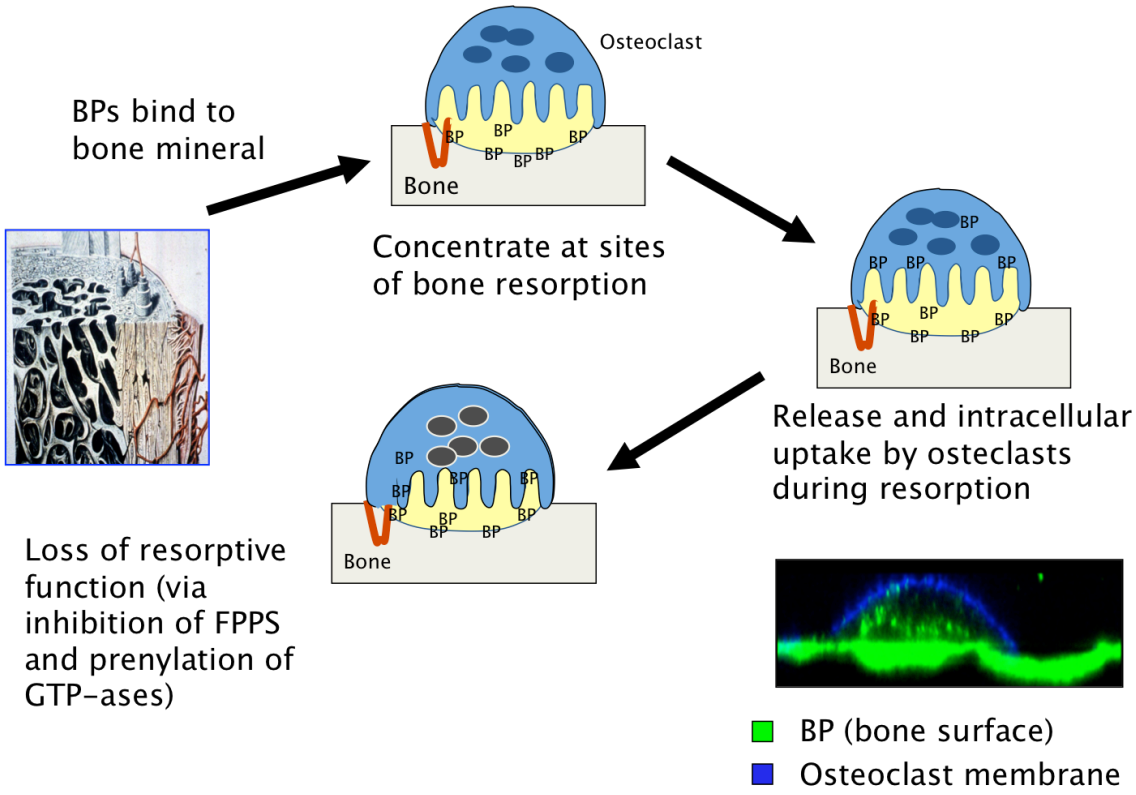

Figure 10 Action of BPs on osteoclasts.

However, the biochemical mechanisms are different between two groups of BPs, namely the simple BPs, i.e., BPs without the nitrogen-containing R2 group (e.g., clodronate and etidronate), and the N-BPs (e.g., pamidronate, alendronate, neridronate, risedronate, ibandronate, zoledronate, etc.) [71] (Figure 11). The simple BPs are able to be metabolised to cytotoxic adenosine triphosphate (ATP) analogues within osteoclasts, which is known to inhibit osteoclast function that causes osteoclast apoptosis and cell death and hence inhibits bone resorption [71]. The more potent N-BPs, on the other hand, inhibit an enzyme called farnesyl pyrophosphate synthase (FPPS) of the mevalonate biosynthetic pathway thereby preventing the prenylation of small GTPase proteins

essential for the function and survival of osteoclasts [74, 75]. Recent studies have shown that N-BPs may have yet another mechanism of action. N-BPs also induce production of an intracellular ATP analogue known as ApppI, which may directly induce osteoclast apoptosis, but this action appears to make a minor contribution to their effect on bone resorption [76].

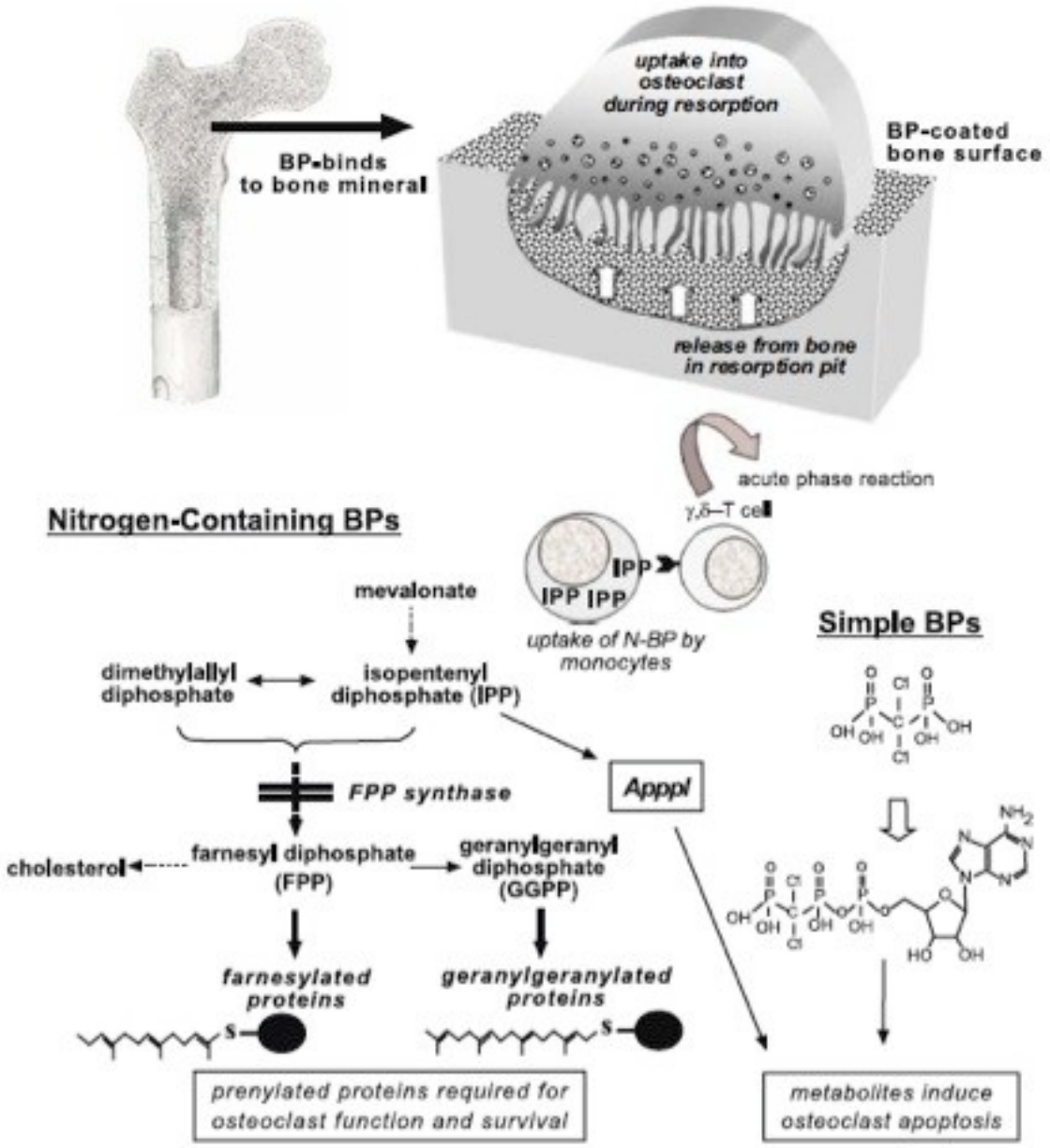

Figure 11 Mode of action of BPs on osteoclasts [69].

After binding to bone mineral, BPs are taken up by osteoclasts through endocytosis. Simple BPs are metabolised to ATP analogues within osteoclasts that induce osteoclast apoptosis. N-BPs inhibit FPPS, thereby preventing the prenylation of small GTPase proteins essential for the function and survival of osteoclasts. Inhibition of FPPS also causes the accumulation of IPP, which is incorporated into ApppI. The ApppI may directly induce osteoclast apoptosis.

Studies over the years have shown that the pharmacological potencies of BPs are mainly dependent on their binding affinities for bone mineral and on their inhibitory actions on osteoclasts. However, more recently protective effects of sub micromolar concentrations of BPs on osteocytes and osteoblasts from glucocorticoid-induced apoptosis have also been reported [77]. This is thought to involve novel membrane actions of the BPs on connexin 43 hemi-channels, and subsequent activation of the extracellular signal-regulated kinases (ERKs) signalling pathway [77] (Figure 12). Effects of BPs on osteocyte apoptosis at low doses were found to be independent of their structure [77, 78]. In addition, by secreting sclerostin, osteocytes may inhibit Wnt signalling and reduce bone formation by osteoblasts [23]. Osteocyte apoptosis may trigger remodelling and play a role in susceptibility to hip fracture [23]. These findings suggest that preservation of the osteocyte network might preserve the function of these cells as mechanosensors and contribute to their anti-fracture efficacy [77]. However, further studies are urgently required to test this hypothesis.

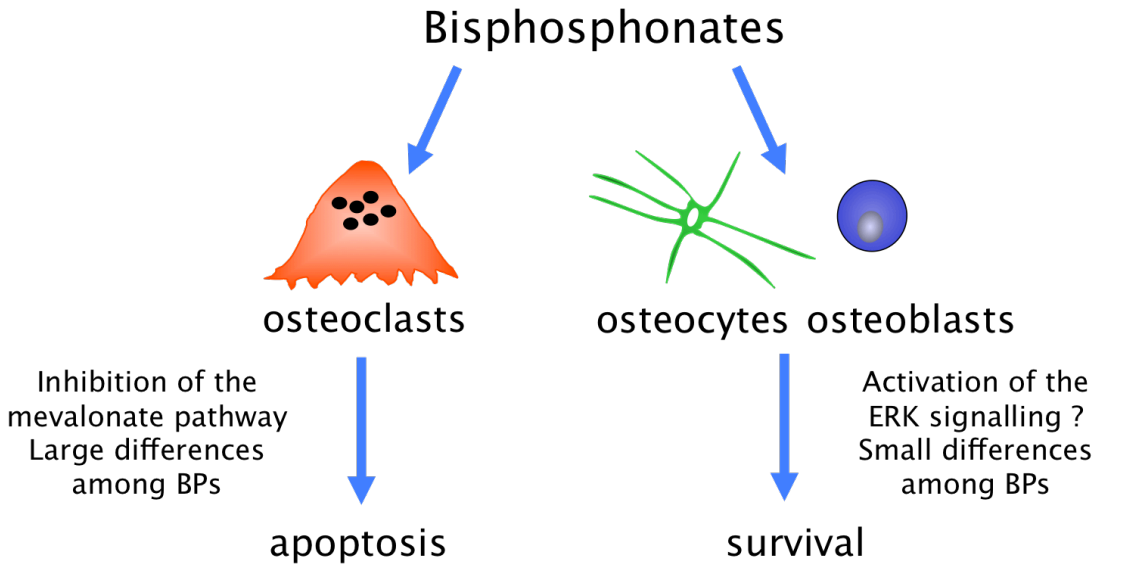

Plotkin, Bellido et al. 2006, Bone
Kogianni, Noble et al, 2004, Life Sciences

Figure 12 Proposed differential effects of BPs on osteoclasts and osteocytes.

Minor changes in the structure or three-dimensional conformation of the R2 substituent of BPs can lead to extensive alterations in their physicochemical, biological, therapeutic and toxicological effects, mainly in inhibition of the FPPS enzyme within the mevalonic acid pathway in osteoclasts, but also in the ability to bind to HAP [67]. For instance, it is shown that the orientation of the nitrogen atom relative to the phosphonate groups affects the ability of N-BPs to inhibit the enzyme [73]. There is a clear correlation between the degree of inhibition of FPPS *in vitro* and the anti-resorptive potencies of N-BPs *in vivo*, and furthermore two compounds with similar bone binding affinity can show vastly different anti-resorptive properties. Over the years, generations of BPs have been developed and changes in chemical structures have

resulted in enhanced potency (Figure 13). For example, incorporation of an amino alkyl side chain as seen in pamidronate and alendronate are up to 100-fold more potent than simple BPs such as etidronate [79]. The length of carbon chain is relevant for two to five carbon derivatives and the highest activity being found is three carbons, as present in alendronate [80]. Moreover, methylation of the amino group or inclusion within a nitrogen heterocyclic ring enhances potency still further. Not surprisingly, the position of the nitrogen moiety within the heterocyclic ring can influence anti-resorptive potency [69]. The newly developed heterocyclic BPs, e.g., zoledronate and risedronate in particular, display wider therapeutic index between anti-resorptive potency and anti-mineralisation effects than the BPs that contain an alkyl side chain and they are determined to be 10,000-fold more potent than etidronate [81, 82].

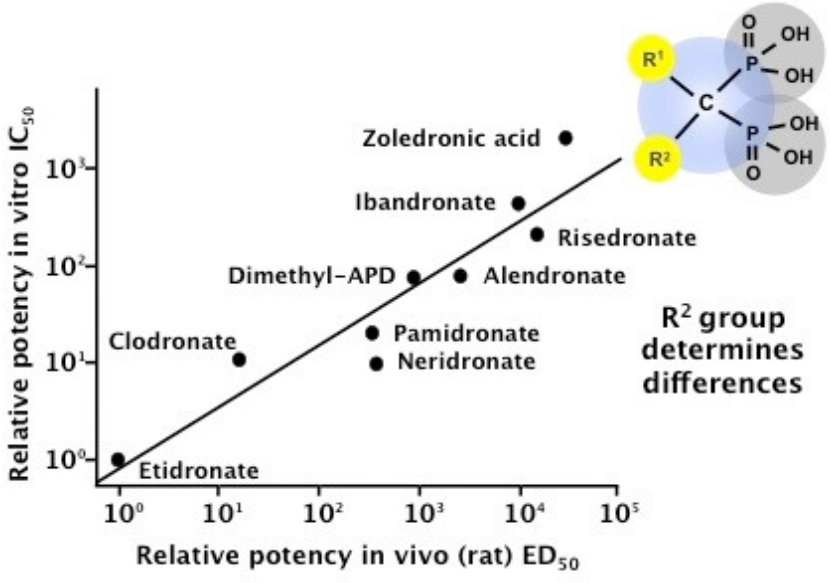

Figure 13 Range of potency of BPs [83].

1.3.3 Pharmacology

The clinical pharmacology of BPs is characterised by low intestinal absorption, but highly selective localisation and retention in bone [84]. When taken orally, only less than 1% of the BP dosage is absorbed from the gastrointestinal tract [81, 85]. Taking a BP in the presence of any food containing calcium or other divalent cations will almost completely block its absorption [81, 86]. BPs are generally not metabolised in serum [86, 87]. Following intravenous infusion, BPs are efficiently cleared from the systemic circulation, up to 50% of the absorbed dose is gathered on the bone surface [86], the binding sites are virtually unsaturable due to the large exchangeable surface capacity of skeleton [81]. The remainder of the dose is excreted unmetabolised rapidly by the kidneys via filtration and possibly by proximal tubular secretion [34, 87] (Figure 14). The long residence time in bone, in contrast to its short circulating half-life, makes BPs conserve bone architecture and strength even after long-term use [69]. The inhibition of bone resorption reaches a new steady-state level within days of administration rather than becoming progressively lower, even when the compounds are given continuously [71]. The reduction in bone turnover is shown to be dose-dependent, therefore appropriate dosing regimens are critical for both safety and efficacy and the long-term use of BPs may well be a progressive labelling of the entire skeleton [88]. In the acid environment of resorption lacunae, BPs are released from bone surfaces, internalised by the osteoclast and cause loss of resorptive

function and eventual apoptosis. There may be some effects of BPs on osteocytes as well [81]. The presence of BP on inactive bone surfaces is not able to influence bone turnover, but it provides a reservoir of drug that potentially available many years later when that newly formed packet of bone is eventually resorbed [88]. Newly developed BPs have been synthesised to display a wide therapeutic index between anti-resorptive potency and inhibition of mineralisation effects, which may also affect the dosing interval and the persistence of effect after medication discontinuation [69].

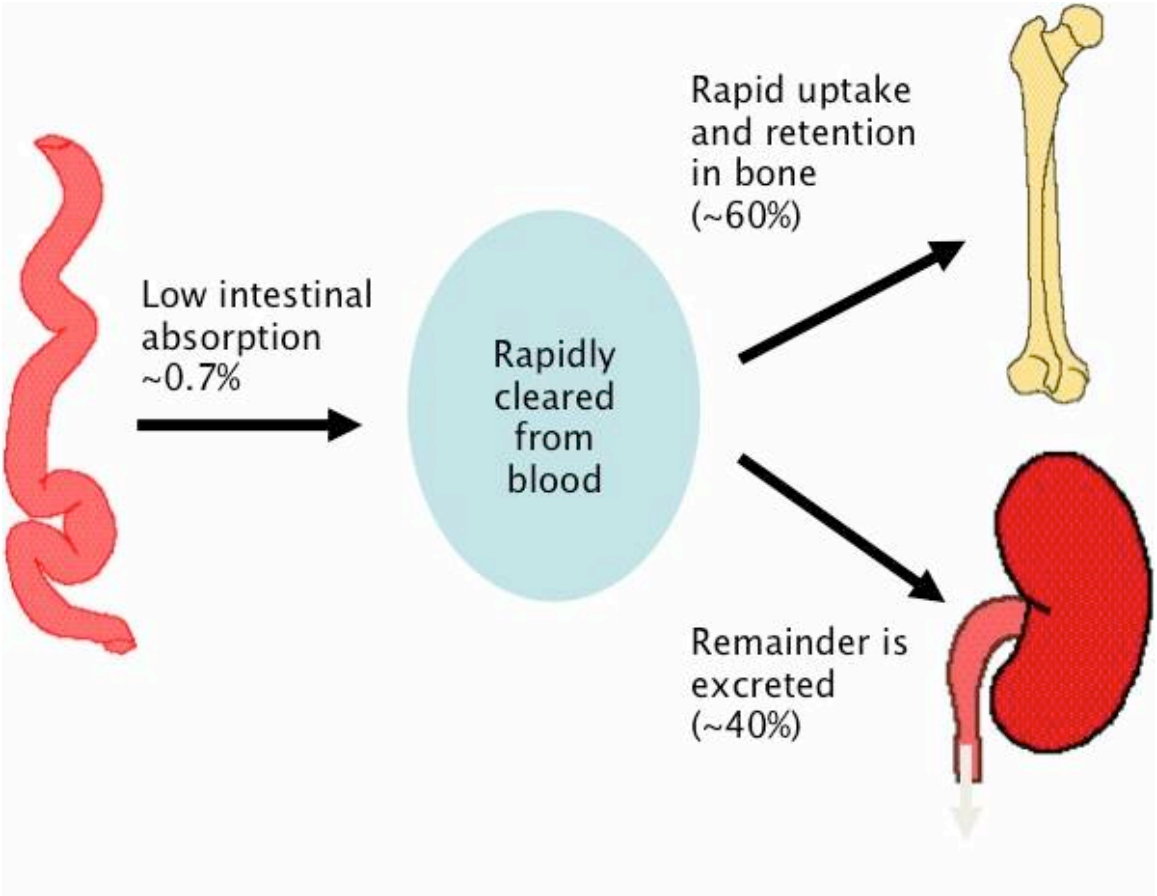

Figure 14 Pharmacology of BPs.

1.3.4 Therapeutic applications of bisphosphonates

The BPs, as synthetic bone-seeking compounds, have been used as radionuclide bone imaging agents [89]. Because of their preferential uptake at sites of increased bone turnover and the ability to be easily linked to a gamma-emitting technetium isotope, BPs for many years have been useful for detecting abnormal metabolic activity of bone, such as, in Paget's disease of bone, bone metastases, and in detecting soft tissue calcifications [60] (Figure 15). In the late 1960s, they began to be used for treatment of fibrodysplasia ossificans progressiva and in patients who had undergone total hip replacement surgery in attempts to prevent subsequent heterotopic ossification and to improve mobility [90].

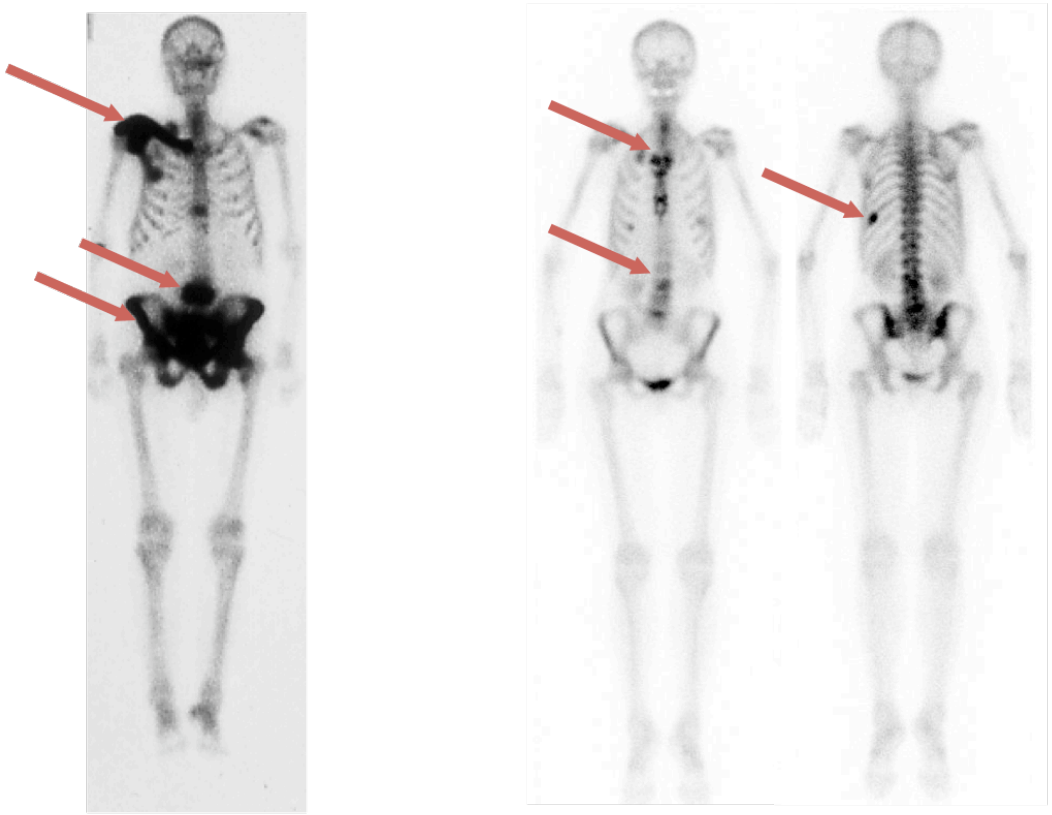

Courtesy of Ignac Fogelman

Figure 15 Use of ^{99m}Technetium BP for bone scans.

Currently, there are at least ten BPs (etidronate, clodronate, tiludronate, pamidronate, alendronate, risedronate, ibandronate and zoledronate, etc.) that have been licensed as drugs for clinical use against osteoporosis, tumoural osteolysis, malignant hypercalcemia associated with multiple myeloma, osteogenesis imperfecta, Paget's disease of bone, rheumatoid arthritis and bone metastases from prostate and breast cancers [85, 91, 92]. Among these diseases, osteoporosis, PDB and metastatic bone disease are the most studied.

Osteoporosis

At the present time, osteoporosis is of great concern as a major health problem in ageing population. Until recently, most agents commonly used to prevent or treat osteoporosis are inhibitors of bone resorption, with BPs as the leading group [41]. Although the widespread introduction of BPs into clinical practice did not occur until 1995 with the approval of alendronate by FDA, BPs, as a class, have been well established as highly effective at limiting bone loss, improving bone mineral density and prevention of fractures in women with postmenopausal osteoporosis and women and men with glucocorticoid-induced osteoporosis [81].

Alendronate was the first BP approved in the United States for treatment of osteoporosis (1995), followed by risedronate (approved for PDB in 1998 and for use in osteoporosis in 2000), zoledronic acid (approved for skeletal complications of malignancy in 2001 and for use in osteoporosis in 2007), and ibandronate (approved in 2005 for use in osteoporosis) [81]. Among them, alendronate, risedronate and zoledronate, have shown to reduce the risk of hip fractures as well as nonvertebral fractures as a composite end point [81]. The effectiveness of BP management in osteoporosis can be explained by the fact that BPs do not only decrease bone turnover but also increase bone mineral density [90]. The decrease in bone resorption is followed by a coupled, induced decrease in bone formation, which leads to a temporary gain in calcium balance. The

lowered bone turnover slows down bone loss and hence permits more complete mineralisation. Based on the broad spectrum anti-fracture efficacy, BPs have established as the agents of choice for most patients with osteoporosis [81].

Paget's disease of bone

The greatly increased bone turnover that causes the major skeletal complications of the PDB is ideally suited to therapy with BPs, since they are selectively delivered to Pagetic lesions [54, 93]. Treatment of PDB with BPs leads to the restoration of normal bone histology and the healing of radiological lesions [54].

The treatment of choice is a potent N-BP, including oral alendronate/ risedronate or intravenous pamidronate/zoledronic acid. The latter ones, especially, have greater potency and prolonged biochemical remissions, usually lasting months to years [53, 58]. New findings suggest that a single infusion of zoledronic acid (5 mg) is significantly more effective than 60 days of daily treatment with oral risedronate in patients with PDB, making it the most potent BP therapy for use in PDB to date [94].

Metastatic bone disease

Metastatic bone disease is a frequent complication of several common solid tumours including breast, lung, prostate and renal cancer, and a

major cause of morbidity for patients [95]. Bone metastases are generally characterised as osteolytic, leading to bone destruction, or osteosclerotic, leading to new bone formation [95]. In addition to the ability to inhibit osteoclast activity, there is increasing evidence showing that N-BPs may have direct anti-tumour effects [48, 96-98] (Figure 16). These effects include the inhibition of adhesion of tumour cells within bone [99-103], the reduction of the release of growth factors that stimulate tumour growth in bone [104-106], and the inhibition of angiogenesis [107, 108]. Furthermore, there are intriguing results from both *in vitro* and *in vivo* models suggesting that the combination of N-BPs with a variety of standard anti-cancer agents has enhanced anti-tumour activity compared to that produced by the single agents [109-111].

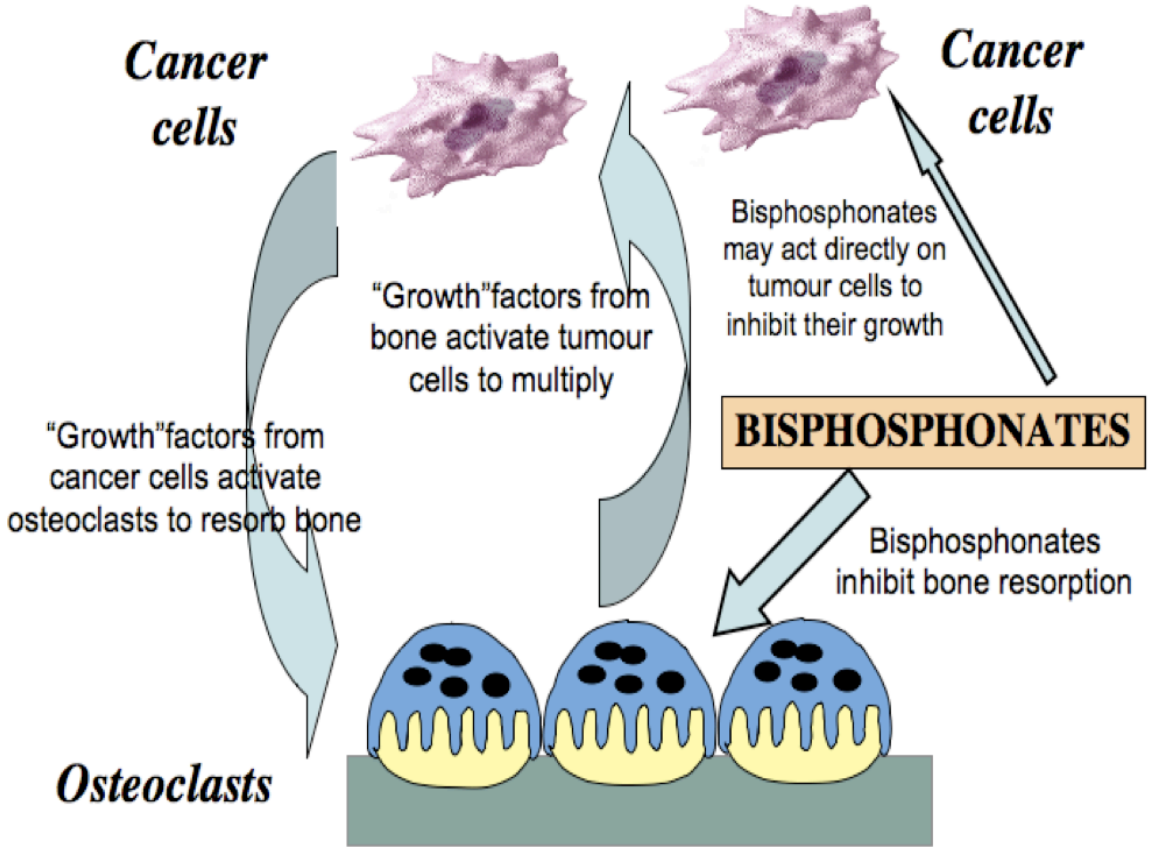

Figure 16 BPs prevent bone resorption caused by metastases and display anti-tumour effects.

Oral and intravenous clodronate and ibandronate, intravenous pamidronate and zoledronic acid used in metastatic bone disease have all shown to significantly reduce skeletal complications [95, 98]. Zoledronic acid (4 mg, i.v. 3-4 weekly), the most potent BP, is shown to consistently reduce the risk of skeletal-related events (SREs) across all tumour types [109] (Figure 17). In addition, BPs have become the treatment of choice for hypercalcemia of malignancy and osteolytic bone disease associated with tumour metastases. With the aim of relieving bone pain, reducing skeletal morbidity and improving quality of life [95], the ongoing research

will hopefully lead to clinically meaningful insights into the anti-tumour mechanisms of N-BPs, and eventually to the development of more specific and potent regimens for clinical use.

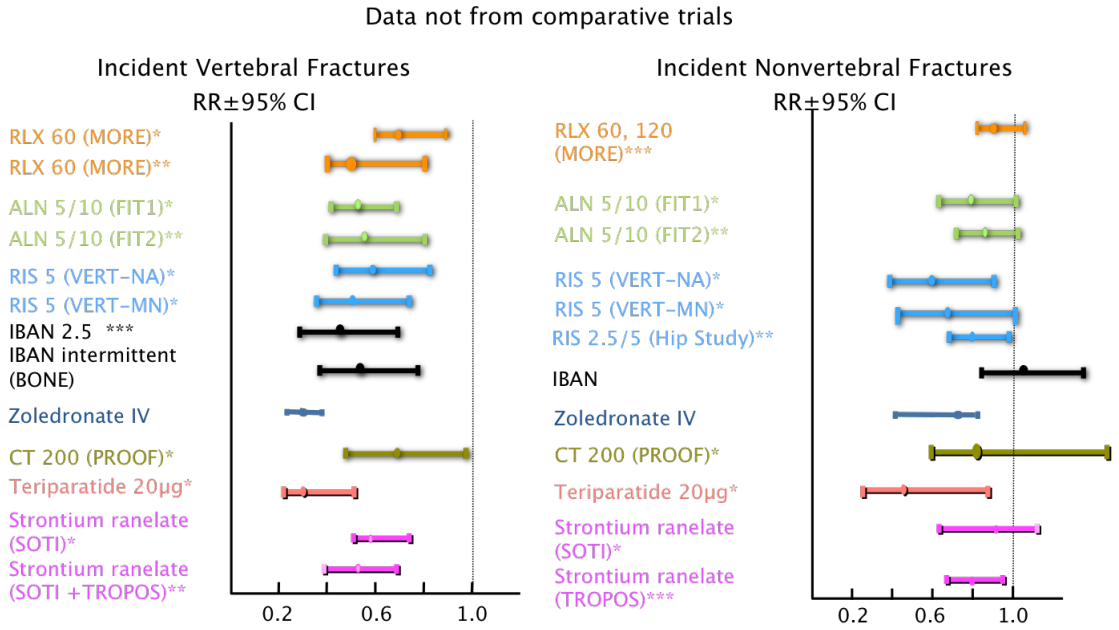

*With prevalent vertebral fracture(s) ; **Without prevalent vertebral fractures; ***With or without prevalent vertebral fractures; †Not from head-to-head studies

Figure 17 Zoledronate (4 mg i.v. 3-4 weekly) consistently reduces the risk of skeletal-related events (SREs) across all tumour types.

Zoledronate 4 mg was significantly more effective than placebo in reducing the risk of SREs in patients with prostate cancer (36% risk reduction; P = .002) and solid tumours other than breast or prostate cancer (31% risk reduction; P = .003). Zoledronate 4 mg also significantly reduced the risk of SREs among patients with lung cancer (32% risk reduction; P = .016), and renal cell carcinoma (58%; P = .010).

1.3.5 Adverse effects of bisphosphonates

BPs are generally well tolerated and safe, which can be partly explained by their strong mineral-binding affinity that prevents their uptake by most other tissues [34, 69]. Nevertheless, adverse effects may occur with BP therapy [85, 112, 113], the incidence of adverse effects may depend on a series of factors, such as the route of administration, the dose and

frequency of administration and the type of BP [112].

For oral BPs, regardless of the structure, upper gastrointestinal irritation is the most common adverse effect [114]. Gastrointestinal symptoms can be minimised by remaining upright for a defined period of time after dosing, taking the medication with sufficient water, and waiting an appropriate interval before consuming food [85, 112].

In patients who receive their first intravenous N-BP, a transient acute-phase reaction may occur [115-117]. The acute-phase reaction includes flu-like symptoms such as fever, myalgias, arthralgias and headache of mild intensity, which generally can be resolved within 48 hours [81, 85, 112]. This is as a result of activation of γ, δ-T cells and has been extensively studied by Rogers and colleagues [118].

Another commonly seen adverse effect with rapid intravenous administration is renal toxicity [119]. Although studies have shown that all BPs have the potential to cause acute tubular necrosis, zoledronic acid is suggested to have a higher risk compared with other N-BPs [112].

The above-mentioned adverse effects are well recognised for their plausible mechanisms and thus in most cases can be avoided or managed effectively [34]. However, there are adverse effects where no clear causal

association or explanation exists. Among these, a striking side effect termed osteonecrosis of the jaw (ONJ) has been documented since 2003 [120]. Almost all cases of ONJ precipitated by a tooth extraction in patients treated with long term, high dose intravenous N-BPs for the management of myeloma, breast or prostate cancer [81, 85, 112, 121]. However, a direct and plausible causal association or the exact mechanism underlying the relationship between BPs and ONJ has not been established [34].

Other rare side effects that have been reported include hypocalcaemia, severe musculoskeletal pain, oesophageal cancer with oral BPs, ocular inflammation, severe suppression of bone turnover and resulting atypical fractures, and most recent, atrial fibrillation [81, 112, 122-124]. However, the association between these cases and BP use is unproven and needs to be comprehensively studied in epidemiology or randomised controlled trials (RCTs) [34].

In conclusion, BP therapy can be associated with mild adverse effects in some patients and, more rarely, with serious adverse effects. Evidence to date suggests that selecting the most appropriate BP based on these factors confers a clear clinical benefit in most carefully selected patients, which outweighs potential risks associated with BP use [34, 85, 112, 125].

1.4 Aims of the project

BPs are potent and effective agents in preserving bone mass in metabolic bone diseases and also in limiting the resorptive consequences of metastatic bone disease in cancer patients. The pharmacological potencies of BPs are dependent both on their binding affinities for bone mineral and on their inhibitory actions on osteoclasts. In addition, potential effects on other cell types present locally in the environment of skeletal tissues have been reported.

Over decades, different strategies have been adopted to reveal the binding affinities of BPs but with contradictory conclusions. Therefore, the present study aims to systematically evaluate the relative mineral-binding affinities of clinically relevant BPs and the effects on binding to HAP. This aspect involves three experimental approaches:

1) Determinations of retention times on ceramic hydroxyapatite (HAP) and fluoroapatite (FAP) columns by using fast performance liquid chromatography (FPLC) combined with mass spectrometric identification and quantitation of the individual BPs.

2) Assessment of the mineral-binding capacities and dissociation constants of BPs by Langmuir adsorption isotherms.

3) Evaluation of the dissociation constants of BPs by development of a competitive binding assay by using fluorescence spectrophotometry.

In addition, in order to obtain new insights into the cellular effects of BPs, *in vitro* cell culture methodology was used. For this purpose, osteocytes and osteoblasts were exposed to a variety of concentrations of BPs. Studies included determinations of the anti-apoptotic effects of BPs as well as investigations on the mechanisms of apoptosis and cell death.

This research should reveal in greater detail the effects of modifications in BP chemical structure on mineral-binding affinities, and hence on their likely retention and diffusion through bone and on their functional efficacies. Also, it attempts to provide the basis for further investigation of the potential role of BPs on osteocyte and osteoblast activities.

CHAPTER 2 MATERIALS AND METHODS

2.1 Materials

Nine clinically relevant bisphosphonate compounds (risedronate, zoledronate, minodronate, alendronate, pamidronate, neridronate, ibandronate, etidronate, and clodronate) (Figure 18), and selected bisphosphonate analogues (see Figure 19 for a full list) were used in this study. All non-fluorescent compounds were synthesised and characterised at Procter & Gamble Pharmaceuticals (OH, USA) (Dr. F. H. Ebetino) and chemical purity determined to be > 99%. The BPs with chromophore attached included 5(6)-carboxylfluorescein-risedronate (5(6)-FAMRIS), Alexa Fluor 647-risedronate (AF647-RIS), rhodamine-risedronate (Rho-RIS), rhodamine-phosphonocarboxylate-risedronate (Rho-RISPC), and 5(6)-carboxylfluorescein-amino-risedronate (5(6)-FAM-amino-RIS). These were all synthesised and characterised at the University of Southern California (Dr. C. McKenna) and the chemical purities of the compounds were > 95%; their structures are listed in Figure 8. Initial wavelength scans were performed for the UV-absorbing BPs, i.e. RIS, ZOL and MIN, by using a Nanodrop spectrophotometer (Thermo Scientific, Wilmington, DE). Potassium phosphate dibasic ACS reagent (≥ 98% purity) and potassium phosphate monobasic ACS reagent (99% purity) were obtained from Sigma-Aldrich (Dorset, UK). Sodium chloride was obtained from Fisher Scientific (Loughborough, UK) and was analytical reagent grade. Deionised water purified with a Milli-Q Ultra-

Pure Water System (Millipore, Bedford, MA) was utilised for all sample preparations. 1 mM phosphate-buffered saline (PBS) with 0.15 M NaCl (pH 7.4) was prepared freshly. Stock solutions of the BPs and analogues were made by dissolving the compounds in 1mM PBS to yield a 10 mM solution and these solutions were adjusted to the desired pH. Solutions were filtered through 0.45 µm Millipore filters (Millipore, Bedford, MA) before use. Hydroxyapatite (HAP; Macro-Prep® Ceramic Hydroxyapatite Type II 20 µm 100 g; specific surface area: 10.63 m^2/g, density: 0.63 g/ml and Ca/P molar ratio: 1.67) used for the pH 7.4 and 6.8 studies, and fluoroapatite (FAP; CFT™ Ceramic Fluoroapatite Type II, 40 µm), used under acidic conditions (pH 5.7), were obtained from Bio-Rad Laboratories, Inc. Hercules, CA.

Bisphosphonate Structures

General BP

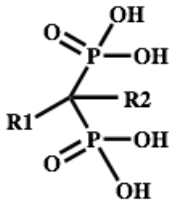

Non N-BPs

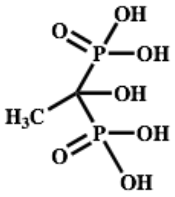

Etidronate (ETI)

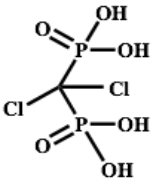

Clodronate (CLO)

Alkyl-amino BPs

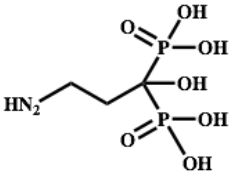

Pamidronate (PAM)

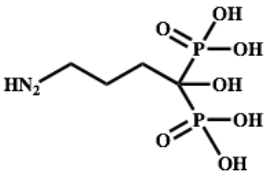

Alendronate (ALN)

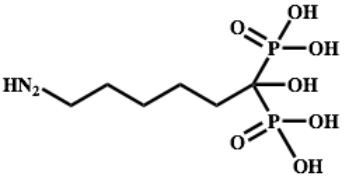

Neridronate (NER)

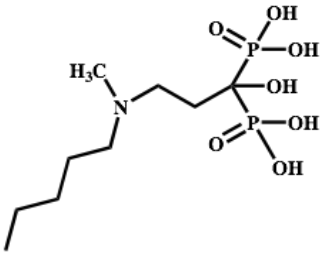

Ibandronate (IBN)

Heterocyclic N-BPs

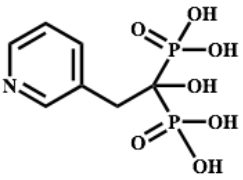

Risedronate (RIS)

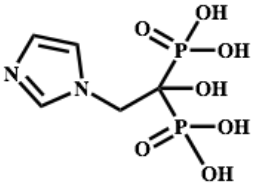

Zoledronate (ZOL)

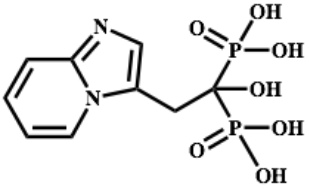

Minodronate (MIN)

Figure 18 Chemical structures of the major clinically relevant BPs used in this study.

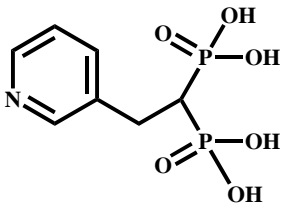

Deoxy-risedronate
(Deoxy-RIS)

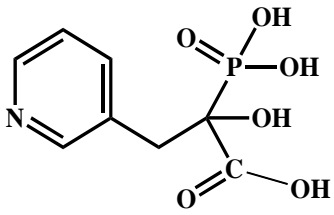

Phosphonocarboxylate-
risedronate
(RIS-PC)

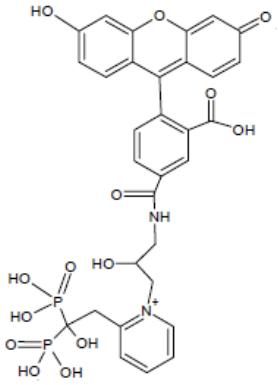

5(6)-
carboxylfluorescein-
risedronate
(5(6)-FAMRIS)

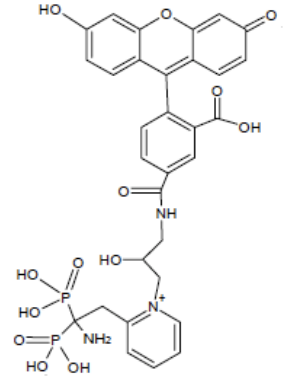

5(6)-
carboxylfluorescein-
amino-risedronate
(5(6)-FAM-amino-RIS)

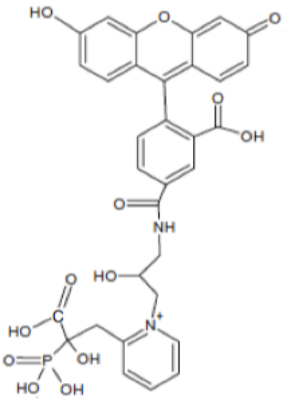

5(6)-
carboxylfluorescein-
phosphonocarboxylate
-risedronate
(FAM-RisPC)

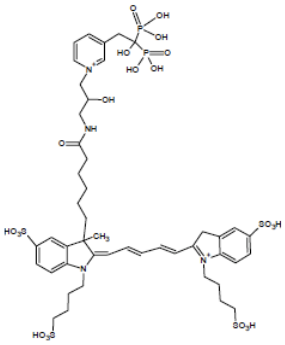

Alexa fluor 647-
risedronate
(AF647-RIS)

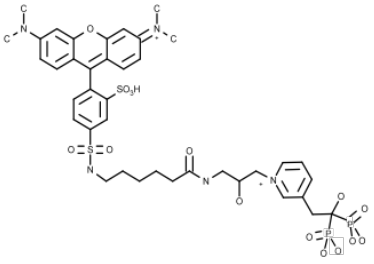

Rhodamine-risedronate
(Rho-RIS)

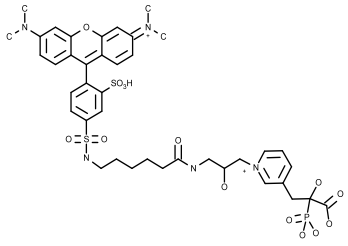

Rhodamine-
phosphonocarboxylate
-risedronate
(Rho-RISPC)

Figure 19 Structures of bisphosphonate analogues used in this study.

2.2 General mass spectrometry (MS) method for detection and quantification of bisphosphonates

2.2.1 Materials and chemicals

The MS analyses for detection and quantification of BPs from hydroxyapatite column chromatography and Langmuir adsorption isotherm studies were developed and conducted by our collaborators (Dr. Roy Dobson and Mr. Mike Quijano) at Procter & Gamble Pharmaceuticals (OH, USA). I spent two weeks in this laboratory to observe and assist the methodology. The BPs specified in section 2.1 were all provided by Dr. F. H. Ebetino at Procter & Gamble and used for quantification by MS. The stable-isotope-labelled internal standard used in the quantitative High-performance liquid chromatography (HPLC)/MS/MS method ($^{2}H_{4}$-risedronate) could not be obtained commercially and was synthesised at Procter & Gamble. Purity was determined to be > 99%.

HPLC-grade acetonitrile was obtained from EMD Scientific and ultra pure water was prepared by a Milli-Q purification system (Millipore Corp., Bedford, MA). All other chemicals (dimethylhexylamine, isopropanol, formic acid, and ammonium formate) utilised in the analytical procedures were obtained from Sigma-Aldrich (Milwaukee, WI) and were reagent grade or better.

2.2.2 Quantification of bisphosphonates by ion-pairing, reverse-phase HPLC/MS/MS

Quantification of targeted BPs was accomplished using a separation on a reverse phase HPLC column by utilising a 10ADVp pumping system (Shimadzu, Columbia, MD), LEAP HTS-PAL autosampler (Carrboro, NC), interfaced to a Sciex API5000 triple quadrupole mass spectrometer (AB Sciex, Foster City, CA), operated in the negative ion mode and employing selected reaction monitoring (SRM), for selective detection of each compound of interest (Figure 20). Separation was carried out using ion-pairing (dimethylhexylamine) reverse phase chromatography employing a rapid/linear gradient over a total time of 6 minutes. HPLC and instrument conditions are detailed below in Table 1.

Table 1 Details of the reverse phase HPLC experimental protocol for BP quantification.

(a): Chromatographic column and elution characteristics

Column	Phenomenex Synergi Max-RP, 2.1 x 50 mm, 5 µm
HPLC Column Temperature	Room Temperature
Mobile Phase A	2/98 acetonitrile/water, 10 mM ammonium formate, 10 mM dimethylhexylamine, 0.4% formic acid
Mobile Phase B	80/20 acetonitrile/water, 10 mM ammonium formate, 10 mM dimethylhexylamine, 0.4% formic acid
Flow Rate	0.85 ml/min
Injection Volume	20 µl (30 µl into a 20 µl loop)

(b) Elution gradient conditions

Time	MP A (%)	MP B %B
0.0–2.0	99	1
4.0	15	85
4.0–5.0	15	85
5.1–6.0	99	1

(c) Mass spectrometry conditions

Ionisation Mode	Turbo–Ion Spray
Polarity	Negative
ISV (Ion Spray voltage)	3500 V
TEM (Source Temp.)	650 °C
G1 (Nebulizer Gas)	70 units (nitrogen)
G2 (Turbo Gas)	70 units (nitrogen)
CG (Curtain Gas)	30 units (nitrogen)
CAD (Collision Gas)	12 units (nitrogen)
Scan Mode	Multiple reaction monitoring (MRM) (one SRM per bisphosphonate and IS)
Dwell Time	80 ms (per SRM transition monitored)

*Settings are typical, and were adjusted as necessary to optimise responses.

(d) MS/MS parameters: Bisphosphonate monitoring and detection schemes

	Individual SRM Detection Schemes			
Compound	Parent Ion (m/z)	Product Ion (m/z)	Declustering Potential* (V)	Collision Energy (eV)
Risedronate	282	200	-40	-24
$^{2}H_{4}$-risedronate (IS)	286	204	-40	-24
Etidronate	205	123	-45	-22
Pamidronate	234	152	-45	-26
Clodronate	243	143	-40	-25
Minodronate	321	239	-45	-26
Zoledronate	271	189	-35	-28
Alendronate	248	166	-40	-22
Ibandronate	318	236	-50	-28
Neridronate	276	194	-50	-26

* Declustering Potential: is an added acceleration voltage that is applied to electrospray-formed ions in the mass spectrometer source. It declusters and strips adducted solvent molecules away from analyte molecules to deliver a much higher proportion of simple M-H species into the vacuum system, and thus, to the first mass analyser.

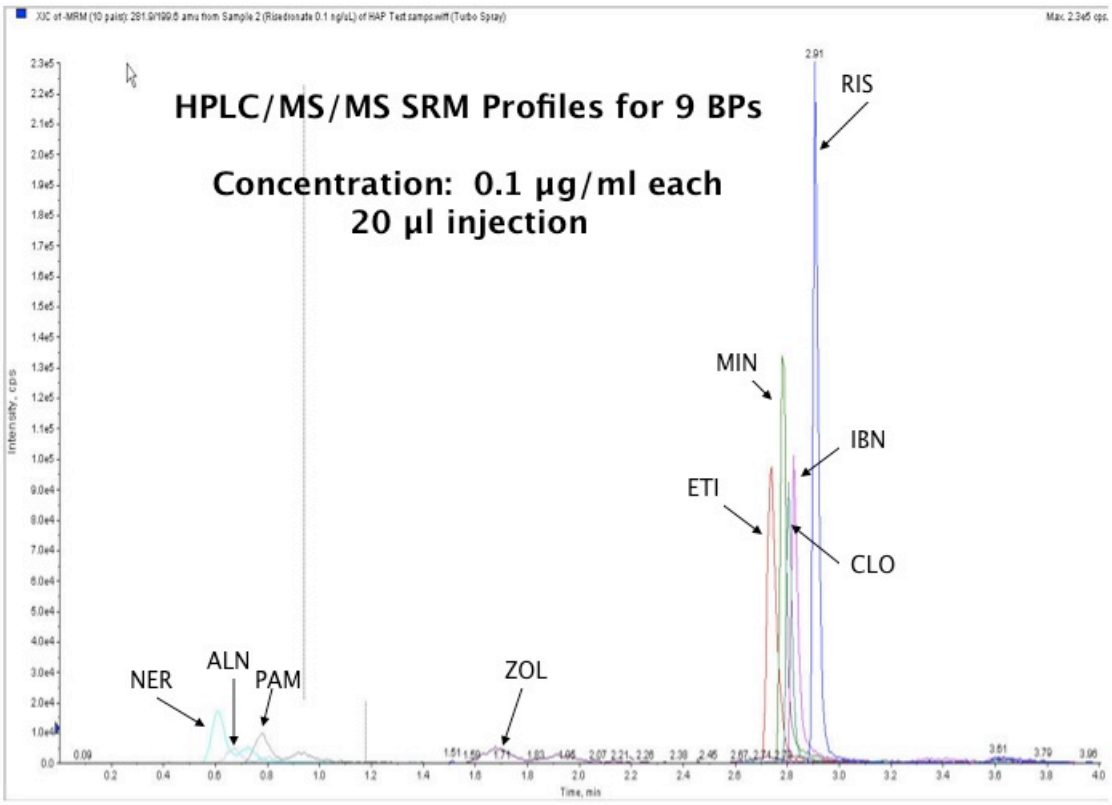

Figure 20 HPLC/MS/MS SRM profiles for 9 BPs.

The SRM profile is from analysis of equal amounts of 9 different BPs. It demonstrates the ability to selectively detect each of these BPs, based on retention time and based on their unique SRMs. It also underscores that each molecular entity has a quite different intrinsic detectability/sensitivity under the collective set of HPLC/MS/MS conditions employed.

2.3 Hydroxyapatite/fluoroapatite column chromatography

2.3.1 Buffer preparation

Running buffers were prepared with 1 mM potassium phosphate (Buffer A) and 1 M potassium phosphate (Buffer C) at either pH 7.4 or 6.8. In the case of the low pH study (i.e., pH 5.7), 25 mM 4-Morpholine ethanesulfonic acid (Mes; Sigma, Dorset, UK) was added to the running buffers (A and C) to maintain the desired pH. Potassium phosphate was

treated in this case as an additive that promotes the elution of the BPs, rather than as a buffer to maintain the pH. All buffers were filtered through a Sartorius® disposable filter units (0.2 µm) (Sartorius, Epsom, UK) and degassed before use.

2.3.2 Equipment and chromatographic conditions

The fast performance liquid chromatography (FPLC) system consisted of a Waters 650E advanced protein purification system (Millipore Corp., Waters chromatography division, Milford, MA), a 600E system controller and a 484 tunable absorbance detector for UV absorbance assessment (Figure 21). Hydroxyapatite [HAP, $Ca_{10}(PO_4)_6(OH)_2$] / fluoroapatite [FAP, $Ca_{10}(PO_4)_6F_2$] was packed in a 0.66 cm (diameter) x 6.5 cm (length) glass column (Omnifit, Bio-chem valve™ inc., Cambridge, U.K.). The column was attached to the Waters 650E advanced protein purification system and equilibrated in the required Buffer A at pH 7.4, pH 6.8 or pH 5.7. Each compound was prepared in 1 mM potassium phosphate buffer at the corresponding pH, and 1 µmol bisphosphonate was injected into the FPLC system. It was calculated that the total binding capacity of the HAP column was much greater than the total BP concentration injected into the column. As a consequence, BP compounds were absorbed and subsequently eluted by using a linear concentration gradient of phosphate from 1 to 1000 mM. The total run lasted 24 min (pH 7.4 and 6.8) or 48 min (pH 5.7) at a flow rate of 2 ml/min. The individual BPs

emerged as discrete peaks either detected by ultraviolet (UV) absorbance at their optimum wavelength (260 nm for risedronate, 220 nm for zoledronate and 287 nm for minodronate) that was recorded on a chart recorder (Vitatron, Figure 21) or their fractions were collected by using an automated fraction collector (Gilson, France, Figure 21) for subsequent mass spectrometric analysis. The HAP elution profile of each compound was determined in triplicate for statistical analysis (Prism, GraphPad Software, USA).

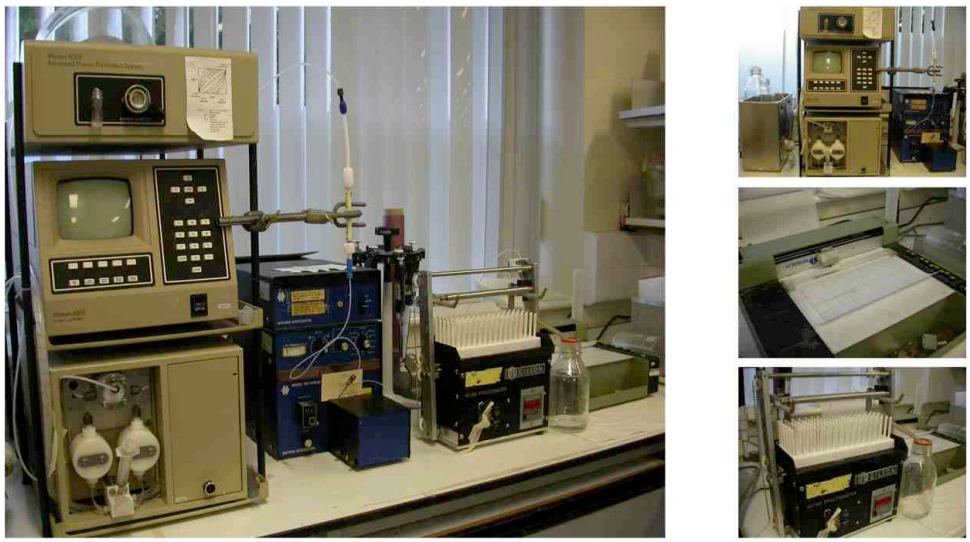

Figure 21 The FPLC system used in the BP HAP/FAP column chromatography study.

Overview of the FPLC equipment set-up (left), FPLC system (upper right), chart recorder (middle right) and fraction collector (lower right).

2.3.3 Mass spectrometry analysis

Preparation of standard solution

All BP standards were accurately weighed into separate plastic vials and diluted to a concentration of 3.0 mg/ml with water. To create the N-in-1

standard solution, an equal volume of each BP was transferred to single plastic vial to achieve a concentration of 10 mM. This sample was then serially diluted 30X for analysis.

Internal standard (IS) solution

The $^{2}H_{4}$-risedronate standard was accurately weighed into a separate plastic vial and diluted with water to a concentration of 1.0 mg/ml. An appropriate aliquot of this solution was transferred to a plastic vial and serially diluted with water to a concentration of 0.10 µg/ml. The total volume of this solution could be adjusted to match the size of the batch run.

HAP sample preparation

Each HAP fractionation study consisted of three separate chromatographic runs, with 80 fractions of 0.3 ml each being collected. A 10 µl aliquot of each sample was diluted with 240 µl of IS solution, vortexed, then analysed. The respective individual diluted standard solution was analysed at the beginning and end of the batch to indicate instrument stability and responsiveness.

Analysis of HPLC/MS/MS data

The overall objective of the MS analysis is to develop a method that has adequate sensitivity to at least reliably detect each BP. Analysis and

reduction of the data were carried out by using the quantitation program within the Analyst software package (version 1.4.2; Applied Biosystems / Sciex mass spectrometry instrumentation, Foster City, CA). The Analyst software package was used to: 1) set up the details of instrument settings for both the mass spectrometer (including detection schemes for each of the analytes), and the HPLC and Autosampler; 2) create a sample list for the batch analysis to be carried out; 3) initiate and carry out the analyses; and 4) provide the tools to do data reduction, including internal standard and analyte MRM peak integration. HPLC/SRM peak integrations were carried out for all BPs and internal standards for each sample. The peak areas derived from peak integration were then used for the subsequent data manipulations. The results were normalised, smoothed, and baseline corrected by using macros, to create a reconstructed HAP chromatogram per BP, for each HAP chromatographic run. The macros are spreadsheet calculations that make calculations of sets of data much more convenient. For example: the normalisation process recognises the highest detection signals for each set of BP data and normalises them to be 1.00, with the other signals being calculated proportional to this. The smoothing process involves using a smoothing algorithm to smooth out the noise in the detection for each BP and the baseline correcting process corrects for a background signal that is present in the analyte detection channel.

This chromatographic spectrum was a representation of all the data points from a study, which provided an indication of reproducibility, when derived over the short period required for triplicate HAP separations. Mean (N=3) reconstructed HAP chromatograms for all nine BPs provided a clear view of relative temporal profiles. The smoothed normalised area ratios have no units and were derived from taking peak area for a BP and dividing it by peak area for internal standard. The mean of smoothed normalised area ratios was calculated from taking the corresponding time point values from the three replicate profiles for each BP. These mean values then represent the y-axis entry that is plotted versus time and these plots were used to calculate the T_{MAX} (peak retention time) and $T_{0.5MAX}$ (retention time at half peak retention time) values. Quantitative comparisons of relative retention were derived from T_{MAX} calculations for all the studies except the BP N-in-1 studies when $T_{0.5MAX}$ calculations were used. The latter was considered to be a more accurate reflection of the elution profiles of the BPs as calculated by using MS. This is because in the HAP chromatography, BP peaks all at least tail, for some BPs (e.g., pamidronate, etidronate, in most cases) a major portion of the loaded material does not elute within the allotted run time, and occasionally a given BP doesn't form a real peak so it can be difficult to assign an appropriate T_{MAX} value at all. On the other hand, a clear $T_{0.5MAX}$ value can be distilled from almost all forms of the BP elution profiles. Using risedronate as a retention time control/comparator, each of the BP

profiles were normalised to risedronate to diminish concerns related to the comparability of the data generated in different chromatographic runs over time.

2.4 Bisphosphonate binding assays

2.4.1 Langmuir adsorption isotherms

To quantitatively measure the interactions between BPs and HAP surfaces, adsorption isotherms of risedronate, ibandronate, pamidronate, clodronate and 5(6)-FAMRIS were carried out by using *in vitro* HAP binding methods described in previous publications [126-128]. All BPs were incubated individually in general. In addition, a 2-in-1 combination for risedronate and ibandronate was included. In general, accurately weighed samples of HAP powder (5.6-6.7 mg) were suspended in a 2 ml clear glass vials containing the appropriate volume of 1 mM PBS with 0.15 M NaCl (pH 7.4) to give a constant solid/solution ratio. The NaCl was used to provide an ionic strength close to physiological conditions. These vials were equilibrated end-over-end on a rotary shaker at room temperature for 3 hours. After premixing, BP stock solutions (or a mixture of equimolar concentrations of risedronate and ibandronate in the case of 2-in-1 study) were added resulting in concentrations of the BP additives ranging from 12.5 to 300 μM (RIS, IBN, RIS and IBN 2-in-1) or 400 μM (PAM, CLO, 5(6)-FAMRIS). Controls were prepared identically

to the samples except that no BP stock solution was added. Each sample was prepared in triplicate. Equilibration with the HAP solution was performed at room temperature for 16 hours. This time period was sufficient for equilibration as determined from preliminary experiments. Subsequent to the equilibration period, the vials were centrifuged at 10,000 rpm for 5 min to separate the solids and the supernatant. The supernatant was carefully collected and used for the corresponding analysis. For example, the equilibrium concentration of alkyl-amino BP containing primary $-NH_2$ side chain, (i.e., pamidronate) was determined spectrophotometrically by the o-phthaldialdehyde (OPA) method (see appendix for details) by using a SPECTRAmax® GEMINI XS Dual-Scanning microplate spectrofluorometer (Molecular Devices Corporation, CA) with an excitation wavelength of 340 nm and an emission wavelength of 455 nm. The amount of 5(6)-FAMRIS not bound to HAP was also quantified with the same device (excitation: 493 nm, emission: 518 nm). Fluorescence intensity was read as relative fluorescent units (RFU) by Softmax® PRO Version 4.0 Software (Molecular Devices Corporation, CA) and later analysed by Microsoft Excel. Mass spectrometry was used to measure risedronate, ibandronate and clodronate (see 2.4.3 for detail).

For the calibration series, BP standards were prepared by serial dilution from the stock solution with the same isotherm buffer to give the range from 0 to 800 μM. Calibration curves were constructed using standard

solutions of the target BP. The adsorbed amounts of BPs (μmol/m^2) were calculated by comparing the end point concentration of BP detected after equilibrium to the initial BP additive concentration (μM) using the following equation:

BP HAP average surface concentration = (Initial BP concentration – end point concentration) / HAP total surface area of the sample

The HAP surface area of the sample was 10.63 m^2/g (density: 0.63 g/ml) (Biorad Laboratories, Inc. Hercules, CA, USA). A plot of BP HAP surface concentration versus BP end point concentration gives the adsorption isotherm.

To describe the equilibrium binding of BP to HAP as a function of increasing BP concentration, the experimental data were fitted to a saturation binding equation:

Y (specific binding) = Bmax * X/(Kd +X)

By using a non-linear curve-fitting algorithm, implemented in the Prism program (Graphpad, USA).

Where X is the concentration of the BP. Y is the specific binding.

Bmax is the maximum number of binding sites, expressed in the same units as the Y-axis.

Kd is the equilibrium dissociation constant, expressed in the same units as the X-axis (concentration). When the drug concentration equals Kd, half the binding sites are occupied at equilibrium.

2.4.2 Competitive binding assays

Competitive binding experiments measure the binding of a single concentration of a fluorescently labelled BP (FL-BP) in the presence of various concentrations of unlabelled BP. They were used to compare the relative mineral affinities of different BPs. In brief, 5(6)-FAMRIS was mixed with specified concentrations of unlabelled BP before adding onto 4 ml clear vials containing accurately weighted amounts (1.4-1.6 mg) of HAP, previously equilibrated with the same buffer, to initiate each reaction. The resulting concentration for 5(6)-FAMRIS used was 3 μM and competitor BP additives ranged from 3 μM to 1000 μM, as noted in the figure legends in Chapter 4. Equilibration with the HAP solution and detection of 5(6)-FAMRIS in the supernatant after separating the solids and the supernatant were performed as described in 2.4.1.

For the calibration series, 5(6)-FAMRIS standards were prepared by serial dilution from the stock solution with 1 mM PBS with 0.15 M NaCl (pH 7.4)

to construct calibration curves within the range from 0 to 5 μM. The amount of 5(6)-FAMRIS binding was assessed as mean of three independent experiments according to the following formula:

Specific binding of 5(6)-FAMRIS (%) = (X – Y) / X * 100%

Where X is the initial amount of BP fluorescence corrected for the degree of dilution and Y is the amount of BP fluorescence in the supernatant corrected for the degree of dilution.

To determine the equilibrium dissociation constant (Ki) of an unlabelled BP, its competition for FL-BP binding was analysed with a competition binding equation (One site – Fit Ki) using the Prism program. The One site – Fit Ki equation assumes one type of ligand binding site, one concentration of labelled-ligand (FL-BP) and multiple concentrations of unlabelled-ligand (BP).

Model:

logEC50=log(10^logKi*(1+FL-BPNM/FL-BPKdNM))

Y=Bottom + (Top-Bottom)/(1+10^(X-LogEC50))

Where FL-BPNM is the concentration of FL-BP in nM. A single concentration (3 μM) of FL-BP is used for the entire experiment.

FL-BPKdNM is the equilibrium dissociation constant of the FL-BP in nM.

Top and Bottom are plateaus in the units of Y axis. The Top is a plateau at a value equal to 5(6)-FAMRIS binding in the absence of the competing unlabelled BP, which is defined by a control measurement to be 99.83. The Bottom should be near the binding observed in the presence of a maximal concentration of competitor. In theory, the competitor BP and FL-BP interact with HAP in a similar way. Assuming the binding is completely exchangeable, the specific binding should approach zero concentration of the FL-BP at high concentration of the competitor BP. In addition, all BPs that bind to the same receptor site should compete all specific FL-BP binding and reach the same bottom plateau value. Therefore, the dissociation constant (Ki) of the unlabelled BP at half specific binding maybe more accurately determined when the bottom is fixed to a constant value of zero than by using experimental high concentration of competitor used in these studies.

logKi is the log of the molar equilibrium dissociation constant of unlabeled BP.

Ki is the equilibrium dissociation constant in mol/L.

2.4.3 Mass spectrometry analysis

HAP adsorption isotherm experiments

An adsorption isotherm study consisted of three runs, per BP, and a concentration range from 12.5-300 μM or 12.5-400 μM. BPs were incubated either as single compounds or as 2-in-1 combinations. BP

standards were also prepared with the samples at the same concentration range and these, were used to calibrate the spectrometric analysis.

Internal standard solution

The $^{2}H_{4}$-risedronate standard was prepared in the same manner as described in 2.3.3.

Isotherm sample preparation

Since the sample BP concentrations ranged from either 12.5-300 µmol or 12.5-400 µmol, the dilution factor necessary for these samples ran between 25-1000X. Briefly, a 20 µl aliquot of each sample was diluted with IS solution and water, then vortexed. Samples were then diluted further with water to the appropriate range (to assure alignment of BP concentration was within the linear-response range of the HPLC/MS/MS system).

Analysis of the HPLC/MS/MS data

Analysis and reduction of the data were carried out using the quantitation program within the Analyst software package. HPLC/SRM peak integrations were carried out for all BPs and the internal standard (used to compensate for any potential instrument variability) for each sample. Peak area ratios (BP-to-internal standard) were then determined. Quantitation was achieved using single-point (single concentration)

calibration. This single-point calibration approach was used for the following reasons: 1) the aim was to measure relative depletion (due to adsorption onto the HAP) at known nominal concentrations and sometimes the differences between nominal concentrations and concentrations within the HAP supernatant environment were small, 2) the MS response is not perfectly linear over a wide concentration range. Therefore, a single-point value that was most relevant to the measurement being made as the reference point for each depletion measurement was used. Given that the intended measure, it was to determine the relative loss from a set concentration value at each concentration level. Then, a standard solution representing the prepared concentration value (single-point calibration) was analysed by calculating the analyte-to-internal standard peak areas. The test sample was analysed the same way and its concentration was determined by comparing the area ratios of the test sample versus the mean of the standard (N=2), which was analysed before and after each concentration group. Test sample concentrations were then transferred to Microsoft Excel using macros to calculate the isotherm curves as described in 2.4.1.

2.5 Cell culture

2.5.1 Cell culture

The murine long bone-derived osteocytic cell line MLO-Y4 was supplied by Dr. Lynda Bonewald (University of Missouri-Kansas City). Cells were grown on collagen I coated plates (Biocoat) or glass coverslips in alpha Modified Minimum Essential Medium (α MEM) supplemented with 5% Fetal Calf Serum (FCS) and 1% penicillin/streptomycin. The murine osteoblastic 2T3 cells obtained from Dr. Lynda Bonewald were cultured in αMEM with 7% FBS and 1% penicillin/streptomycin on 10 cm^2 petri dishes at 37°C in 5% CO_2. Cells were cultured until 70%-80% confluent, before passage for experimental use.

2.5.2 Nick translation assay

Murine osteocytic MLO-Y4 cells and osteoblastic 2T3 cells in normal growth medium were pre-treated with a nitrogen-containing heterocyclic BP, risedronate and a non-nitrogen BP, etidronate, at concentrations of 10^{-8} to 10^{-6} M for 1 hour, prior to the addition of etoposide (50 μM), which is a commonly used apoptosis inducer. All pre-treatment agents were maintained in cultures in the presence of etoposide. After 24 hours, cells were fixed in 4% paraformaldehyde, for Nick Translation assay (NT assay) and for staining.

The NT assay was applied to quantify the extent of MLO-Y4 and 2T3 cell apoptosis. Flow cytometry was performed on a FACSCalibur flow cytometer (BD Biosciences, Oxford, UK) and data were analysed using CellQuest Pro software (BD Biosciences).

2.5.3 TUNEL staining

Terminal deoxynucleotidyl transferase-mediated biotin-dUTP nick end labelling (TUNEL) is a method for detecting DNA fragmentation by labelling the terminal end of nucleic acids. It is a common method for identifying cells in the last phase of apoptosis [126]. In this study, TUNEL staining was performed to detect the presence of apoptotic MLO-Y4 cells; counterstaining was done with DAPI (4', 6-diamidino-2-phenylindole). Multiple images were captured across the surface of the cover slips. TUNEL-positive staining and cells characterised by condensed and irregular nucleus, two or more nuclear fragments, or blebbing were counted as apoptotic cells.

TUNEL staining was achieved by applying the Roche POD In Situ Death Detection kit (Penzberg, Germany). The stain was visualised using DAB substrate. Coverslips were counterstained with DAPI nuclear stain and mounted on glass slides with FluorSave Reagent (CalBiochem, San Diego, California).

2.5.4 Western blotting

To evaluate activation of the ERK pathway, MLO-Y4 cells and 2T3 cells were serum starved in 1% Fetal Calf Serum overnight before treatment with risedronate at 10^{-8} M, or 20% FCS as positive control. Following a 5, 30 or 60 minute incubation, the cells were harvested and the cell lysates were used for Western blots.

For Western blotting, samples with equal amount of protein were resolved by sodium dodecyl sulfate-polyacrylamide gel electrophoresis (SDS-PAGE) in a 10% bisacrylamide SDS gel, and then transferred to a polyvinylidene difluoride (PVDF) membrane (Amersham, UK). Prestained molecular weight markers were used. Antibodies to phospho-ERK1/2 (1:1000 dilution) and ERK1/2 (1:20,000 dilution) (Cell Signaling Technology, Beverly, Massachusetts) were used and incubated with goat anti-rabbit horseradish peroxidase-conjugated secondary antibody (1:50,000 dilution). The enhanced chemiluminescence detection system was employed to visualise immunoreactive proteins by use of Supersignal West Dura kit (Thermo Scientific, Rockford, IL). Intensity of the bands was quantitated using Image J software (NIH).

2.6 Data analysis

Langmuir adsorption isotherms and competitive binding assays were performed three times for each compound tested. Data are presented as mean ± standard deviation (SD). Scatchard plot and Kd determination of the Langmuir adsorption isotherm data and competitive binding curves were performed using the GraphPad Prism software program (GraphPad software, Inc., San Diego, USA).

Statistical analyses were conducted using Prism. Significant differences between treatment groups were determined by Student's t test (for two means), one-way analysis of variance (ANOVA) (for FPLC studies) or one-way ANOVA followed by Dunnett's Multiple Comparison Test (for cell culture studies). All data are presented as means ± SD unless stated otherwise. Significance was assumed at $p<0.05$.

CHAPTER 3 EVALUATION OF THE RELATIVE MINERAL-BINDING AFFINITIES OF BISPHOSPHONATES BY USING COLUMN CHROMATOGRAPHY

3.1 Introduction

Mineral-binding affinities of BPs are of crucial biological importance since they can influence a number of important activities of the drug, including their uptake and retention by the skeleton, their differential distributions within bone and diffusion through the osteocyte network, the release and potential recycling of the drug and their cellular functions within bone [69, 70]. The mineral-binding affinity may also affect the appropriate dosing interval and the persistence of effect after discontinuation of medication when BPs are used clinically to treat disorders of bone resorption [41, 123].

Over many years, different strategies have been adopted by a variety of investigators to reveal the binding affinities of BPs but with contradictory conclusions [61]. For instance, a constant composition potentiostatic method was conducted by Nancollas *et al*. to study the kinetic mineral-binding affinities of BPs. It was suggested that significant differences exist between compounds with a rank order of binding with clodronate < etidronate < risedronate < ibandronate < alendronate < pamidronate < zoledronate at pH 7.4, these differences are thought to be due to the structural differences in the side-chains [127]. The same rank order was also shown in a carbonated apatite (CAP) affinity study, except that the differences between individual BPs were larger than for HAP affinity at the

same pH [128]. Most recently, a nuclear magnetic resonance (NMR)-based *in vitro* assay to measure binding affinities of small molecules to HAP or bone powder was reported. Using a competition assay, binding affinities of BPs for HAP were ranked as ibandronate < risedronate < zoledronate < alendronate < pamidronate [129]. In addition, a novel approach using HAP column chromatography has been developed by previous researchers in our group, which demonstrated that there were significant differences in the HAP binding affinities of different BPs [69, 130]. These studies indicate that individual BPs differ substantially in their binding affinities for HAP and bone mineral and that the P-C-P moiety, the R1-OH group and the R2 side chain contribute to this binding [13, 14]. In contrast, a radioactive competition assay using ^{14}C-alendronate with powdered bone found that although clodronate exhibited a weaker affinity than most tested BPs, structural differences in BPs with R1-OH groups may have little effect on binding to human bone [131]. These findings are in line with work using mouse bone explants investigated by a similar radioactive tracer method [67].

Therefore, it is highly desirable to develop a robust and generally applicable method to assess the binding affinities of BPs, especially newer generation N-BPs that are being developed. For this purpose, we have conducted a series of studies to comprehensively compare the mineral-binding affinities of BPs in, and intended for, clinical use (Figure 18), and

selected analogues (Figure 19), using a variety of complementary techniques. In this chapter, the focus is on the approach of using ceramic hydroxyapatite or fluoroapatite fast performance liquid chromatography combined with mass spectrometric identification and quantitation of BPs.

Hydroxyapatite as a chromatographic medium column has been used extensively in both analytical and biological systems for separations of proteins and other heterogeneous biological substances for several decades [10, 132, 133]. Due to its similarity to bone mineral, in the studies presented here, synthetic HAP chromatography was applied to mimic the interaction between BPs and bone mineral HAP *in vivo*. HAP contains multiple adsorption sites that are involved in the adsorption-desorption process, namely C-sites that consist of pairs of positively charged calcium ions, and P-sites that are clusters of negatively charged phosphate groups [132, 133]. In the case of BPs, it can be deduced that the phosphonate groups on the molecular surface can adsorb onto C sites, presumably due to chelating interactions with the calcium ions in the apatite structure. On the other hand, phosphate ions from the phosphate buffer are also adsorbable onto C sites whereas potassium or sodium ions from the same buffer can be adsorbed only onto P sites. In the process of chromatography, especially with gradient elution using potassium or sodium phosphate buffer at pH $\approx$ 6.8, competition occurs between BPs and phosphate ions for adsorption onto C crystal sites. As a

result, the BP molecules initially adsorbed at the top of the column are driven out of the crystal surface. Due to different affinities of BPs for HAP, the time taken for the BP to elute from the HAP column varies, which can in turn reflects its affinity [133-135].

Previously, the feasibility of this approach has been demonstrated by measuring the differential binding affinities on crystalline HAP columns of several BPs and other biologically relevant phosphate-containing compounds with detection by using UV spectrometry [130]. Nevertheless, there are certain drawbacks with using this approach that restrict its broad application: 1) the crystalline form of HAP is fragile as a column packing material, therefore columns cannot be reused and have to be freshly prepared for each cycle of experiment, 2) the low detection limit of UV spectroscopy, and since most BPs either lack or have weak UV chromophores, a UV detector cannot be used in such cases, and 3) crystalline HAP does not have defined particle size and surface areas, therefore the variable crystal shape and sizes affect the performance of HAP and data generated over time may thus vary. Based on the facts above, in this study, a rapid method was developed for separation and quantitation of both low and high binding BPs by mixing an array of BPs in one run as a N-in-1 (N>1) approach rather than individually (N=1) by using chromatography on ceramic HAP columns combined with mass spectrometry. The recently available ceramic HAP is a spherical,

macroporous form of HAP, which overcomes many of the limitations of crystalline HAP, yet retains the separation properties of crystalline HAP [136] (Figure 22). The ceramic HAP is vastly superior to crystalline material, for example, it is of consistent particle size and extremely stable, both chemically and physically [137]. It can be packed into large columns and used at high flow rates for hundreds of cycles with no change in either separation or operating pressure [138-140] (Table 2). Furthermore, mass spectrometry is a highly specific method for determining or confirming identity or structure of chemicals of drugs. The combination of FPLC with MS should provide an accurate, precise and robust method for quantitative analysis of BPs.

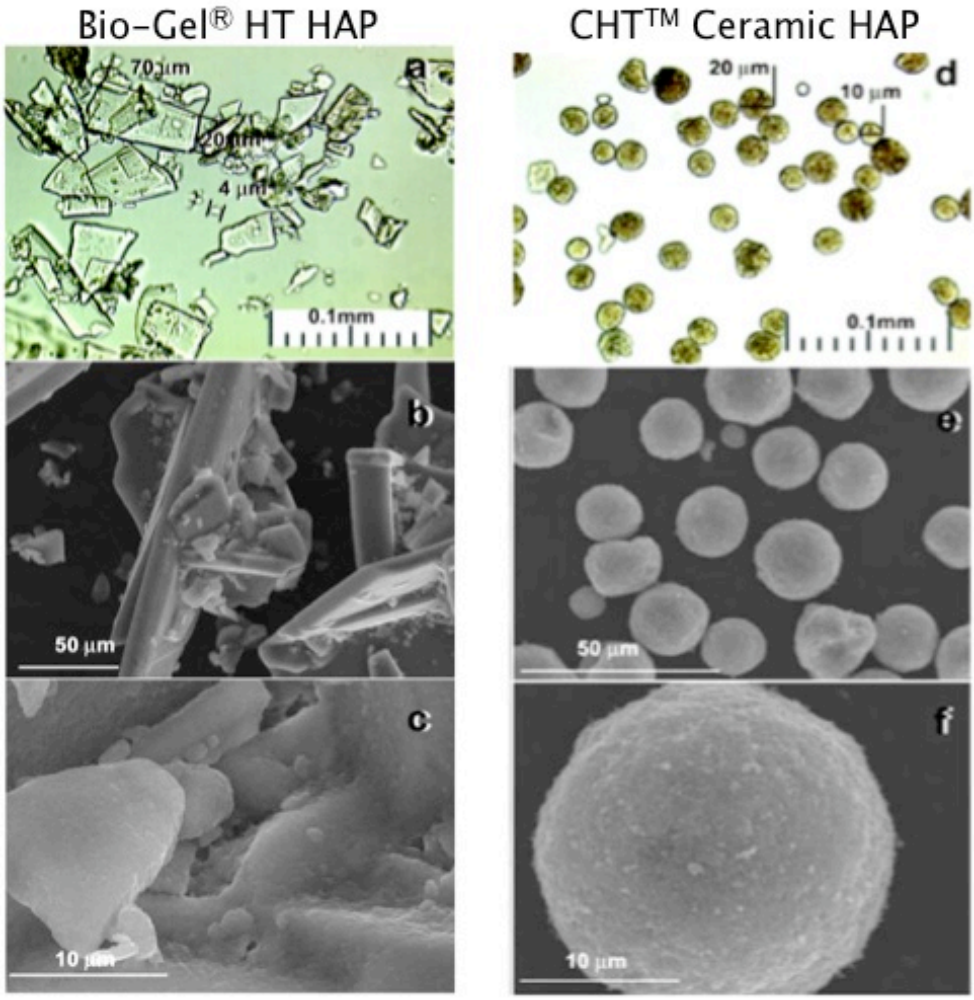

Figure 22 Comparison of the Bio-Gel® HT crystalline HAP particles and the CHT™ macroporous ceramic HAP particles.

Table 2 Comparison of the crystalline HAP column and the ceramic HAP column.

	Crystalline HAP column	Ceramic HAP column
Reproducible and reliable	Yes	Yes
Easy to pack and operate	Yes	Yes
Flow rate	Low	High
Operating pressure	Low	High
Reuse of the column	No	Yes
Defined particle size and surface areas	No	Yes
Conclusion	Inefficient compared with ceramic	Highly efficient rapid throughput

BPs have high affinity for calcium ions, as a result, they localise to bone mineral, particularly at sites of bone resorption [138]. It has been well described that resorbing osteoclasts on bone are capable of generating an acidic microenvironment with a mean pH of 6.0 and a lower limit of 4.7 [12, 13]. It is believed that the acidic pH of the resorption lacuna protonates the phosphonate groups of previously adsorbed BPs and hence facilitates their release from the acidified bone surfaces into solution [138]. Thus, in addition to evaluating the mineral-binding affinities of BPs under physiological conditions, the function of pH was studied to compare the potential affinity differences of BPs that may be exhibited at bone resorption sites.

In this study, experiments were conducted at pH values 7.4, 6.8 and 5.7, respectively. As hydroxyapatite is unstable at low pH [133], ceramic fluoroapatite ($Ca_{10}(PO_4)_6F_2$) was employed at the more acidic chromatography conditions. FAP is a ceramic apatite with similar separation characteristics to ceramic HAP, but is stable even at pH 5 [135]. In addition, phosphate buffer is a weak buffer outside the pH range of 6.0 to 7.5 [139], and to study the mineral affinities of BPs at pH 5.7, a second buffer system that broadens the pH range of HAP separation while maintaining a properly buffered environment was introduced [139]. For this purpose, mixed buffer of potassium phosphate combined with Mes (4-Morpholine ethanesulfonic acid) was used, where the potassium

phosphate was treated as an additive that promotes the elution of BP, rather than as a buffer that maintains the pH [139].

3.2 Results

3.2.1 Comparison of retention times of BPs and selected analogues on ceramic HAP at pH 6.8

Comparison of risedronate and selected risedronate analogues on ceramic HAP at pH 6.8

Previous studies have shown that the phosphonocarboxylate analogues of BPs were able to inhibit bone resorption to some extent, yet, their retention times on crystalline HAP column were significant lower than their BP counterparts. In addition, BPs with the R1-OH group have been shown to have enhanced chemisorption to HAP [69].

To explore the observation further by the means of ceramic HAP column chromatography, peak retention times (T_{MAX}) of RIS, RIS-PC (phosphonocarboxylate analogue of risedronate) and deoxy-RIS (analogue of risedronate without the R1-OH group) (Figure 19) were compared. As expected, the data indicate that both RIS-PC and deoxy-RIS show statistically reduced retention times compared to RIS ($P<0.001$) (Figure 23), suggesting that both phosphonate groups and the R1-OH group are of major importance for the high affinity of BPs to HAP.

Notably, RIS-PC has the lowest retention time on the column, indicating that the phosphonate groups are playing a dominant role in HAP binding, however, the R1-OH group is also clearly playing a direct role in binding, since its absence resulted in a significant loss of retention on the HAP column, presumably owing to the bidentate rather than tridentate binding of deoxy-BPs to Ca^{2+} in HAP.

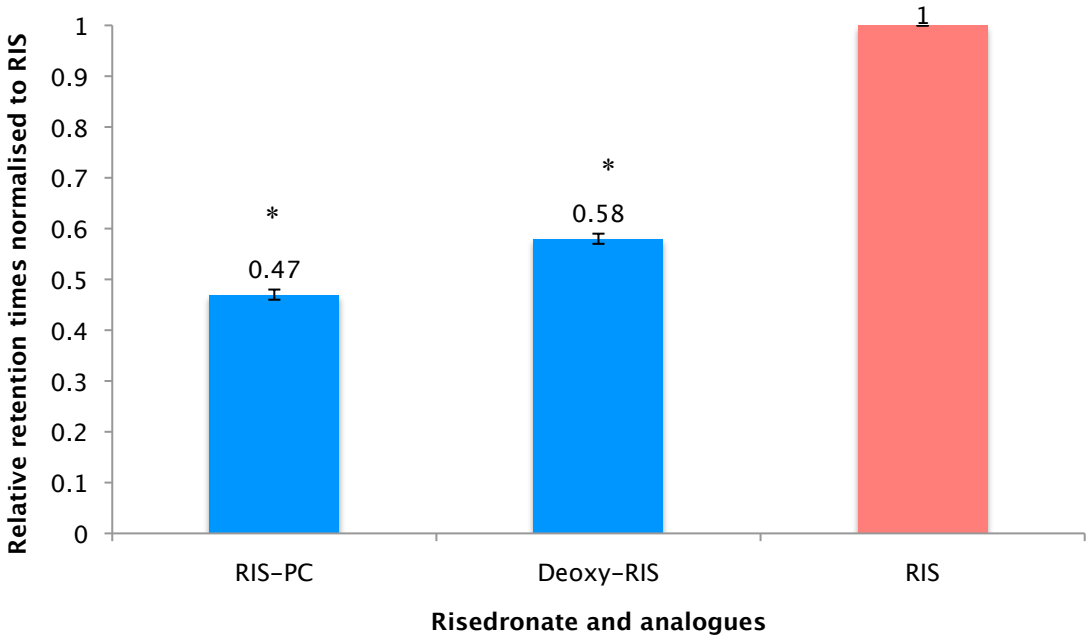

Figure 23 Comparison of the peak retention times of RIS-PC, deoxy-RIS and RIS at pH 6.8 on HAP columns.

Data are shown as means ± SD from three individual studies shown as relative retention times normalised to RIS. *Significantly different from parent compound RIS ($p<0.001$).

Comparison of risedronate and fluorescent risedronate conjugates on ceramic HAP at pH 6.8

FL-BPs are of increasing interest as specific imaging probes to study the *in vivo* localisation and cellular uptake of BPs [140]. In addition, FL-BPs

can be useful tools for designing novel *in vitro* competition assays to study the relative mineral-binding affinities of BPs. This will be covered in the next Chapter. Recently, two fluorescently labelled conjugates of risedronate, 5(6)-FAMRIS and AF647-RIS, have been successfully prepared [140, 141].

To investigate whether the different fluorophores conjugated to risedronate could interfere with the binding affinity for HAP, and to make a general comparison of a variety of fluorescent risedronate conjugates that might be used for different applications, risedronate labelled with AF647, 5(6)-FAM and rhodamine; risedronate-PC labelled with 5(6)-FAM and rhodamine; as well as 5(6)-FAMRIS with R1-NH_2 substitution were tested on the HAP columns.

Interestingly, as illustrated in Figure 24, the peak retention time on HAP columns of three fluorescent risedronate compounds varied, with Rho-RIS displaying the highest retention time for HAP, which was almost the same as the parent drug, whereas the retention time for AF647-RIS was only 68% of risedronate. These results are in good accordance with others using a HAP crystal growth assay method [140]. As from previous studies and the present measurements, the two fluorescent RIS-PC compounds had significantly decreased in retention times compared to their BP parent counterparts. Rho-RISPC showed only a moderate decrease of 32%

retention time compared to Rho-RIS and risedronate, but still about the same retention time as AF647-RIS, suggesting the high affinities of these rhodamine labelled compounds. On the other hand, 5(6)-FAMRISPC was hardly retained on the HAP column. These two findings further support the importance of the P-C-P structure of BP for high mineral-binding affinity. Again, as predicted, the substitution of R1-OH of 5(6)-FAMRIS with an amino group did not significantly alter its affinity, which supports the hypothesis that the amino group could also provide tridentate binding of BP molecule to HAP with similar affinity to OH [142].

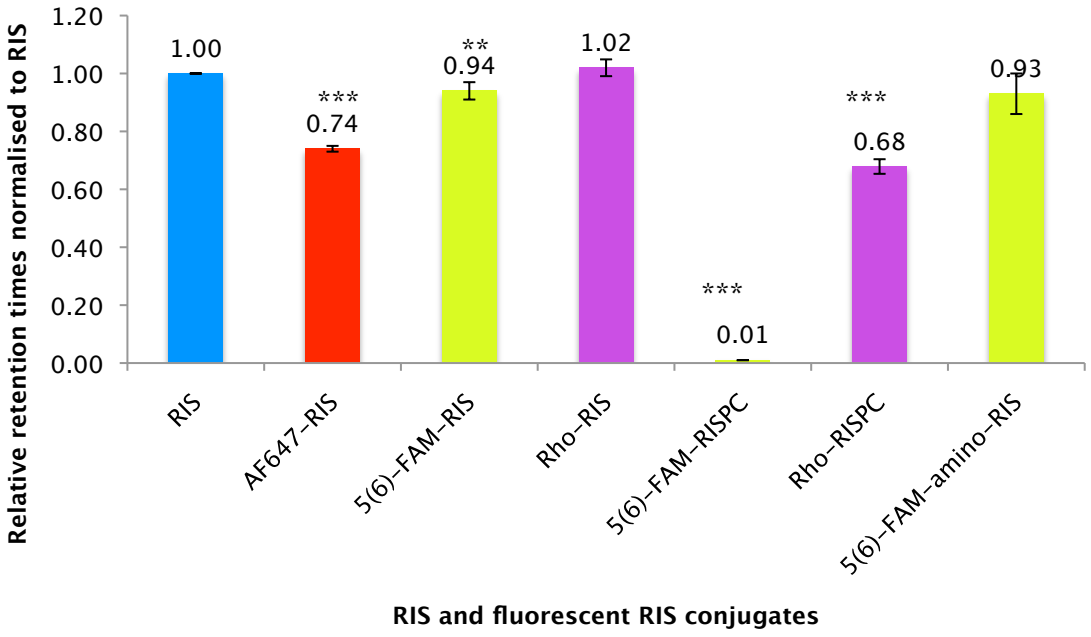

Figure 24 Comparison of the peak retention times of RIS and fluorescent RIS conjugates including AF647-RIS, 5(6)-FAMRIS, Rho-RIS, 5(6)-FAMRISPC, Rho-RISPC and 5(6)-FAM-amino-RIS at pH 6.8 on HAP columns.

Void volume was taken out prior to the calculation. Data are shown as means ± SD from three individual studies shown as relative retention times normalised to RIS. *** $p<0.001$ significantly different from parent compound RIS. ** $p<0.05$ significantly different from parent compound RIS.

3.2.2 Retention times of individual BPs versus BP 2-in-1 on ceramic HAP at pH 6.8

The purpose of this study was to investigate whether, when different BPs were mixed together (N-in-1, N>1), there was an effect on their individual behaviours under the chromatographic conditions used and if this procedure was an appropriate alternative to the testing of BPs individually. Preliminary work included using two BPs, ibandronate and risedronate, for HAP column chromatography. Both compounds were run through the FPLC system individually and as a mixture of the two.

Typical retention profiles derived from mass spectrometric analysis of HAP-separated fractions of IBN and RIS when ran individually at pH 6.8 are shown in Figure 25 (N-in-1, N=1). It can be seen that the retention profiles from three different runs were very consistent, indicating the reproducibility of this method. Interestingly, IBN and RIS exhibited the same mean peak retention time of 9.85 min. Likewise, these two compounds eluted from the HAP column distinctively at the same time when mixed together as a single run (Figure 26, N-in-1, N=2, Table 3). Thus, it can be concluded that when IBN and RIS were mixed together under the chromatographic conditions used there was no significant change (P>0.05) to either of their individual relative retention times.

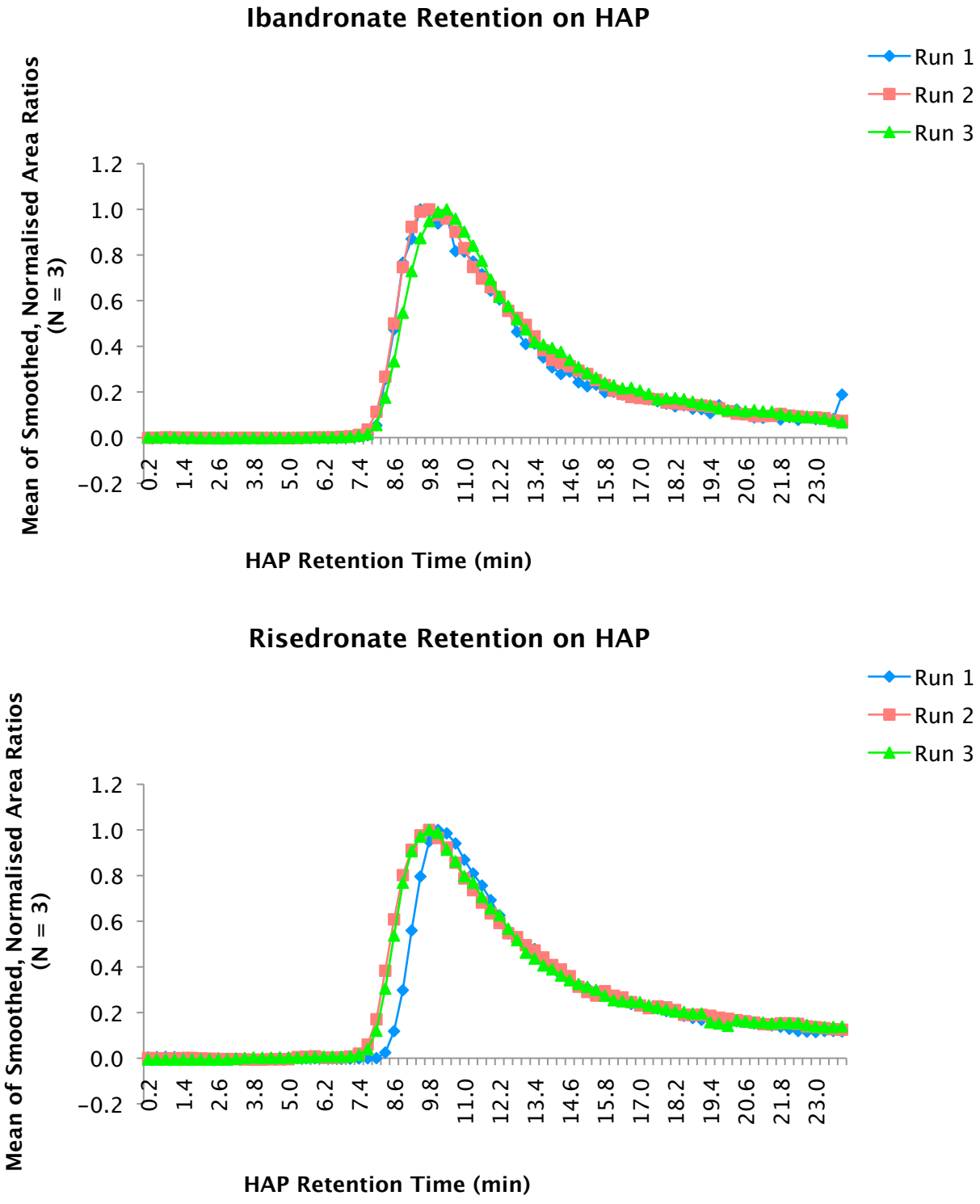

Figure 25 Elution profiles of ibandronate (upper) and risedronate (lower) run individually (1-in-1) on HAP columns at pH 6.8, derived from HPLC/MS/MS analysis of HAP-separated fractions.

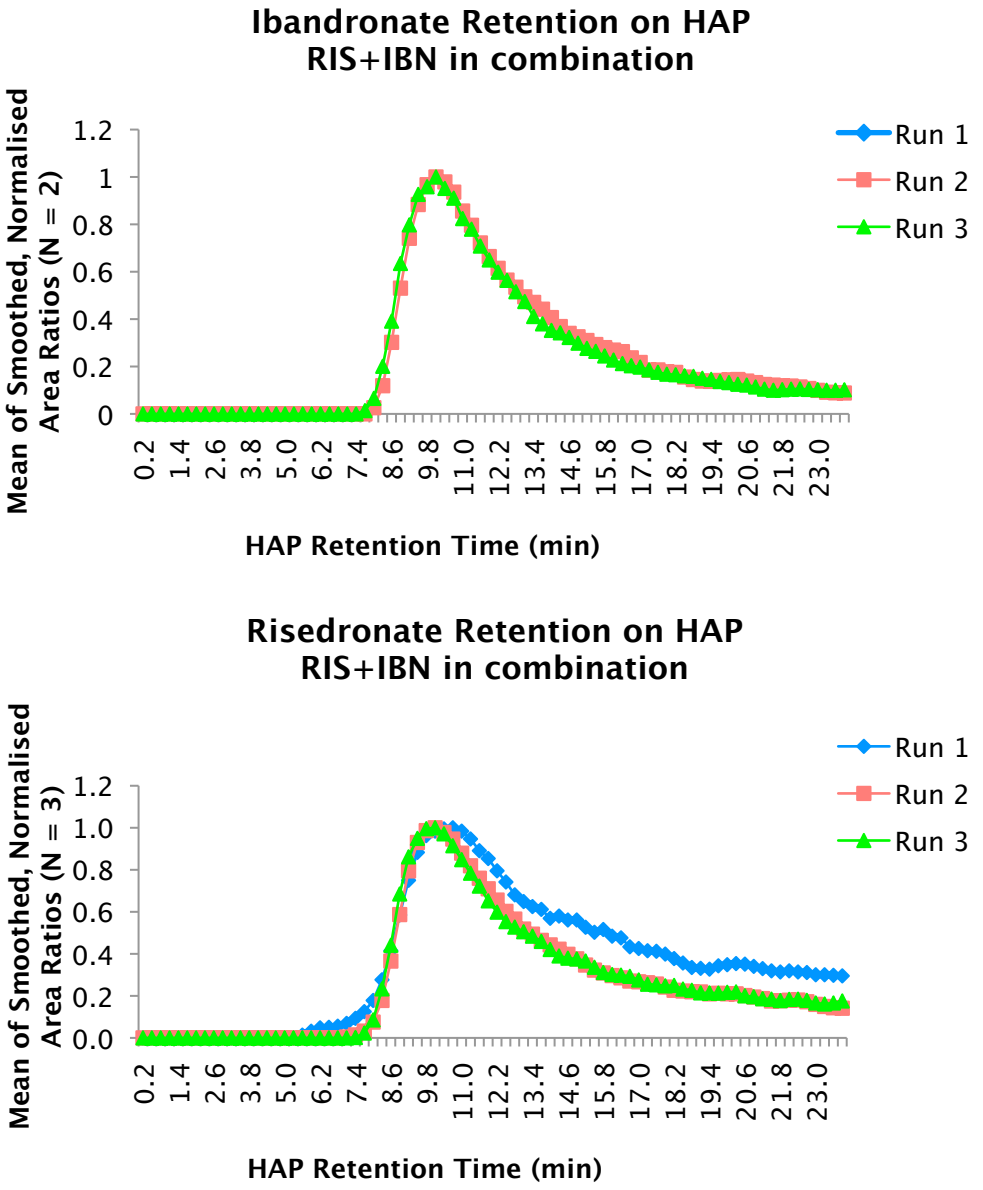

Figure 26 Elution profiles of ibandronate (upper) and risedronate (lower) run as a mixture (2-in-1) on HAP columns at pH 6.8, derived from HPLC/MS/MS analysis of HAP-separated fractions.

Table 3 Summary of N-in-1 (N=2) versus IBN alone and RIS alone HAP retention.

Values represent the mean value of three experiments ± SD.

Bisphosphonate	Peak retention time (min) Alone	Peak retention time (min) Run together
Ibandronate	9.85±0.46	10.05±0
Risedronate	9.85±0.17	10.05±0.35

3.2.3 Retention times of BP N-in-1 on ceramic HAP at pH 7.4

As the relative mineral-binding affinities of IBN and RIS could be assessed in a mixture without showing any major interference of the two compounds, it was assumed that a series of BPs with different binding affinities for HAP when mixed together as in one chromatographic run (N-in-1, N>1) could be separated by using this technique. In addition, the effect of pH on the mineral-binding affinities of BPs was examined by using the combined procedure.

To test the hypothesis that, under the conditions used, similar adsorption characteristics are exhibited by BPs when applied to the column either in combination or in isolation, a mixture of nine clinically relevant BPs (as seen in the figure legend of Figure 27) was first run through the FPLC system at physiological pH, i.e., pH 7.4. Reconstructed 9-in-1 HAP chromatograms obtained from the MS analysis (Figure 27) demonstrate that each BP had their discrete retention time in the HAP column, which reflects their respective bone mineral affinity. At pH 7.4, the alkyl-amino BPs, such as pamidronate, alendronate and neridronate, had the highest binding with retention times at half peak retention times ($T_{0.5MAX}$) (min; mean ± SD) of 12.21 ± 0.17, 11.12 ± 0.18, 9.86 ± 0.17, respectively. This suggests the importance of the nitrogen moiety and its position in an alkyl chain is playing a role in the different HAP binding affinities. However, clodronate, the only non-hydroxybisphosphonate tested,

showed a significantly shorter ($P < 0.0001$) retention time (6.36 ± 0.01) compared to all other compounds, again emphasising the importance of the R1-OH group in the HAP binding. Zoledronate, minodronate and risedronate displayed intermediate binding values, suggesting the additional importance of the nitrogen position within the pyridyl ring with regard to HAP binding.

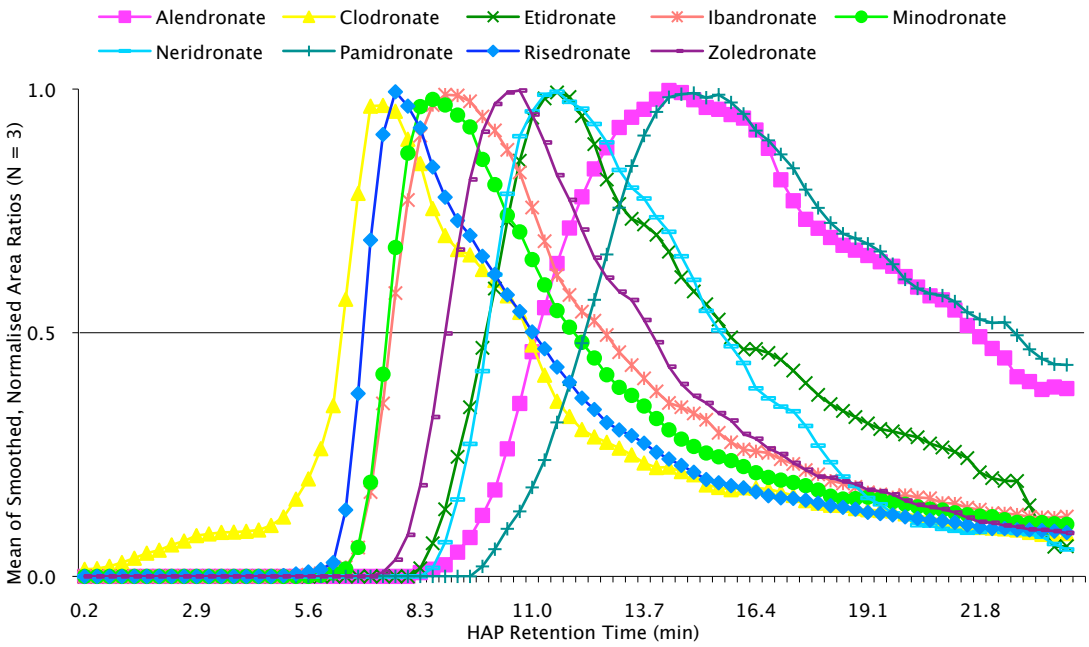

Figure 27 Reconstructed chromatograms of a mixture of 9 BPs (pH 7.4), derived from 9-in-1 HPLC/MS/MS analysis of HAP-separated fractions.

1 µmol of BP 9-in-1 sample was injected into the FPLC system. Elution was performed with a linear gradient of phosphate buffer from 1 mM to 1 M at pH 7.4. The total run lasted 24 min at a flow rate of 2 ml/min. 80 fractions of the sample were collected and used for subsequent MS analysis.

3.2.4 Retention times of BP N-in-1 on ceramic HAP at pH 6.8

Experiments were then done at pH 6.8. Interestingly, at pH 6.8, the data (Figure 28) were reproducible enough to see a difference in affinities with significant longer retention times compared to those seen at pH 7.4

(Figure 27) ($p<0.001$ for all BPs except CLO, $p<0.05$ for CLO), as a function of pH.

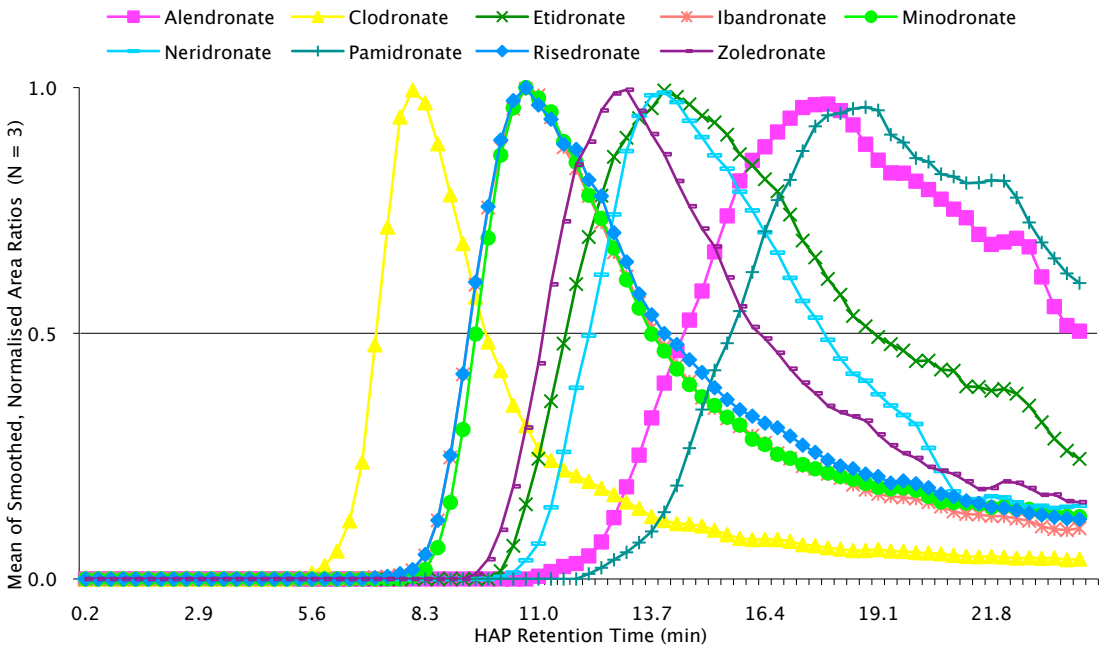

Figure 28 Reconstructed chromatograms of a mixture of 9 BPs (pH 6.8), derived from 9-in-1 HPLC/MS/MS analysis of HAP-separated fractions.

1 µmol of BP 9-in-1 sample was injected into the FPLC system. Elution was performed with a linear gradient of phosphate buffer from 1 mM to 1 M at pH 6.8. The total run lasted 24 min at a flow rate of 2 ml/min. 80 fractions of the sample were collected and used for subsequent MS analysis.

3.2.5 Retention times of BP N-in-1 on ceramic FAP at pH 5.7

Since HAP is less stable at low pH, we used fluoroapatite, which is a more stable alternative to HAP, together with the mixed-phosphate buffer system to investigate the mineral-binding affinities of BPs under acidic buffered chromatography conditions. Preliminary results with RIS, MIN and ZOL (Figure 29) detected by UV absorbance at their optimum wavelength confirmed that using a FAP column did not alter the elution

patterns and relative retention times of BPs ($p>0.05$), hence the results generated from FAP columns should be comparable to those using HAP columns.

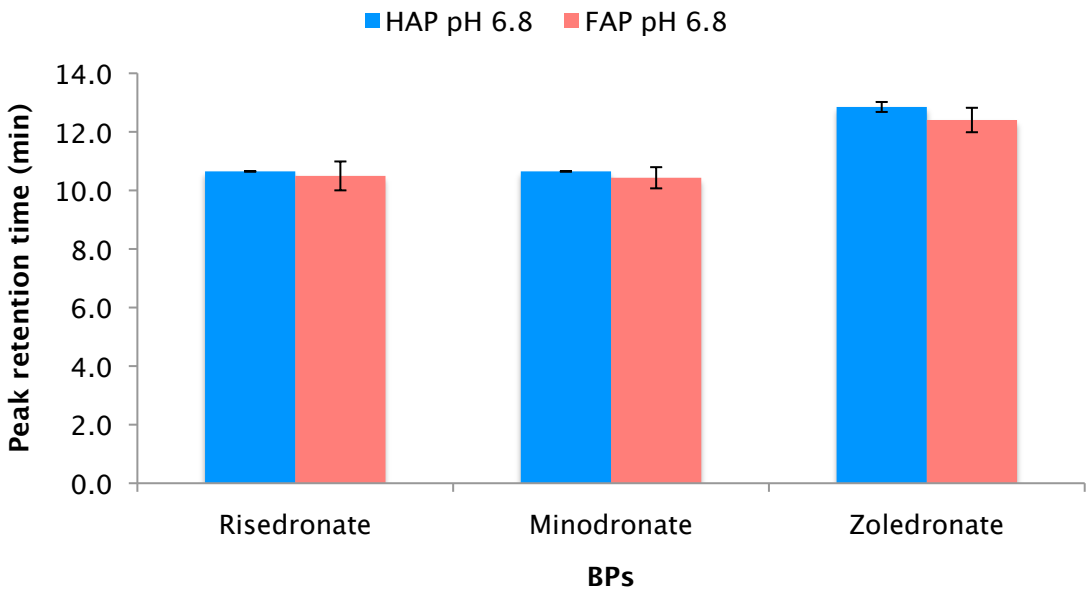

Figure 29 Comparison of the peak retention times of risedronate, minodronate and zoledronate on HAP columns and FAP columns at pH 6.8.

Data are shown as mean ± SD from three individual studies.

The BP 9-in-1 study was thus conducted by using FAP columns at pH 5.7. The results indicate that by changing pH profound effects on the binding and release from HAP are observed, and that BPs appear to have significantly higher affinities at lower pH as shown by increased retention times (Figure 30) ($p<0.001$ for all BPs except CLO, $p<0.05$ for CLO compared to retention times at pH 6.8 and $p<0.0001$ for all BPs except CLO, $p<0.001$ for CLO compared to retention times at pH 7.4).

Changing pH will affect the ionisation of the phosphonate and R2 functional groups that are important for HAP binding. These observations have implications for detachment of BPs during bone resorption, and may help to explain some of the clinical differences between BPs and their potencies.

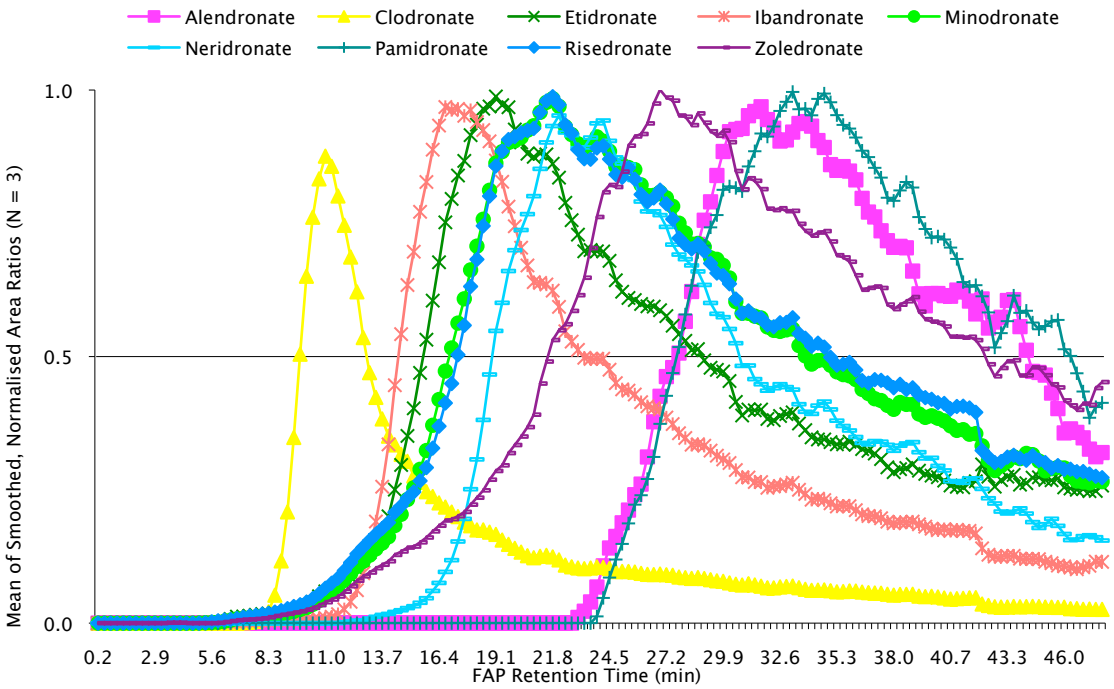

Figure 30 Reconstructed chromatograms of a mixture of 9 BPs (pH 5.7), derived from 9-in-1 HPLC/MS/MS analysis of HAP-separated fractions.

1 µmol of BP 9-in-1 sample was injected into the FPLC system. Elution was performed with a linear gradient of phosphate buffer from 1 mM to 1 M at pH 5.7. The total run lasted 48 min at a flow rate of 2 ml/min. 160 fractions of the sample were collected and used for subsequent MS analysis.

3.3 Discussion

The mineral-binding property is one of the key features contributing to the differences in the pharmacology and clinical effects of BPs. The binding affinity of any BP for HAP should predict the likelihood of

attachment to bone and the subsequent duration of attachment [69]. It has been well characterised that the binding of BPs to HAP is based on their common structure of P-C-P and R1, as a hydroxyl group or amino group could enhance bone affinity [69, 127, 143], whereas a lesser effect is expected from the R2 group. An early binding study of N-BPs, using organ culture techniques, demonstrated significant differences in apparent affinity with differing R1 groups and only small or no differences due to differing R2 groups [8]. In addition, Leu *et al*. used competition binding assays with ^{14}C-alendronate on bone powders to assess the relative binding affinities of BPs. Except for clodronate and tiludronate having a significantly weaker affinity for bone, all the hydroxyl-substituted BPs (etidronate, ibandronate, pamidronate, risedronate, and zoledronate) showed only small differences in affinity and these were not significantly different [19]. Furthermore, compared to the much higher affinities obtained in other studies [17, 42], the affinity constants in the competition binding assays were too weak to explain the high skeletal uptake and retention of BPs observed in experimental and clinical studies. On the contrary, as mentioned previously the studies by Nancollas *et al*. [127] have demonstrated that the R2 side chain may also contribute to mineral-binding affinity.

In order to better simulate the interactions of BPs with bone surfaces and to yield results that would be used to contribute to the ongoing debate

on the differences of interactions of BPs with bone mineral, in our current studies we have used column chromatography with ceramic hydroxyapatite and fluoroapatite combined with mass spectrometric identification and quantitation to assess the relative mineral-binding affinities of individual clinically relevant BPs in mixtures of these compounds and the changes with elution pH.

Some BP derivatives might show interactions when mixed in solutions, however, for the compounds used in this study it is unlikely that such interactions have major influences on elution profiles. This is because similar profiles are seen when they were run individually or as mixed samples (IBN and RIS 2-in-1 study vs. 1-in-1 study). It is of interest to note that the notion of using mixture of BPs (N-in-1) (with RIS always included as a control) as the standard study design represents a new and novel way of assessing BP candidates quickly by co-administration of several compounds of similar class into a single animal or HAP-based column chromatography system. Because the HPLC/MS/MS instrument can be used to assay multiple compounds in the presence of each other in one analysis, these (N-in-1) studies offer the possibility of obtaining more information from fewer samples, and yield more robust results.

Generally speaking, all test compounds are evaluated literally in the same HAP run and the end measurement is relative across all BPs. Each BP

serves as a control for all the others, so any run-to-run variability in HAP performance is eliminated as a source of variability and the HAP experimental, relatively brief, timeframe also minimises any potential for drift in the HAP system performance. In practice, quantitative comparisons of relative retention were derived from $T_{0.5MAX}$ calculations. Using risedronate as a retention time control/comparator, each of the BP profiles were normalised to risedronate which should take care of any concerns related to the comparability of the data generated over time.

Moreover, the speed or efficiency has improved dramatically in terms of running the actual HAP column experiment and in final sample preparation for MS analysis. Using the HAP procedure as an example and using a 9-in-1 analysis approach (N=3 replicates), 2160 data points are collected using 240 6-min LC/MS/MS runs (24 vs. 216 hour MS time, if done singly). Sample preparation time is reduced from 50 hours to less than 5 hours. The experiment reduces 27 HAP column runs down to 3.

Our results are consistent with previous data that show the structures of P-C-P and R1 as OH are essential for high bone mineral affinity of BPs and support the idea that a nitrogen moiety and its position in an alkyl chain or heterocyclic ring in the R2 side chain may play a role in the different HAP binding affinities [69, 127, 143]. For instance, both RIS-PC and Rho-RISPC exhibited significantly lower retention times than their

corresponding BP, supporting the idea that both phosphonate groups are essential for HAP binding. Deoxy-RIS was a particular example used to confirm the importance of the R-OH group. Furthermore, our result with 5(6)-FAM-amino-RIS supports the hypothesis that an amino group can substitute the R1-OH group and maintain similar affinity as the hydroxy BPs [142].

FL-BPs have been recently applied in imaging to investigate the cellular and skeletal uptake of BPs *in vitro* and *in vivo* [141]. Roelofs *et al.* reported that 5(6)-FAMRIS intensely labelled the surface of dentine, and the newly exposed surface of resorption pits beneath actively resorbing osteoclasts. These findings imply that 5(6)-FAMRIS binds to newly exposed mineral surfaces with high affinity after being released by osteoclast resorption. In this study, our aim was to investigate whether the fluorescent conjugates would affect the mineral-binding affinities of fluorescently labelled BPs, which may help, together with imaging technique, to investigate the action of BPs *in vitro* and *in vivo* in more detail. By measurement of the retention time on HAP columns, it was shown that the addition of rhodamine fluorophore to risedronate did not change the affinity of risedronate for bone mineral. The affinities of 5(6)-FAMRIS and AF647-RIS were also comparable, even though to a lower extent, to that of unlabelled risedronate. These results agreed with findings that both 5(6)-FAMRIS and AF647-RIS significantly inhibited HAP

crystal growth demonstrated by a HAP crystal growth assay [140]. On the other hand, an *in vivo* study with 5(6)-FAMRIS confirmed that the molecule was bound to bone mineral through the BP moiety [140], in agreement with the present results.

Results generated from this study have shown that, in general, the alkyl-amino BPs, such as pamidronate, alendronate and neridronate, have the highest binding, whereas clodronate, a non-amino BP, shows the lowest binding, with zoledronate, minodronate and risedronate displaying intermediate binding values (Figure 31). The rank order of ALN, RIS and CLO were in accordance with results of 24-hour urinary recovery from a bolus rat study, as viewed later in this thesis, indicating the capability of coupling the excretion with skeletal uptake of BPs. Plus, HAP retention times of PAM, ZOL, ALN, RIS and deoxy-RIS, correlate well with the available results by NMR investigations on the basis of integrated ^{31}P CP-MAS NMR peak areas [144]. Moreover, our novel approach of using HAP chromatography has shown that the relative mineral-binding affinities of BPs tested were in a similar but not identical order to the binding affinity ranking found by Nancollas *et al.* [127]. This subtle difference may be attributed to the different methods used to measure bone affinity (static vs. nonstatic), which will be influenced by various factors to different degrees (e.g., adsorption vs. desorption rates), yet the mechanism of

interactions between BPs and the calcium sites of HAP would be the same.

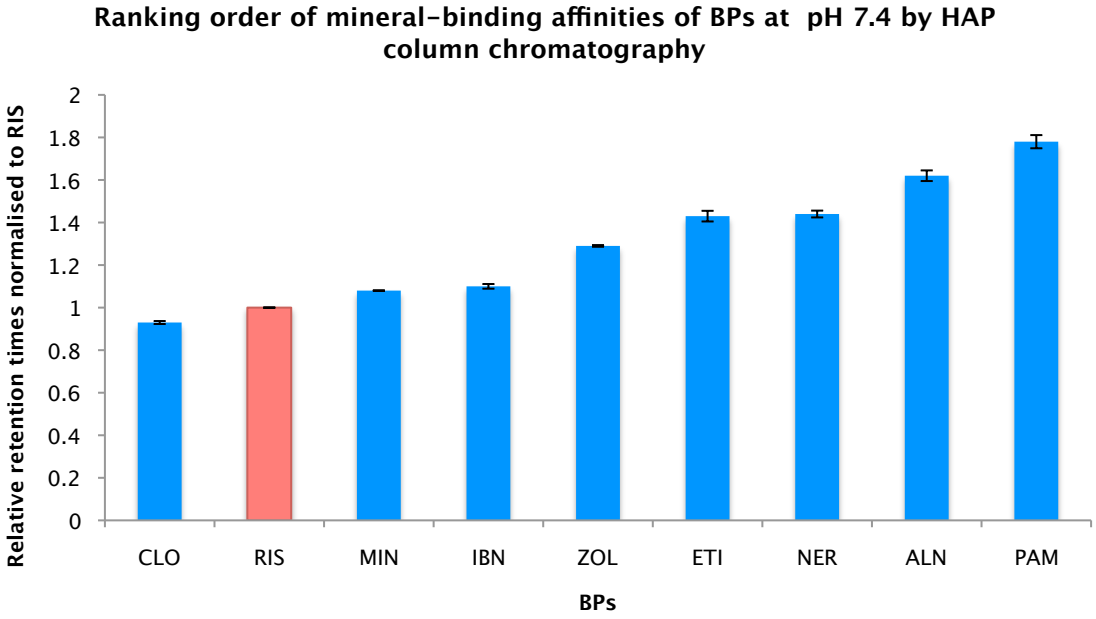

Figure 31 Ranking order of mineral-binding affinities of BPs at pH 7.4 by HAP column chromatography.

Data are shown as mean ± SD from three individual studies shown as relative retention times normalised to RIS.

The effect of pH on BPs binding on HAP can be seen from the example of RIS, MIN and IBN (Figure 32). At pH 6.8, RIS, MIN and IBN were not significantly different in retention time ($P>0.05$) (Figure 33), indicating they have similar affinities for HAP. However, when the pH was switched to 7.4 (Figure 34), those three compounds were dissimilar ($P<0.05$), with IBN having greater affinity shown by a longer retention time than MIN and RIS. Conversely, at pH 5.7, IBN became the lowest affinity compound among those three (Figure 35). The proposed explanation for this phenomenon is based on the protonation of the BP nitrogen functional

group in the R2 position. As in the example of RIS and IBN (Figure 36), the pKa values of the nitrogen substituents in this position are 5.25 and 9.8, respectively. Thus, at pH 7.4, the pyridine ring in RIS is almost completely deprotonated, while the tertiary amine group in IBN remains protonated, which results in its higher affinity at this pH.

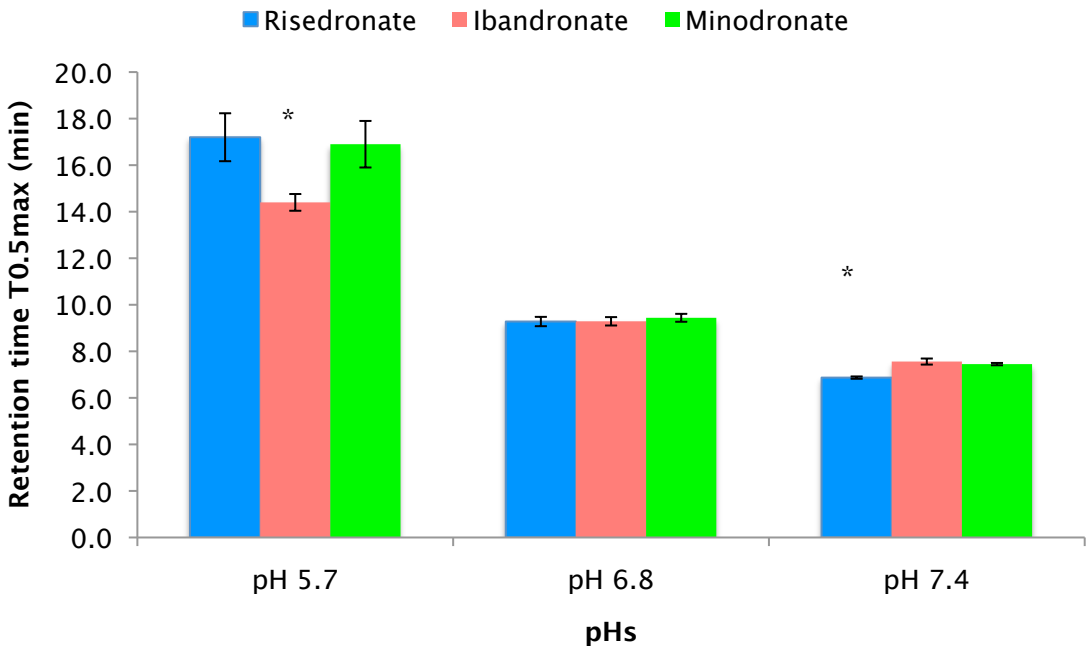

Figure 32 Comparison of the retention times at half peak retention times ($T_{0.5MAX}$) of risedronate and ibandronate on FAP/HAP columns at pH 5.7, pH 6.8 and pH 7.4.

Bars indicate the mean ± SD (n=3). * $p<0.05$.

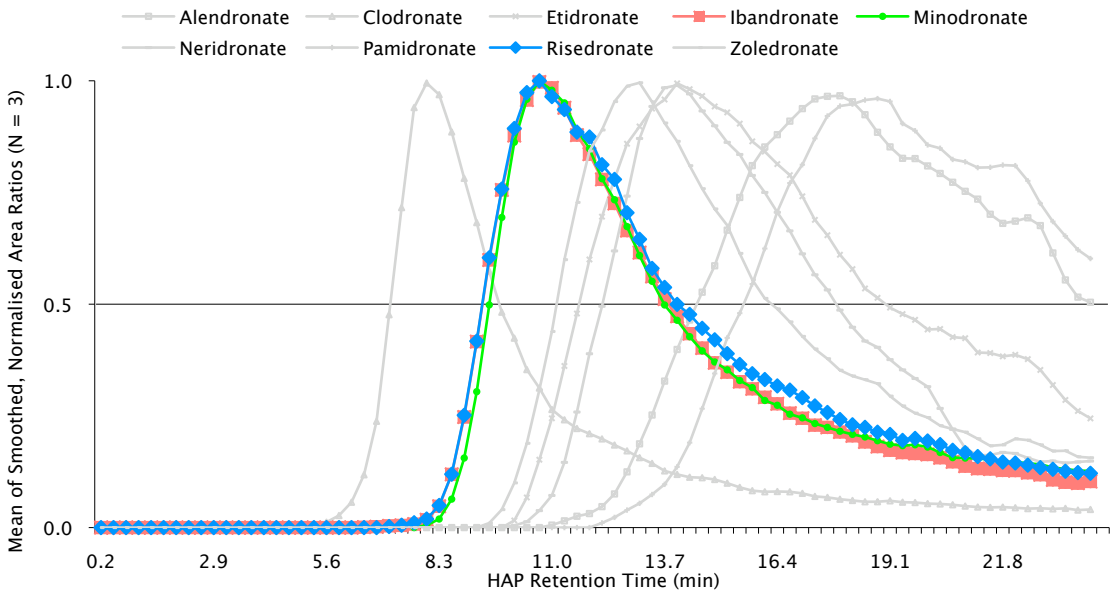

Figure 33 Reconstructed chromatograms of RIS, MIN and IBN (pH 6.8), derived from 9-in-1 HPLC/MS/MS analysis of HAP-separated fractions.

Risedronate and ibandronate were not significantly different in retention time (P>0.05) at pH 6.8, indicating they have similar affinities for HAP.

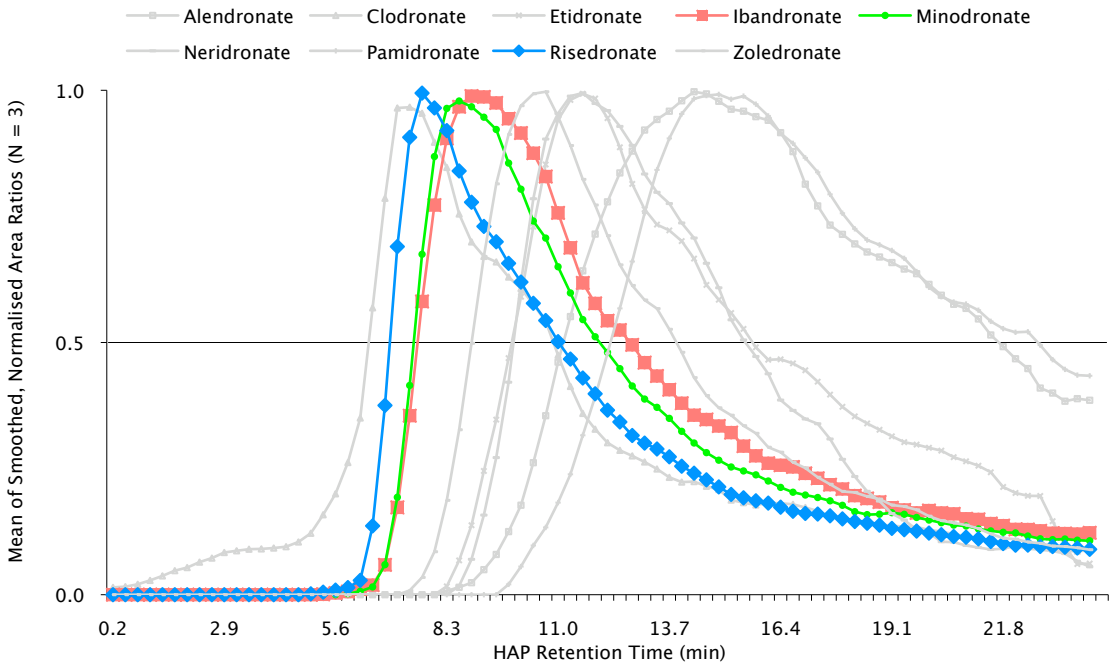

Figure 34 Reconstructed chromatograms of RIS and IBN (pH 7.4), derived from 9-in-1 HPLC/MS/MS analysis of HAP-separated fractions.

Risedronate and ibandronate were dissimilar in retention time (P<0.05) at pH 7.4, with ibandronate having greater affinity shown by a longer retention time than risedronate.

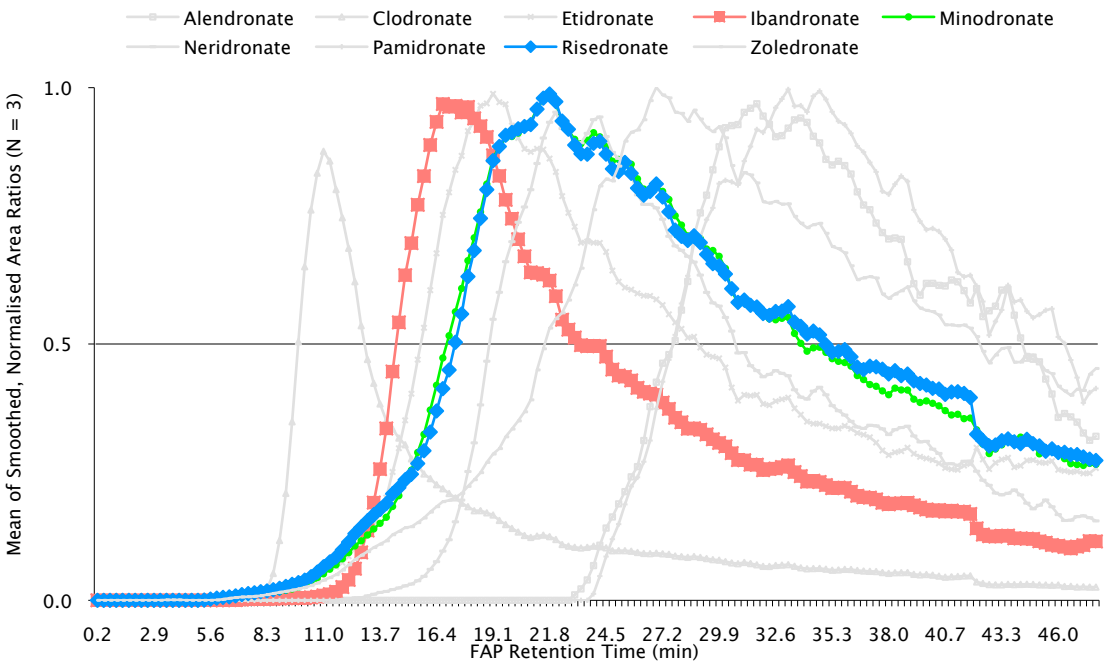

Figure 35 Reconstructed chromatograms of risedronate and ibandronate (pH 5.7), derived from 9-in-1 HPLC/MS/MS analysis of FAP-separated fractions.

Risedronate and ibandronate were dissimilar in retention time ($P<0.05$) at pH 5.7, with ibandronate having less affinity shown by a shorter retention time than risedronate.

	N functional group pKa
RIS	5.25
IBAN	9.8

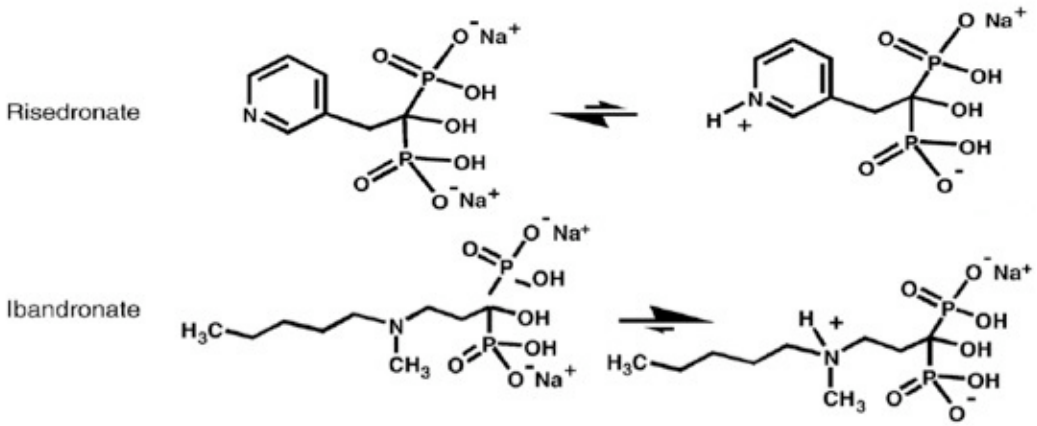

Figure 36 Differing nitrogen charges/species between RIS and IBN at pH 7.4 [127].

The pKa values of the nitrogen substituents in this position of risedronate and ibandronate are 5.25 and 9.8, respectively. At pH 7.4, the pyridine ring in risedronate is almost completely deprotonated, while the tertiary amide group in ibandronate remains protonated, which results in its higher affinity at this pH.

In addition, we found that the chromatographic elution of all BPs could be delayed significantly ($P<0.0001$ for all BPs except CLO, $p<0.001$ for CLO) by decreasing the pH from 7.4 to 5.7 (Figure 37). We speculate that it is mainly the change in ionisation of the phosphonate residues that results in BPs be retained longer on the column at lower pH. The use of fluoroapatite as the column material and a mixed phosphate buffer system at acidic pH allowed optimisation of the phosphate-mediated elution of the test BP as a function of pH and under properly buffered conditions.

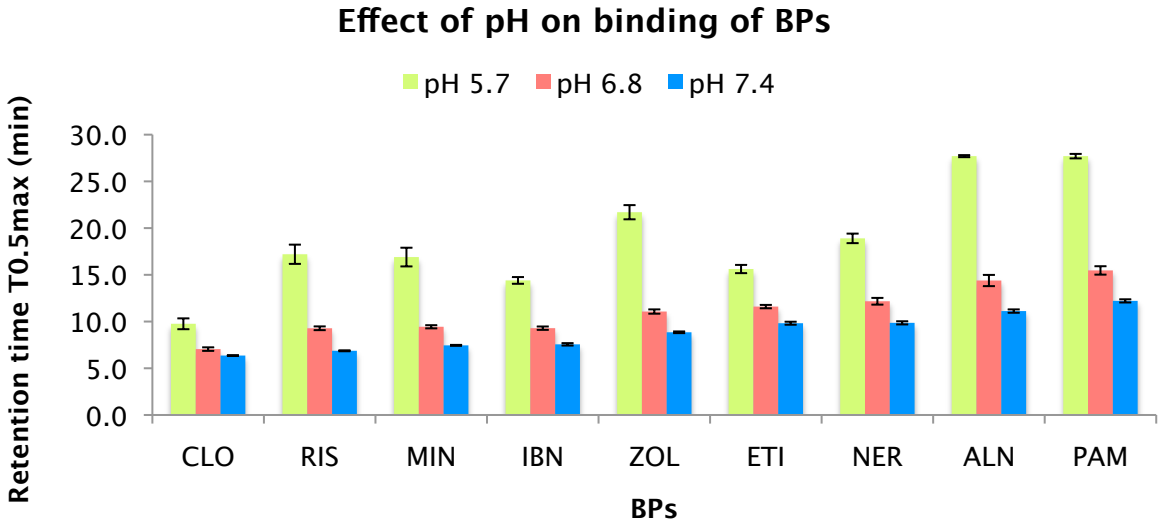

	CLO	RIS	MIN	IBN	ZOL	ETI	NER	ALN	PAM
pH 5.7	9.8	17.2	16.9	14.4	21.7	15.6	18.9	27.7	27.7
SD	0.58	1.03	1.00	0.36	0.76	0.44	0.51	0.11	0.24
pH 6.8	7.05	9.28	9.44	9.29	11.07	11.60	12.17	14.39	15.47
SD	0.19	0.20	0.17	0.18	0.23	0.18	0.36	0.60	0.45
pH 7.4	6.36	6.87	7.45	7.56	8.85	9.82	9.86	11.12	12.21
SD	0.01	0.05	0.05	0.13	0.09	0.16	0.17	0.18	0.17

Figure 37 Retention times at half peak retention times ($T_{0.5MAX}$) of 9 BPs at pH 5.7, pH 6.8 and 7.4 on FAP/HAP columns under conditions defined in Figures 26, 27 and 29.

Bars indicate the mean ± SD (n=3).

While much work has been performed thus far on the study of interactions between BPs and HAP by using HAP/FAP column chromatography, these observations are highly dependent on the utilisation of mass spectrometry. Indeed, the FPLC combined with MS is a powerful technique with respect to quantitative analysis of BPs. However, the MS instrumentation is expensive and requires support by highly trained personnel and regular maintenance. In addition, the FPLC method does not allow for calculation of affinity constants that represents the binding capacity and affinity of BPs. For these reasons, other approaches were developed for characterising mineral-binding affinities of BPs *in vitro* and *in vivo* and these will be covered in Chapter 4 and Chapter 7.

CHAPTER 4 EVALUATION OF THE RELATIVE MINERAL-BINDING AFFINITIES OF BISPHOSPHONATES BY USING BINDING ASSAYS

4.1 Introduction

According to the published literature, several different methods have been used for determination of the binding affinity of BPs for HAP or bone powder. These methods include:

1) Inhibition of HAP crystal growth using a constant composition method [127].

2) Radioactive competition assays of BPs binding to human bone [131].

3) NMR-based competition assays of BPs binding to bone powder and HAP [129].

4) Retention of BPs on HAP column by using FPLC (Chapter 3 of this thesis) [130].

Each of these methods has its advantages and disadvantages and, in addition, the materials used in each model system, i.e., HAP vs. bone powder, may contribute to the different conclusions derived from these studies. With respect to the present FPLC approach described in this thesis, this method of analysis relies on the utilisation of mass spectrometry to identify and quantify all clinically used BPs. Moreover, it does not allow for ready calculation of affinity constants that represent the binding capacities and affinities of BPs. For these reasons, development of robust and comparable assays that can not only

compensate for the weaknesses of the FPLC method but also have general applications will be the main focus of this chapter.

When BPs are added to HAP crystals, the binding characteristic of BP to HAP fits the model of a Langmuir adsorption isotherm (Figure 38). As the concentration of BP increases in solution, the amount bound increases up to a saturation level that indicates the maximum of binding to HAP. A measure of affinity can be obtained from such curves where 50% binding is achieved. According to the law of mass action, these bindings are reversible so that an equilibrium of free and bound BP will exist at different concentrations. The fact that differential uptake occurs at different concentrations of BP is important to explain how BPs bind to bone mineral. Indeed, the use of Langmuir adsorption isotherms can be a highly relevant model to investigate the binding of BP to HAP, and thus was applied in the present study to obtain an estimate of the equilibrium dissociation constant (Kd) of the BP-HAP complex and also the maximal number of binding sites (Bmax) from the non-linear adsorption isotherm. Adsorption isotherms of clodronate, pamidronate, 5(6)-FAMRIS, together with risedronate and ibandronate, either individually or as a mixture of two compounds, were performed.

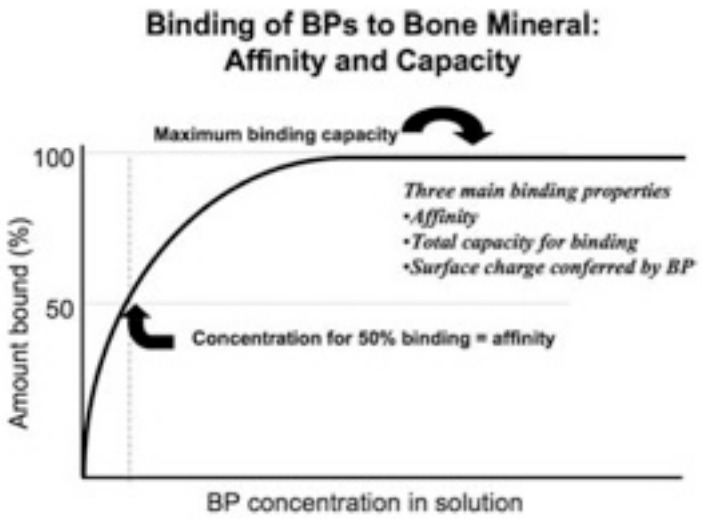

Figure 38 Adsorption isotherm for the binding of BPs to HAP [70].

In addition, as proposed from the FPLC findings, the affinities of BPs should be different from each other, due to their unique structures. Therefore competitive binding assays based on the Langmuir adsorption isotherms should be able to demonstrate the binding of a range of clinically used BPs to HAP. Unlike the competition assays conducted by other research groups that involved radioactively labelled BP or NMR-based detection, which either restricts the universal application or lacks high sensitivity, our work was based on measurement of competition with a FL-BP (5(6)-FAMRIS). Fluorescence competition analysis is a well-established assay in quantitative studies of protein or enzyme-ligand binding and antigen-antibody binding [145]. It is a sensitive method for measuring small amounts of drug and allowing drugs that fluoresce to be assayed in the presence of other compounds that would interfere in an UV assay [146, 147]. In our studies, the competing BPs had no

fluorophore, and they were mixed with 5(6)-FAMRIS prior to applying to the HAP. Their ability to compete with 5(6)-FAMRIS for binding sites is a measure of their affinity for HAP and is reflected by an increase of 5(6)-FAMRIS fluorescence in the supernatant at equilibrium compared with binding of 5(6)-FAMRIS alone. With the Kd of 5(6)-FAMRIS derived from the adsorption isotherm, an estimate of the equilibrium dissociation constant (Ki) of nine clinically relevant BP-HAP complex was obtained via the competition experiments in a direct comparison.

Relatively speaking, the competitive binding assay is preferred for the following reasons. First, this robust and straightforward assay only depends on the measurement of fluorescence of the FL-BP, the amount of nonlabelled BP bound on HAP simply correlates inversely with the fluorescence in the supernatant. In contrast, all data from the Langmuir adsorption isotherms depend upon accurate measurement of BPs especially at low concentrations and light absorbance and MS were shown not to be adequate for most results in the preliminary studies. Second, the presence of nonlabelled BP in the mixture does not interfere with fluorescence quantification, so that many different nonlabelled BPs can be studied via the competition experiments in a direct comparison. Third, the high sensitivity of this fluorometric assay allows for low use of labelled BP and low cost.

4.2 Results

4.2.1 Langmuir adsorption isotherms of BPs on HAP at pH 7.4

To estimate the binding affinities of BPs for HAP, Langmuir adsorption isotherms were performed across a range of 0–300 μM or 0–400 μM over a period of 16 hours. Bound BP was then removed by centrifugation, and the BP remaining in solution was quantified fluorimetrically (5(6)-FAMRIS), spectrophotometrically by the OPA method (pamidronate), or by mass spectrometry (risedronate, ibandronate and clodronate). Differences in solution concentrations upon incubation with HAP directly reflect binding of the BP to HAP. Figures 39–43 illustrate adsorption isotherms for the binding of pamidronate, risedronate, ibandronate, clodronate and 5(6)-FAMRIS, respectively, to HAP. The Scatchard plots inset are linearised forms of the isotherms that is valuable displaying the data.

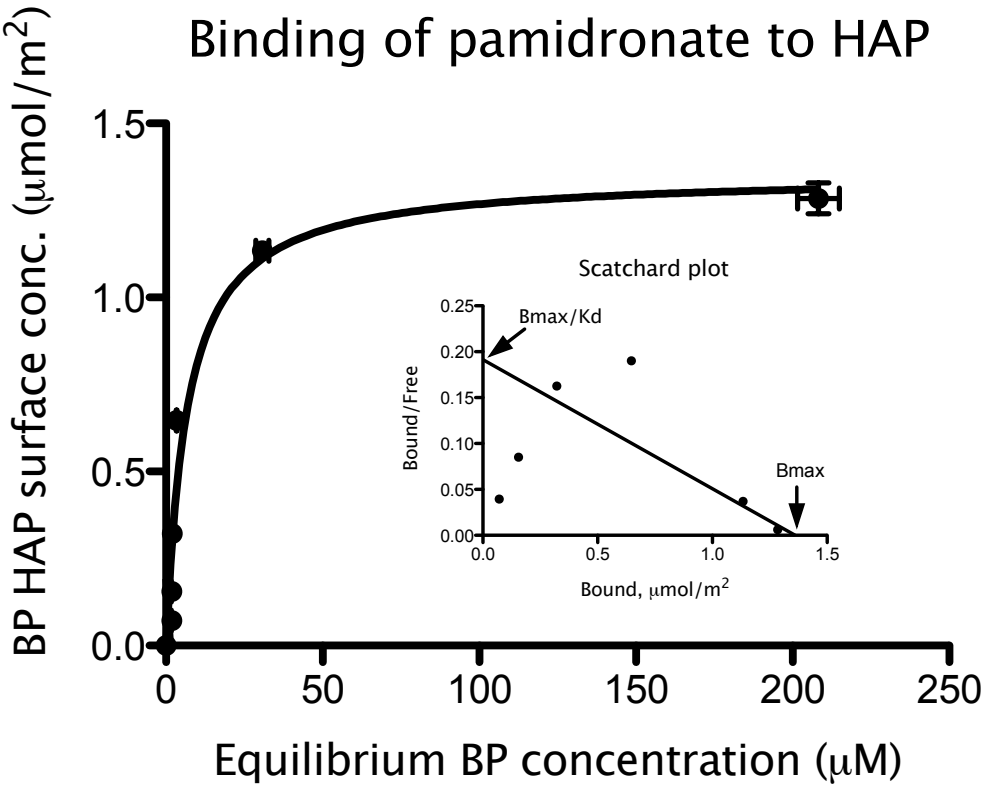

Kd= 6.671 ± 1.131 μM

Bmax= 1.353 ± 0.0654 μmol/m^2

Figure 39 Representative adsorption isotherm for the binding of pamidronate to HAP at pH 7.4 with Scatchard plot of the same data as inset.

Data are shown as mean ± SD (n=3). Kd= 6.671 ± 1.131 μM, Bmax= 1.353 ± 0.654 μmol/m^2. Langmuir adsorption isotherm of pamidronate was performed across a range of 0-400 μM over a period of 16 hours. Bound pamidronate was then removed by centrifugation, and the pamidronate remaining in solution was quantified spectrophotometrically by the OPA method.

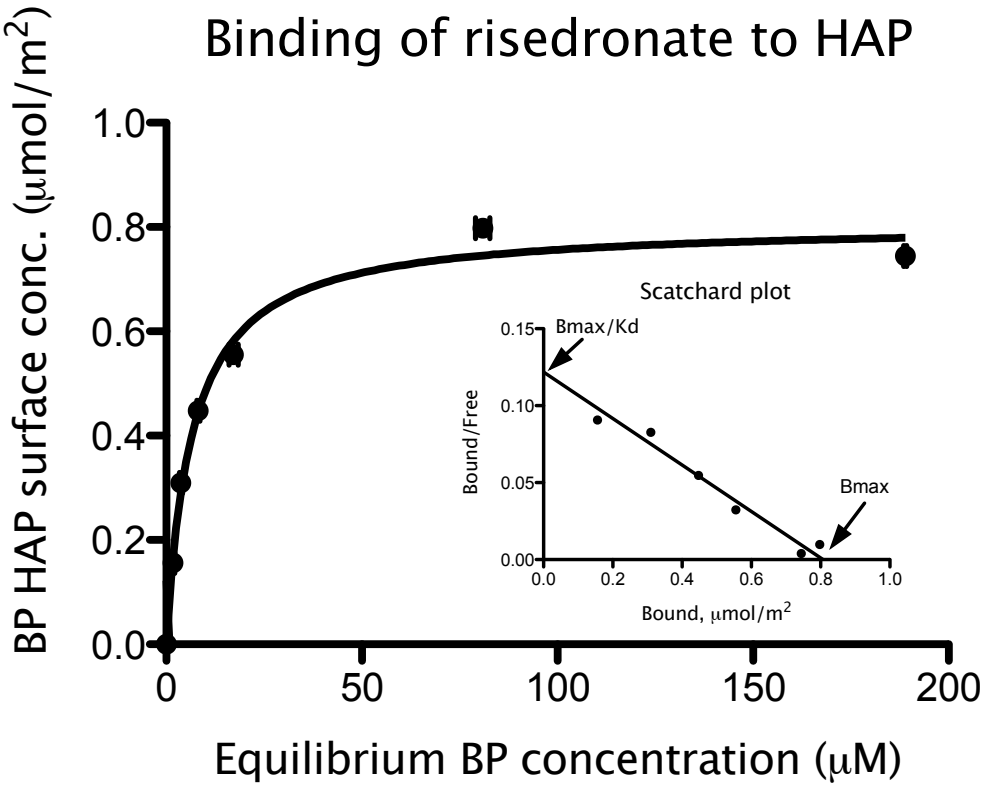

Kd= 6.625 ± 0.4347 μM

Bmax= 0.8067 ± 0.0137 μmol/m^2

Figure 40 Representative adsorption isotherm for the binding of risedronate to HAP at pH 7.4 with Scatchard plot of the same data as inset.

Data are shown as mean ± SD (n=3). Kd= 6.625 ± 0.4347 μM, Bmax= 0.8067 ± 0.0137 μmol/m^2. Langmuir adsorption isotherm of risedronate was performed across a range of 0-300 μM over a period of 16 hours. Bound risedronate was then removed by centrifugation, and the risedronate remaining in solution was quantified by mass spectrometry.

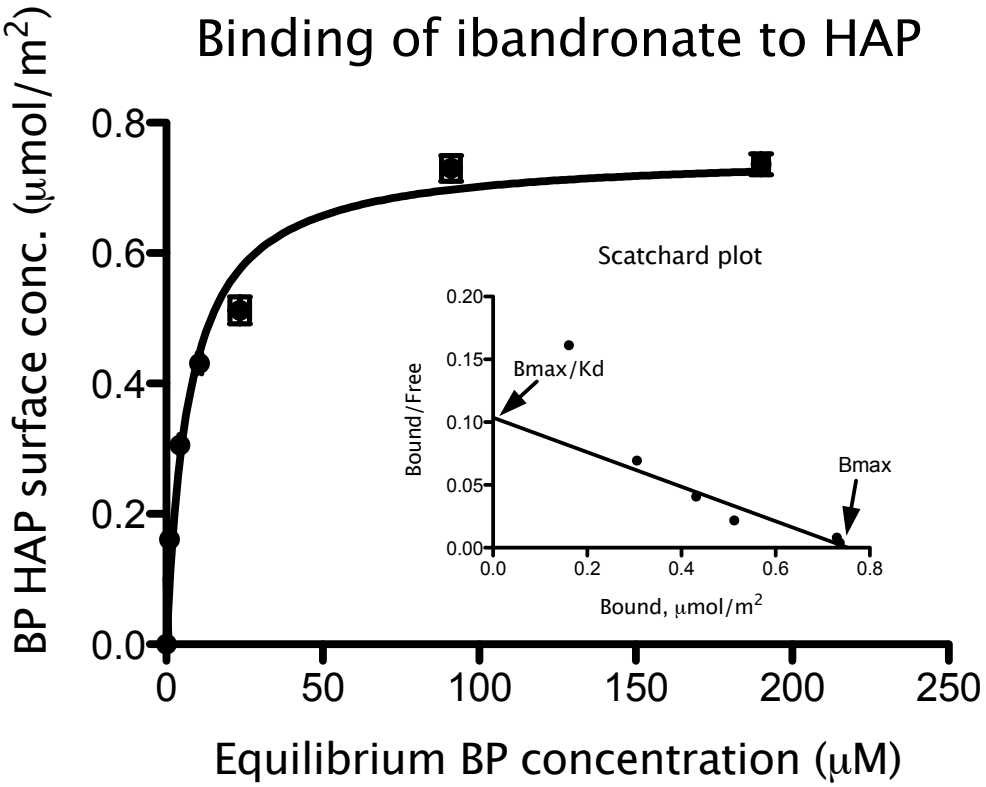

Kd= 7.266 ± 0.8232 μM

Bmax= 0.7531 ± 0.0203 μmol/m^2

Figure 41 Representative adsorption isotherm for the binding of ibandronate to HAP at pH 7.4 with Scatchard plot of the same data as inset.

Data are shown as mean ± SD (n=3). Kd= 7.266 ± 0.8232 μM, Bmax= 0.7531 ± 0.0203 μmol/m^2. Langmuir adsorption isotherm of ibandronate was performed across a range of 0-300 μM over a period of 16 hours. Bound ibandronate was then removed by centrifugation, and the ibandronate remaining in solution was quantified by mass spectrometry.

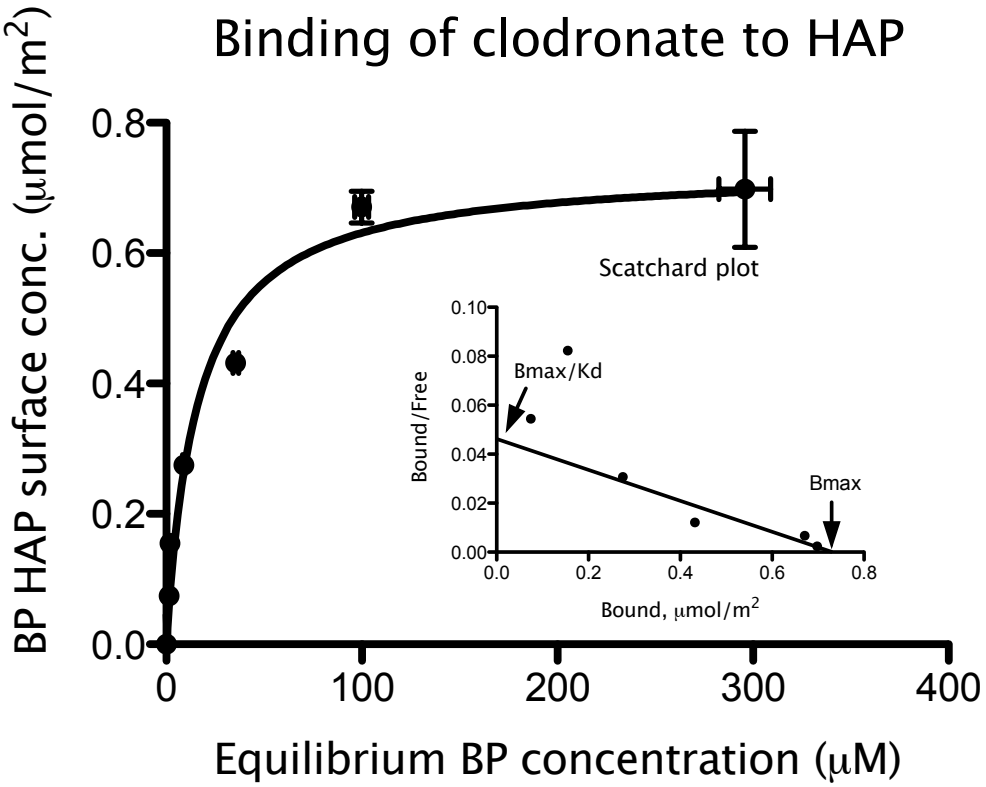

Kd= 15.81 ± 2.784 μM

Bmax= 0.731 ± 0.0307 μmol/m^2

Figure 42 Representative adsorption isotherm for the binding of clodronate to HAP at pH 7.4 with Scatchard plot of the same data as inset.

Data are shown as mean ± SD (n=3). Kd= 15.81 ± 2.784 μM, Bmax= 0.731 ± 0.0307 μmol/m^2. Langmuir adsorption isotherm of clodronate was performed across a range of 0-400 μM over a period of 16 hours. Bound clodronate was then removed by centrifugation, and the clodronate remaining in solution was quantified by mass spectrometry.

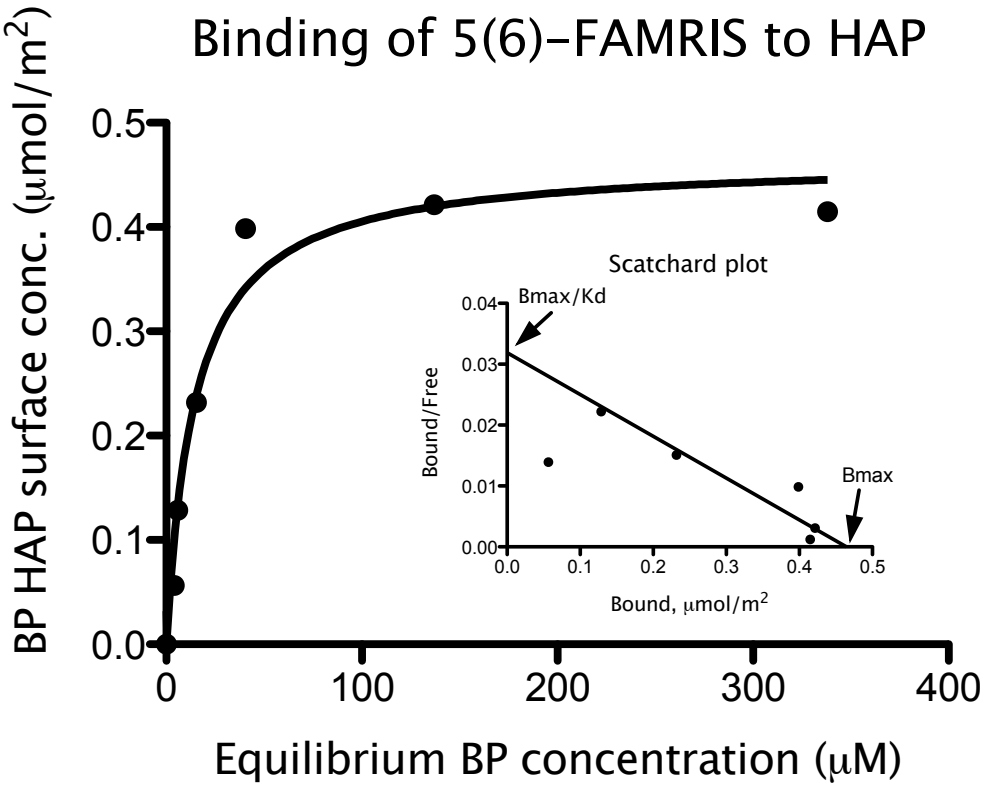

Kd= 14.56 ± 3.645 μM

Bmax= 0.4644 ± 0.0302 μmol/m^2

Figure 43 Representative adsorption isotherm for the binding of 5(6)-FAMRIS to HAP at pH 7.4 with Scatchard plots of the same data as inset.

Data are from a single experiment. Kd= 14.56 ± 3.645 μM, Bmax= 0.4644 ± 0.0302 μmol/m^2. Langmuir adsorption isotherm of 5(6)-FAMRIS was performed across a range of 0-400 μM over a period of 16 hours. Bound 5(6)-FAMRIS was then removed by centrifugation, and the 5(6)-FAMRIS remaining in solution was quantified fluorimetrically.

By analysing the binding data, the Kd and Bmax of pamidronate, risedronate, ibandronate, clodronate and 5(6)-FAMRIS were derived from the non-linear curves, as illustrated in Table 4. A small Kd means that the HAP has a high affinity for the BP while a large Kd means that the HAP has a low affinity for the BP. In these experiments, the units for Kd and Bmax are μM and μmol/m^2, respectively. Interestingly, pamidronate, risedronate and ibandronate were found to exhibit similar Kds of approximately 7 μM, which is roughly two-fold lower than the Kds of 5(6)-FAMRIS and clodronate. The similarity in affinity between risedronate and ibandronate, and the low affinities of 5(6)-FAMRIS and clodronate are in good accordance with the results obtained from the FPLC study. With respect to maximal binding capacities of BPs, pamidronate was shown to be the greatest among the BPs tested. Risedronate, ibandronate and clodronate appeared to have similar binding capacities and were about 60% of the value of pamidronate. In addition, the Bmax of 5(6)-FAMRIS was the lowest, with only 34% in the amounts that can be bound at saturation levels compared with pamidronate. These data suggest that the effect of using a wide range of BP concentrations should be studied in order to achieve estimates of the maximum affinity of any BP to bone mineral. Whilst these levels may never be reached *in vivo*, their relative levels at sites of high exchange may affect potencies of the individual BPs.

Table 4 Dissociation constants (μM) and maximal binding capacities (μmol/m^2) of BPs for HAP.

Data are shown as mean ± SD (n=3) except for 5(6)-FAMRIS which are from a single experiment.

BPs	Kd (μM)	Bmax (μmol/m^2)
Pamidronate	6.671±1.131	1.353±0.06535
Risedronate	6.625±0.4347	0.8067±0.01373
Ibandronate	7.266±0.8232	0.7531±0.02032
5(6)-FAMRIS	14.56±3.645	0.4644±0.03018
Clodronate	15.81±2.784	0.7310±0.03070

Figure 44 summaries the HAP surface concentrations of all BPs tested at various equilibrium solution concentrations. The concentration of each BP adsorbed on to 1 m^2 of HAP surface was calculated as a function of the equilibrium solution concentration. It can be seen that binding to HAP began to plateau at BP concentration in the solution of approximately 100 μM in most cases. The quantity of adsorbed BP near the saturation point is a direct indicator of its capacity of adsorption, which represents the Bmax of HAP for BP. In addition, the measure of affinity of BP for HAP, expressed as Kd, is the concentration of BP that occupies half of the HAP adsorption sites at equilibrium. This data plot demonstrates the potential binding capacities and affinities of HAP for different BPs.

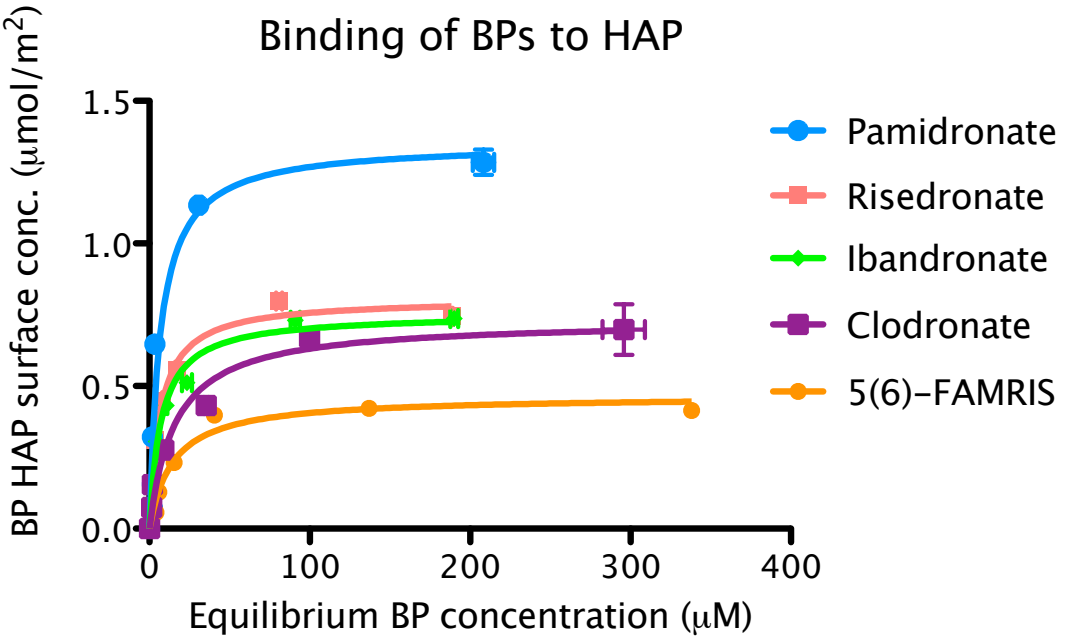

Figure 44 Comparison of the HAP surface concentrations of BPs (pamidronate, risedronate, ibandronate, clodronate, and 5(6)-FAMRIS) at various equilibrium solution concentrations at pH 7.4 and physiological ionic strength.

Data are shown as mean ± SD (n=3) except for 5(6)-FAMRIS which are from a single experiment.

4.2.2 Langmuir adsorption isotherms of competitive binding of RIS and IBN to HAP, at pH 7.4

As demonstrated by comparing the FPLC studies of risedronate and ibandronate run individually (1-in-1) versus as a mixture of the two BPs (2-in-1), the relative retention times of these two compounds did not change when mixed together. This finding is the basis for the BP N-in-1 approach, which allows quantification of one compound to be determined in the presence of other compound. In this study of adsorption isotherms, we also tested whether a mixture of BPs risedronate and ibandronate incubated together (2-in-1) would behave in a similar way.

Adsorption isotherms for the binding of risedronate and ibandronate to HAP obtained from 2-in-1 mixtures show that the two BPs yielded almost superimposable profiles (Figure 45). Noting that this is effectively 0-150 μM of each compound, so that the sum of these essentially represents a 0-300 μM composite load to the HAP material.

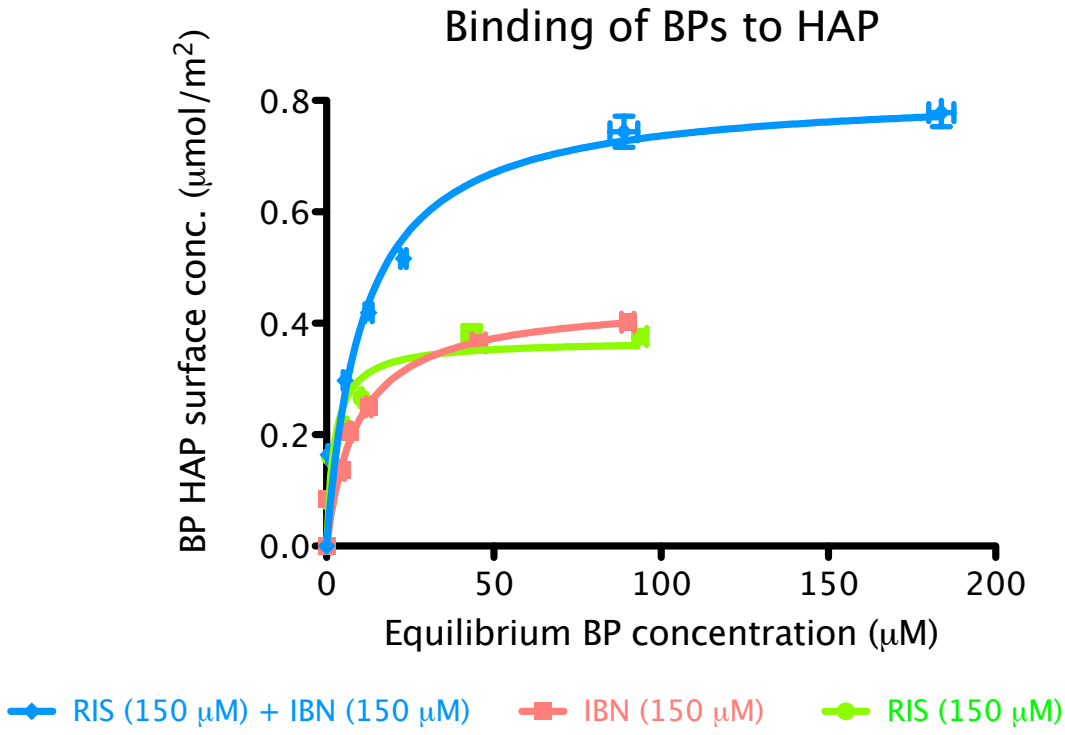

Figure 45 Langmuir adsorption isotherms for the binding of risedronate and ibandronate to HAP in a mixture (2-in-1) at 0-150 μM, respectively, together with calculated total HAP surface concentrations of the mixture (risedronate: ibandronate = 1:1) at pH 7.4 and physiological ionic strength.

Data are shown as mean ± SD (n=3).

Results from the 1-in-1 risedronate and ibandronate at 0-300 μM are shown in Figure 46. As with the 2-in-1 results (Figure 45), these were still almost superimposable, when incubated separately. For further

comparison, Figure 46 shows both the 0–300 μM plots for risedronate and ibandronate, together with the risedronate + ibandronate plot from the 2-in-1 leg. Again, these were nearly identical, which leads to the conclusion that the 2-in-1 approach, in this case, at least gives a nearly identical assessment to the independent incubations. It may be observed that risedronate has a slightly steeper rise (relative to ibandronate) in both study legs, but there was not a statistically significant difference. Based on the above evidence, binding of BPs to HAP has been proved to be reversible, saturable, specific and competitive.

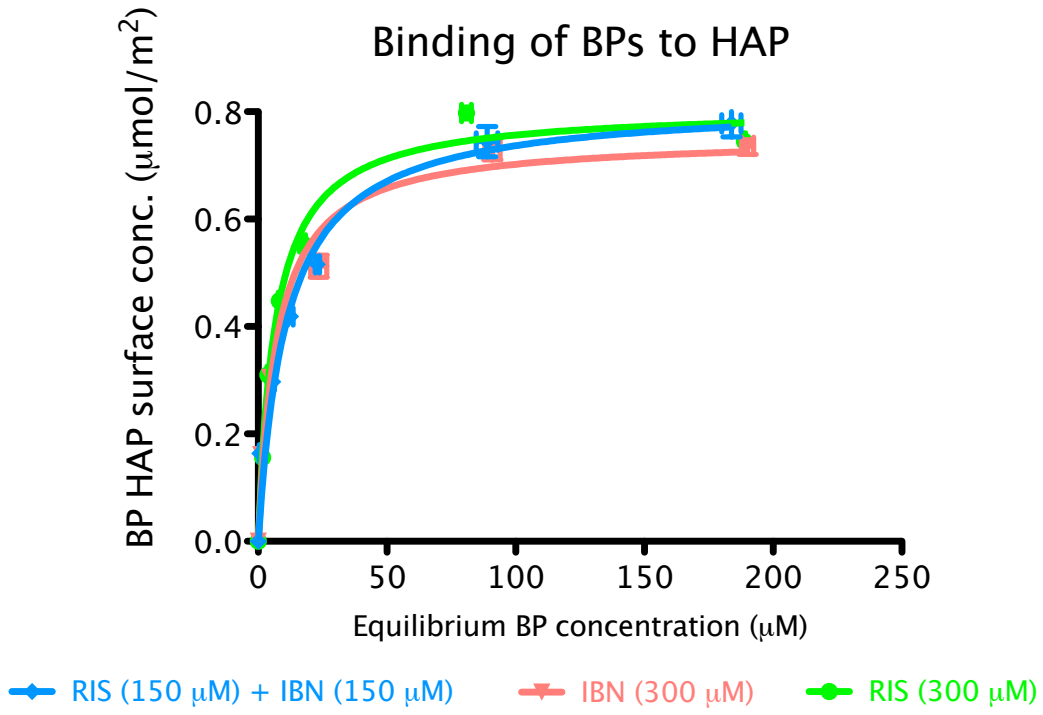

Figure 46 Langmuir adsorption isotherms for the binding of risedronate and ibandronate to HAP at 0–300 μM when incubated separately, together with calculated total HAP surface concentrations of the mixture (risedronate: ibandronate = 1:1) at pH 7.4 and physiological ionic strength.

Data are shown as mean ± SD (n=3).

4.2.3 Competitive binding assays of 9 BPs vs. 5(6)-FAMRIS

The above sections have shown that the Langmuir adsorption isotherms were able to determine the binding affinities of BPs. However, this approach has a high requirement for the sensitivity of measurement device since free BP concentrations below the dissociation constant of the complex must be determined. In order to obtain an accurate quantitative evaluation of dissociation constants for BP binding, competitive binding assays were performed by using various concentrations of unlabelled BP to compete with FL-BP in binding to HAP.

Nine BPs including PAM, ALN, ETI, NER, ZOL, RIS, IBN, MIN and CLO were tested to competitively inhibit 5(6)-FAMRIS binding to HAP, and their competitive binding curves are shown in Figures 47-55. The Top and Bottom of the competitive binding curves are defined in section 2.4.2 of this thesis. The Kd value of 5(6)-FAMRIS was 14.56 μM, based on the Langmuir adsorption isotherm determined in Figure 43. By using these criteria, Kis were calculated from non-linear fitting of the competition curves (see section 2.4.2 for details) and used to setup a relative table of HAP affinity as shown in Table 5.

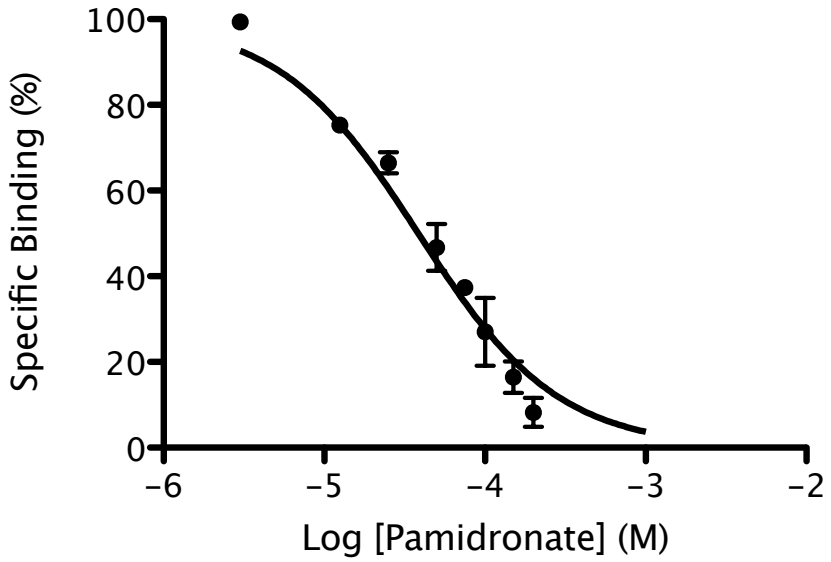

Figure 47 Competitive binding of pamidronate with 5(6)-FAMRIS to HAP.

5(6)-FAMRIS (3 μM) was co-incubated with various concentrations of pamidronate (3-1000 μM), as indicated in the inset key. Results were analysed with Graphpad Prism software using a one-site competition model. The data were normalised for specific binding and the percentage shown. The error bars indicate SD and a representative curve is shown. A mean Ki was determined for three independent experiments and reported in Table 5.

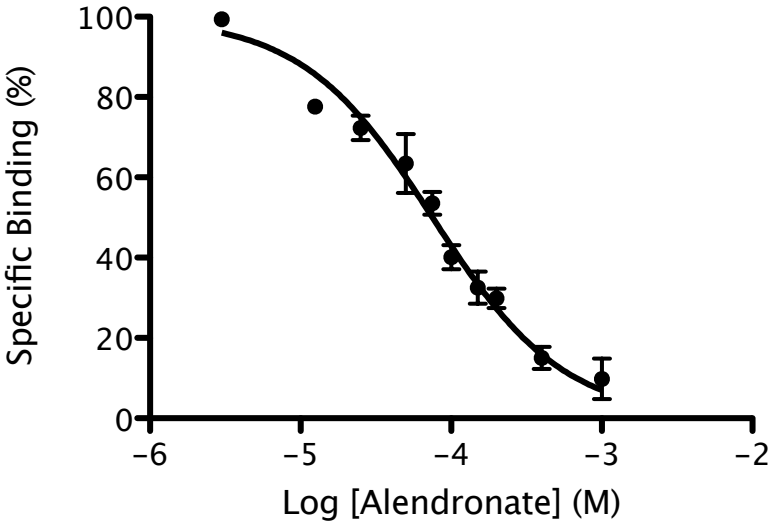

Figure 48 Competitive binding of alendronate with 5(6)-FAMRIS to HAP.

5(6)-FAMRIS (3 μM) was co-incubated with various concentrations of alendronate (3-1000 μM), as indicated in the inset key. Results were analysed with Graphpad Prism software using a one-site competition model. The data were normalised for specific binding and the percentage shown. The error bars indicate SD and a representative curve is shown. A mean Ki was determined for three independent experiments and reported in Table 5.

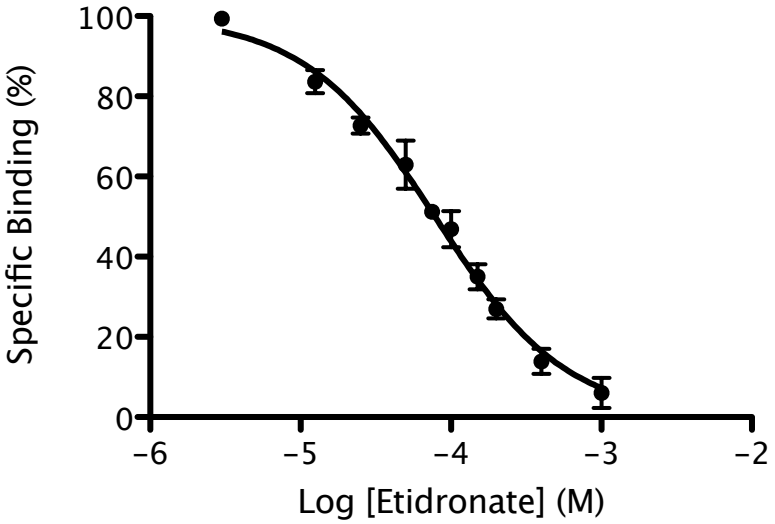

Figure 49 Competitive binding of etidronate with 5(6)-FAMRIS to HAP.

5(6)-FAMRIS (3 μM) was co-incubated with various concentrations of etidronate (3-1000 μM), as indicated in the inset key. Results were analysed with Graphpad Prism software using a one-site competition model. The data were normalised for specific binding and the percentage shown. The error bars indicate SD and a representative curve is shown. A mean Ki was determined for three independent experiments and reported in Table 5.

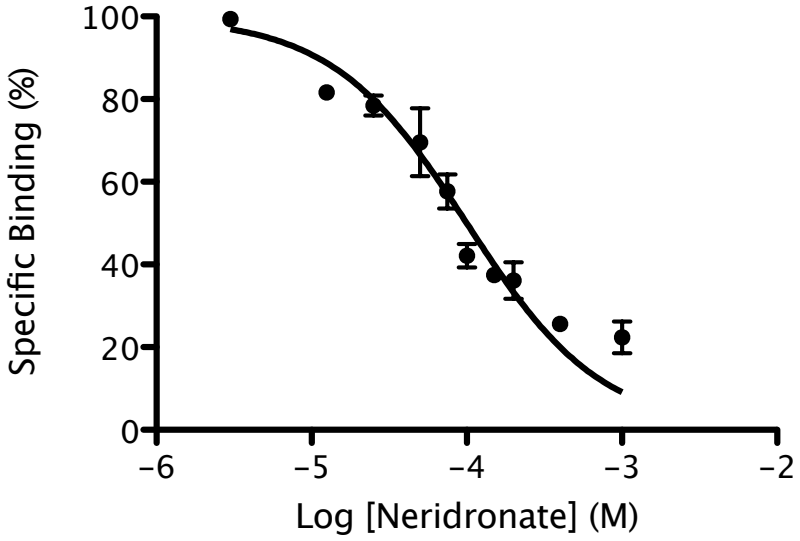

Figure 50 Competitive binding of neridronate with 5(6)-FAMRIS to HAP.

5(6)-FAMRIS (3 μM) was co-incubated with various concentrations of neridronate (3-1000 μM), as indicated in the inset key. Results were analysed with Graphpad Prism software using a one-site competition model. The data were normalised for specific binding and the percentage shown. The error bars indicate SD and a representative curve is shown. A mean Ki was determined for three independent experiments and reported in Table 5.

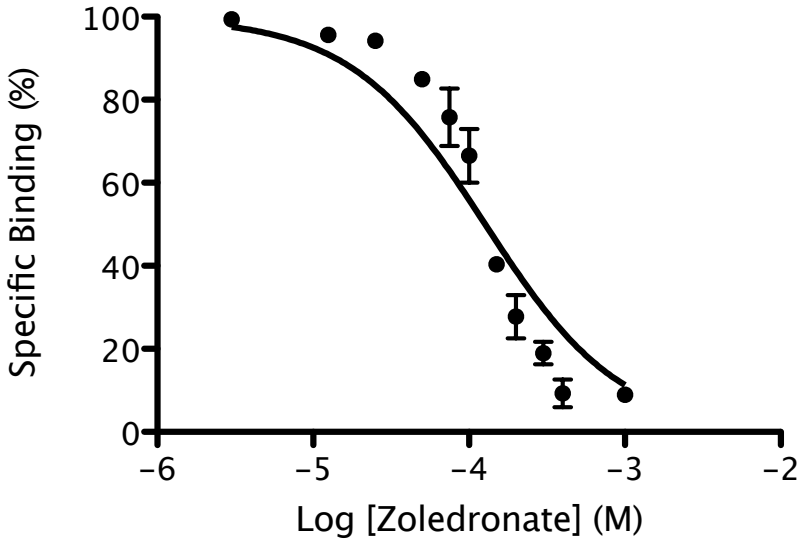

Figure 51 Competitive binding of zoledronate with 5(6)-FAMRIS to HAP.

5(6)-FAMRIS (3 μM) was co-incubated with various concentrations of zoledronate (3-1000 μM), as indicated in the inset key. Results were analysed with Graphpad Prism software using a one-site competition model. The data were normalised for specific binding and the percentage shown. The error bars indicate SD and a representative curve is shown. A mean Ki was determined for three independent experiments and reported in Table 5.

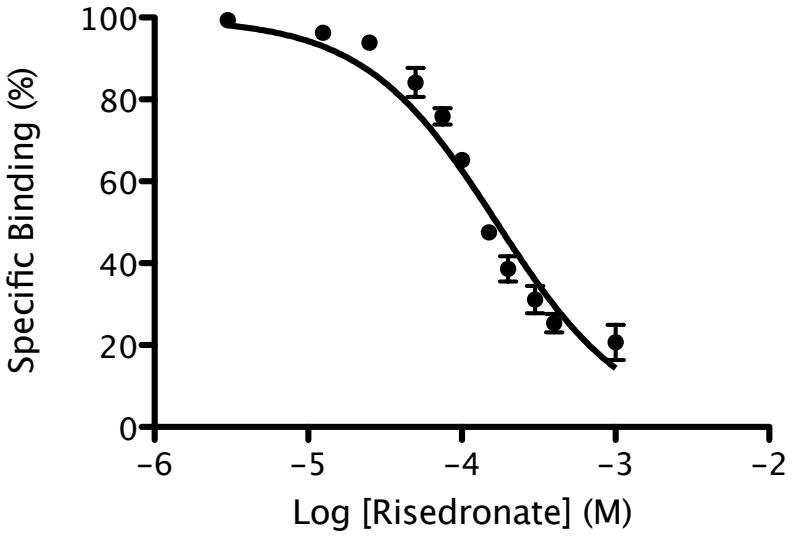

Figure 52 Competitive binding of risedronate with 5(6)-FAMRIS to HAP.

5(6)-FAMRIS (3 μM) was co-incubated with various concentrations of risedronate (3-1000 μM), as indicated in the inset key. Results were analysed with Graphpad Prism software using a one-site competition model. The data were normalised for specific binding and the percentage shown. The error bars indicate SD and a representative curve is shown. A mean Ki was determined for three independent experiments and reported in Table 5.

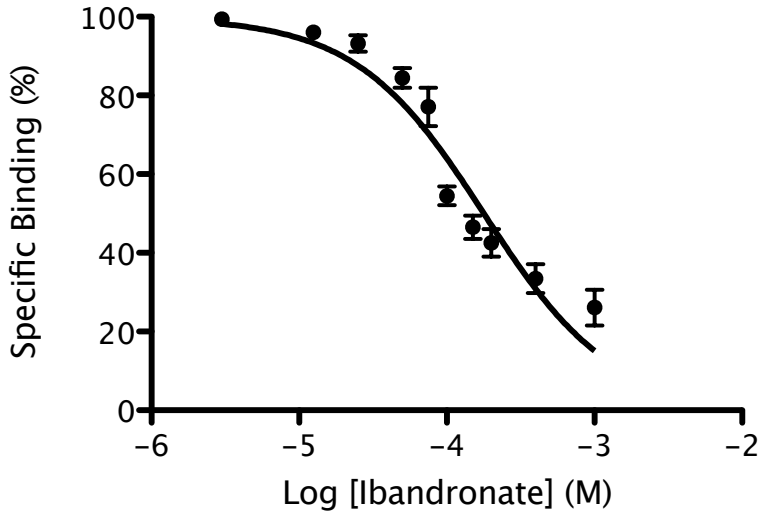

Figure 53 Competitive binding of ibandronate with 5(6)-FAMRIS to HAP.

5(6)-FAMRIS (3 μM) was co-incubated with various concentrations of ibandronate (3-1000 μM), as indicated in the inset key. Results were analysed with Graphpad Prism software using a one-site competition model. The data were normalised for specific binding and the percentage shown. The error bars indicate SD and a representative curve is shown. A mean Ki was determined for three independent experiments and reported in Table 5.

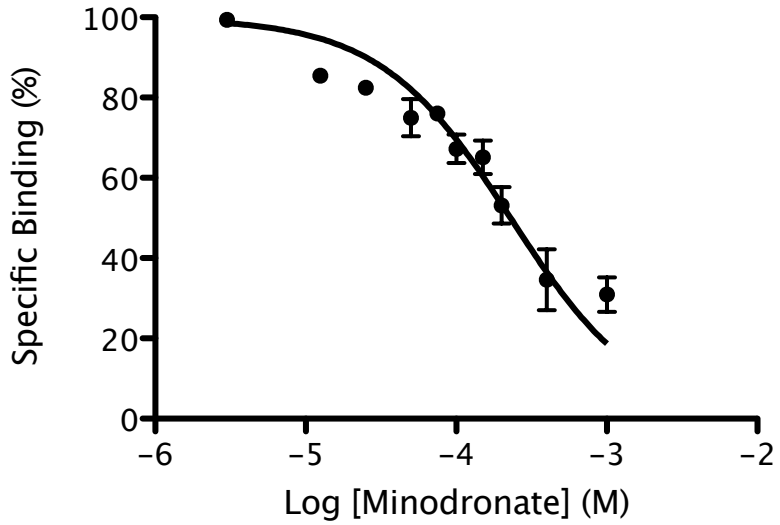

Figure 54 Competitive binding of minodronate with 5(6)-FAMRIS to HAP.

5(6)-FAMRIS (3 μM) was co-incubated with various concentrations of minodronate (3-1000 μM), as indicated in the inset key. Results were analysed with Graphpad Prism software using a one-site competition model. The data were normalised for specific binding and the percentage shown. The error bars indicate SD and a representative curve is shown. A mean Ki was determined for three independent experiments and reported in Table 5.

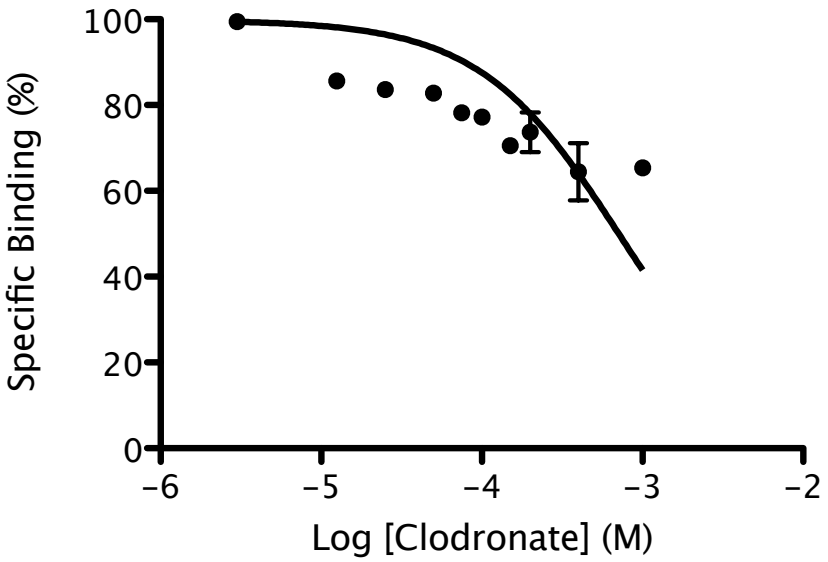

Figure 55 Competitive binding of clodronate with 5(6)-FAMRIS to HAP.

5(6)-FAMRIS (3 μM) was co-incubated with various concentrations of clodronate (3-1000 μM), as indicated in the inset key. Results were analysed with Graphpad Prism software using a one-site competition model. The data were normalised for specific binding and the percentage shown. The error bars indicate SD and a representative curve is shown. A mean Ki was determined for three independent experiments and reported in Table 5.

Table 5 Relative affinities (Kis) of BPs for HAP.

BP	Ki (μM)	SD
PAM	32.01	1.01
ALN	62.62	2.76
ETI	65.13	2.20
NER	83.06	9.61
ZOL	105.6	16.29
RIS	139.9	5.09
IBN	148.2	9.69
MIN	190.8	25.27
CLO	591.7	98.84

As summarised in Figure 56, each of the BPs showed an ability to inhibit 5(6)-FAMRIS binding to HAP. However, differences in mineral-binding affinities exist between the BPs, represented by Kis falling between 32.01 and 591.7 μM. Interestingly, the binding pattern of BPs observed in this study at pH 7.4 is in agreement to the results we found using the FPLC approach, i.e., the alkyl-amino BPs (pamidronate, alendronate and neridronate) and etidronate displayed the highest binding with Kis lower than 100 μM, the heterocyclic N-BPs (zoledronate, risedronate and minodronate) and ibandronate had intermediate Kis ranging between 100-200 μM, while the BP without the R1-OH group (clodronate), showed the lowest affinity at competing 5(6)-FAMRIS from binding to HAP (Ki=591.7 μM). Above all, our data once again support the hypothesis that the R2 side chain of BPs contributes to the mineral binding of BPs, suggesting the nitrogen position in the alkyl chain or within the pyridyl ring may play an important role in the different binding affinities of BPs.

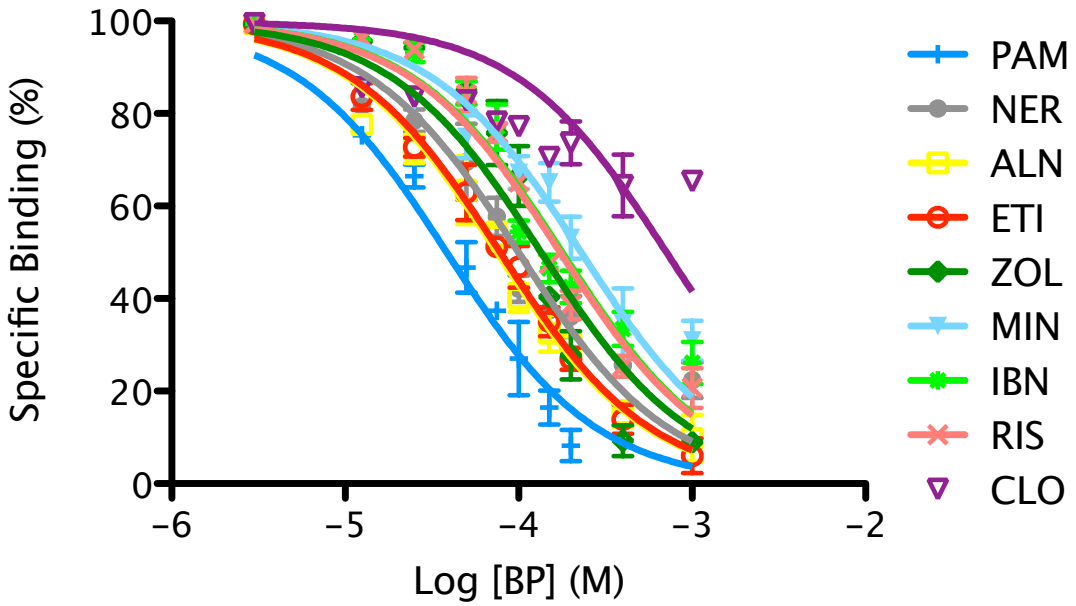

Figure 56 Competitive binding of clinically used BPs with 5(6)-FAMRIS to HAP.

5(6)-FAMRIS (3 μM) was co-incubated with various clinically used BPs (3-1000 μM), as indicated in the inset key. Results were analysed with Graphpad Prism software using a one-site competition model. The data were normalised for specific binding and the percentage shown. The error bars indicate SD and a representative curve is shown. A mean Ki was determined for three independent experiments and reported in Table 5.

4.3 Discussion

Langmuir adsorption isotherms have been widely applied to quantitatively estimate interactions between macromolecules and mineral interfaces [148]. The attachment and release of BPs on bone mineral surfaces is considered as a dynamic reversible process illustrated by the adsorption isotherm. HAP is an ionic compound with Ca^{2+}, PO_4^{3-}, and OH^- ions presented on its surface. In the chromatographic adsorption experiments, we found that discrete levels of PO_4^{3-} were required to elute BPs from HAP, indicating a displacement by phosphate groups of binding by one or both of the phosphonate residues on BPs. BPs show a high affinity for the

Ca^{2+} ions, thus coordination of the BPs on the Ca^{2+} ion on the surface and/or substitution of the surface phosphate anions are believed to be the main mechanism of the adsorption [144, 149]. In addition, there are other physicochemical properties of the N-BPs that may be important for their effects on HAP, for example the molecular charges on the nitrogen atom in the R2 side chain of the N-BPs may influence binding capacity of BPs on HAP as revealed by adsorption isotherms [127]. The adsorption of BP is, however, mainly explained as a bidentate coordination via two phosphonate oxygen atoms or tridentate coordination via two phosphonate oxygen atoms and a hydroxyl or amino group bound at the α-carbon atom [143] (Figure 57). On the other hand, the release of BPs from bone occurs via at least two mechanisms, namely physicochemical desorption and osteoclastic resorption.

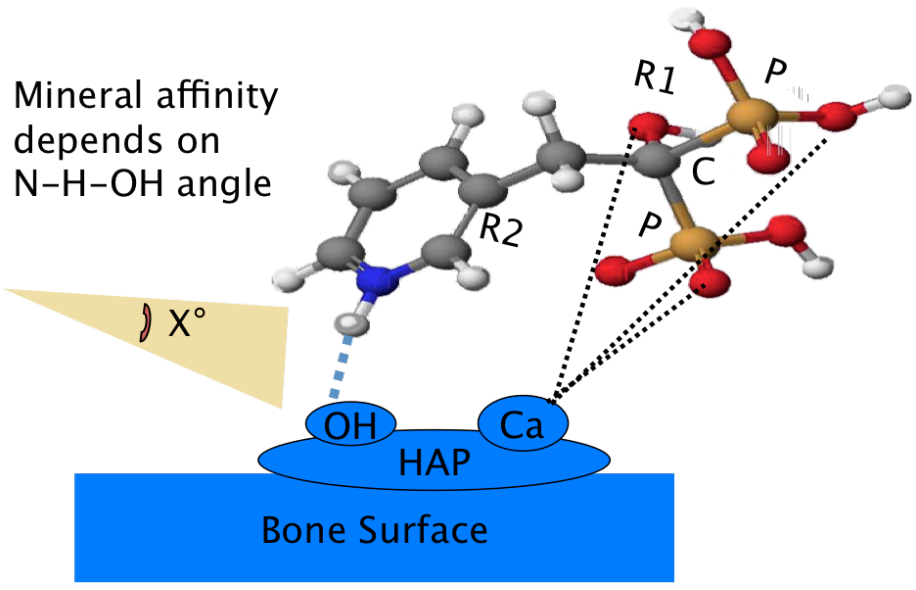

Figure 57 BP binds to bone mineral HAP.

This study, began by examining the equilibrium bone mineral-binding affinities of pamidronate, risedronate, ibandronate, clodronate and 5(6)-FAMRIS by means of Langmuir adsorption isotherms. Unlike the FPLC method, which does not allow for ready calculation of affinity constants, with this approach, we quantitatively estimated the interactions between BPs and HAP surfaces. Interestingly, we found that the binding affinities of pamidronate, risedronate and ibandronate were very similar, compared with the significant lower affinities of clodronate and 5(6)-FAMRIS. The lower affinities of clodronate and 5(6)-FAMRIS were also revealed by the FPLC method, probably due to the lack of R1-OH group and the addition of fluorophore that lowers the affinity of the parent drug, respectively. It is important to note that the Kd of 5(6)-FAMRIS was determined to be 14.56 μM, which was used to calculate the Kis of unlabelled BPs by the competitive binding assays. In addition, the risedronate and ibandronate 2-in-1 versus 1-in-1 competitive adsorption isotherms not only proved the BP binding to HAP is saturable and competitive in our experimental setup, but also supported the findings from our FPLC study that risedronate and ibandronate had similar affinities for HAP at pH 7.4. Altogether, the fact that BP binding to HAP can be described by the Langmuir adsorption isotherm is intriguing and suggests that BP interacts with HAP surfaces as interacting units with defined capacity and affinity.

In further studies, we assessed the mineral-binding affinities of nine clinically used BPs by using the adsorption isotherm-based competitive binding assays. With the competitive binding assays, it was shown that most BPs bearing a hydroxyl at R1 had an affinity for HAP within the range of 32-190 μM. On the other hand, clodronate remained at the weak end of the affinity spectrum. The BP with highest affinity for HAP was pamidronate, followed by alendronate, etidronate, neridronate, zoledronate, risedronate, ibandronate, minodronate and clodronate. Interestingly, this rank order is identical to the relative binding affinities measured towards HAP by previous NMR-based competition assay [129]. With the NMR-based competition assay, the affinity span between alendronate and ibandronate for HAP was a factor of 2.1, which is similar to 2.37 found in our study. In addition, the data from the competition assays are in general agreement with our FPLC results measured at the same pH, although there are slight differences in the ranking of risedronate, ibandronate and minodronate. Moreover, Nancollas *et al.* established indirectly a significant difference in the kinetic binding affinity (i.e., the binding of BP molecules during crystal growth) of several BPs to HAP surfaces. Finally, differences in the binding capacities between BPs have been observed with the following rank order at pH 7.4: risedronate < zoledronate < ibandronate < etidronate < alendronate [22], possibly attributed to various physicochemical properties of the N-

BPs including binding affinity, molecular charge and interfacial tension [11].

With regard to reported investigations of BPs binding to bone, competitive binding studies of radiolabelled BPs to fetal mouse bones or to bone powder showed only small differences for the clinically relevant BPs [131]. Also, NMR studies have been used to probe how different BPs bind to bone and a model has been proposed in which a BP-PO_3^{2-} group displaced Pi, while the cationic side chains interacted electrostatically with anionic surface groups [144]. Later, the detailed thermodynamic description of the binding of BPs to human bone was investigated further, by using isothermal titration calorimetry (ITC). The ITC results showed that there were two binding sites of BP to bone, with binding to each based on the structural features present in each molecule, which suggests the importance of R1-OH group for bone mineral binding. The binding strength was shown to be alendronate > pamidronate > zoledronate > risedronate and thought to be attributed to the pKa values of the side chains [150].

In general, the rank order for affinity of the various BPs for HAP differs vs. that for bone, although in both model systems, clodronate stands out as having significantly weaker affinity compared with the hydroxy-bearing BPs. These differences are likely due to differences in methodology and

the composition of the binding surface (natural bone vs. HAP crystal). Even though HAP is related to bone mineral in bone, it lacks both surface and embedded protein components, such as type I collagen and specific non-collagenous moieties that may modify the different BP binding properties. Despite these differences, the general agreement is noteworthy and the results of all these investigations contribute to a fuller understanding of interactions between BPs and bone/bone mineral that are likely to be of major importance in a clinical context.

CHAPTER 5 EFFECT OF BISPHOSPHONATES ON APOPTOSIS IN OSTEOCYTES AND OSTEOBLASTS

5.1 Introduction

The biological potencies of BPs with respect to bone metabolism and treatment of bone disease are thought to be related mainly to their binding affinities for bone mineral and their inhibitory actions on osteoclasts. Recent literature, reviewed in Chapter 1, suggests that osteocytes may also be important target cells for BPs in bone [77].

BPs, at sub-micromolar concentrations, have been shown to have protective effects on osteocytes and osteoblasts, thought to involve novel membrane actions of the BPs on connexin 43 hemi-channels, and subsequent activation of the extracellular signal-regulated kinases (ERKs) signalling pathway (Figure 58) [151]. It is also worth noting that the potential effect of BPs on osteocyte apoptosis at low doses is independent of their particular structure [23, 24]. However, most studies of this possible mechanism are reported from the same research group [28, 77, 151-154], hence many of these observations remain to be independently verified.

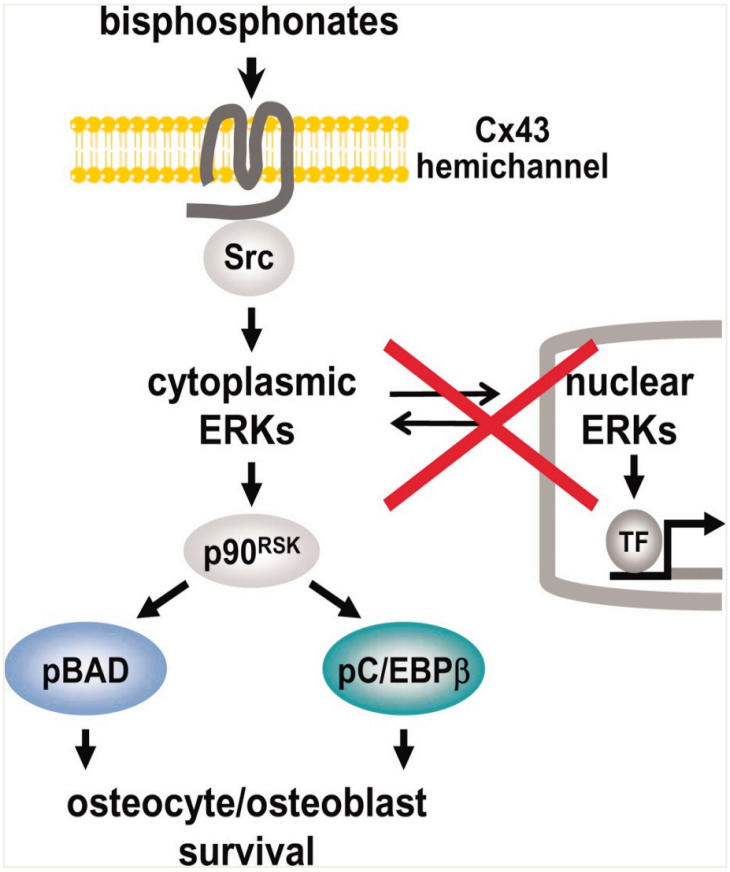

Figure 58 Anti-apoptotic effect of BPs on osteocytes (MLO-Y4 cells) [28].

In this study, the specific aims are 1) to examine the ability of risedronate (a nitrogen-containing BP) and etidronate (a simple BP) to exert anti-apoptotic effects on osteocytes and osteoblasts, and 2) to understand the possible prosurvival signalling pathways involved in these cells.

5.2 Results

5.2.1 Nick Translation (NT) assay

Earlier studies have demonstrated that apoptosis of osteocytic MLO-Y4 cells and osteoblastic 2T3 cells is inhibited by several BPs and this inhibition is independent of the anti-resorptive potencies of BPs on osteoclasts [77]. To verify these observations, the ability of risedronate, which inhibits FPPS, and etidronate, which does not inhibit FPPS, to prevent etoposide-induced apoptosis of osteocytes and osteoblasts were examined.

Osteocytes and osteoblasts were exposed to one hour pre-treatment with risedronate or etidronate at concentrations of 10^{-8} to 10^{-6} M, before adding 50 μM etoposide as apoptotic promotion agent for 24 h. As illustrated in the NT results, risedronate (10^{-6} M) (Figure 59) reduced the apoptosis induced by 24 h etoposide (50 μM) treatment by an average of 35.6%, in murine osteocytic MLO-Y4 cells. However, no significant effect of etidronate (Figure 60) or dose-dependent response of either BP on etoposide-induced apoptosis of osteocytic cells was observed, which cannot verify the findings of Plotkin *et al.* [77].

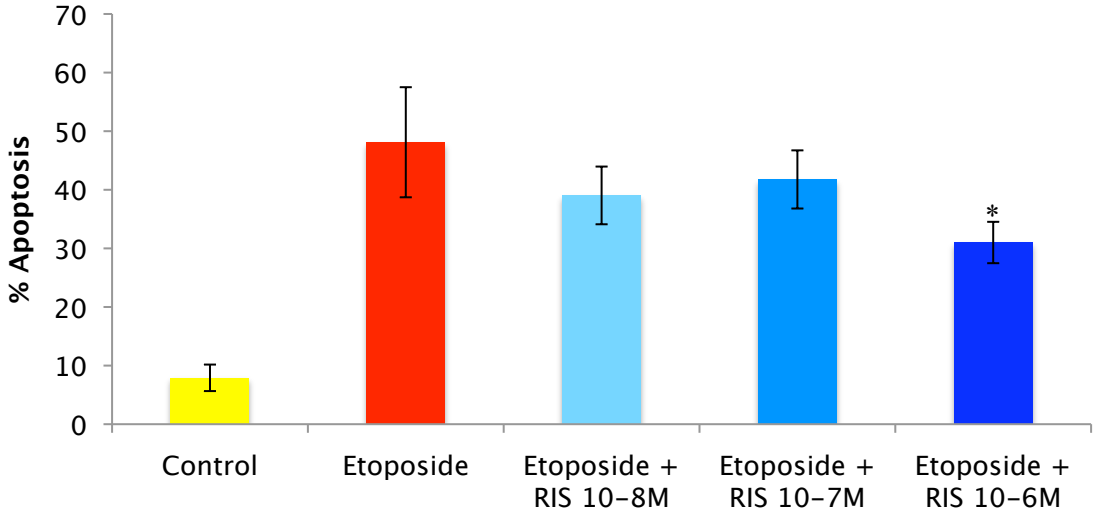

Figure 59 Protection by risedronate of apoptosis induced by etoposide in MLO-Y4 cells.

MLO-Y4 cells were pretreated with vehicle or the indicated concentrations of risedronate for 1 h, prior to the addition of 50 μM etoposide for 24 h. Apoptosis was assessed by NT assay in three replicas per condition. Results are expressed as percentage of apoptosis ± SD. One hour pre-treatment with risedronate (10^{-6} M) reduced the apoptosis induced by etoposide treatment by an average of 35.6% in MLO-Y4 cells. * $p<0.05$ compared to etoposide (50 μM)-treated cultures by one-way ANOVA followed by Dunnett's Multiple Comparison Test.

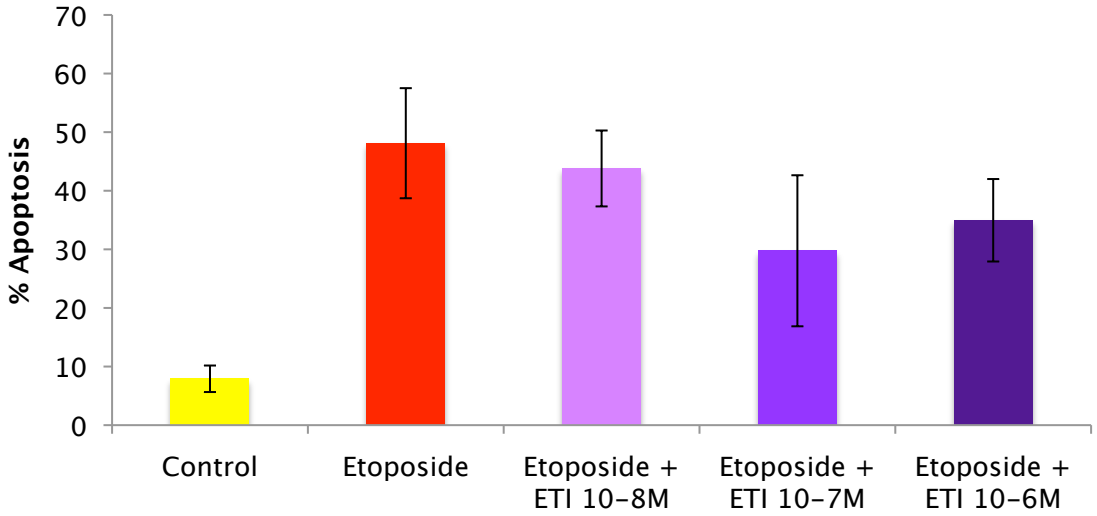

Figure 60 Protection by etidronate of apoptosis induced by etoposide in MLO-Y4 cells.

MLO-Y4 cells were pretreated with vehicle or the indicated concentrations of etidronate for 1 h, prior to the addition of 50 μM etoposide for 24 h. Apoptosis was assessed by NT assay in three replicas per condition. Results are expressed as percentage of apoptosis ± SD. There was no significant reduction in apoptosis induced by etoposide treatment with etidronate at any concentration tested in MLO-Y4 cells.

With respect to osteoblastic 2T3 cells, surprisingly, all doses of risedronate (Figure 61) and etidronate (Figure 62) did not show any anti-apoptotic effect. Under these circumstances, the percentage of apoptotic cells in cultures treated with etoposide and BPs is not statistically different from the percentage of apoptotic cells in cultures treated with etoposide alone.

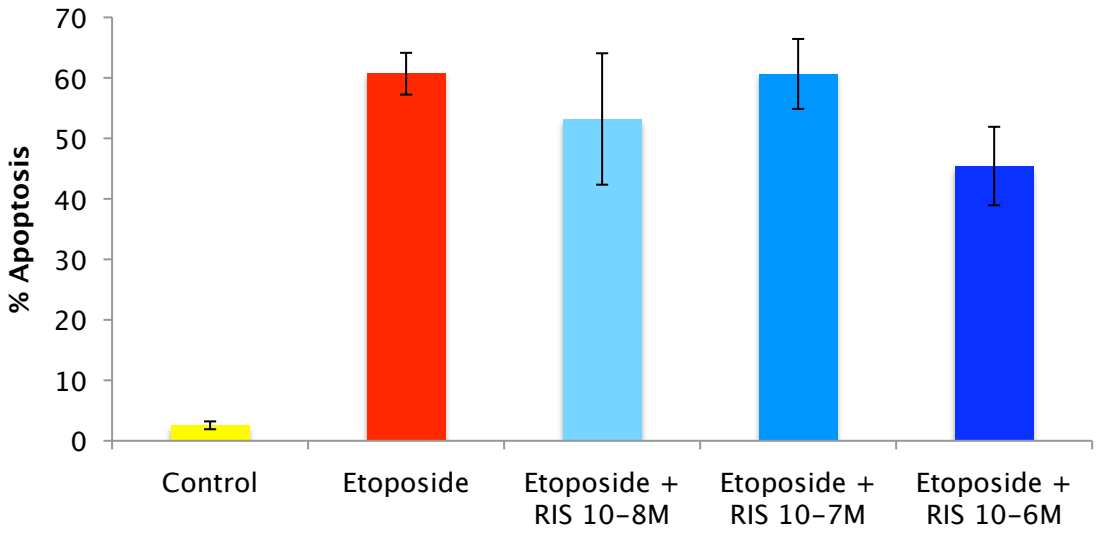

Figure 61 Protection by risedronate of apoptosis induced by etoposide in 2T3 cells.

2T3 cells were pretreated with vehicle or the indicated concentrations of risedronate for 1 h, prior to the addition of 50 µM etoposide for 24 h. Apoptosis was assessed by NT assay in three replicas per condition. Results are expressed as percentage of apoptosis ± SD. There was no significant reduction in apoptosis induced by etoposide treatment with risedronate at any concentration tested in 2T3 cells.

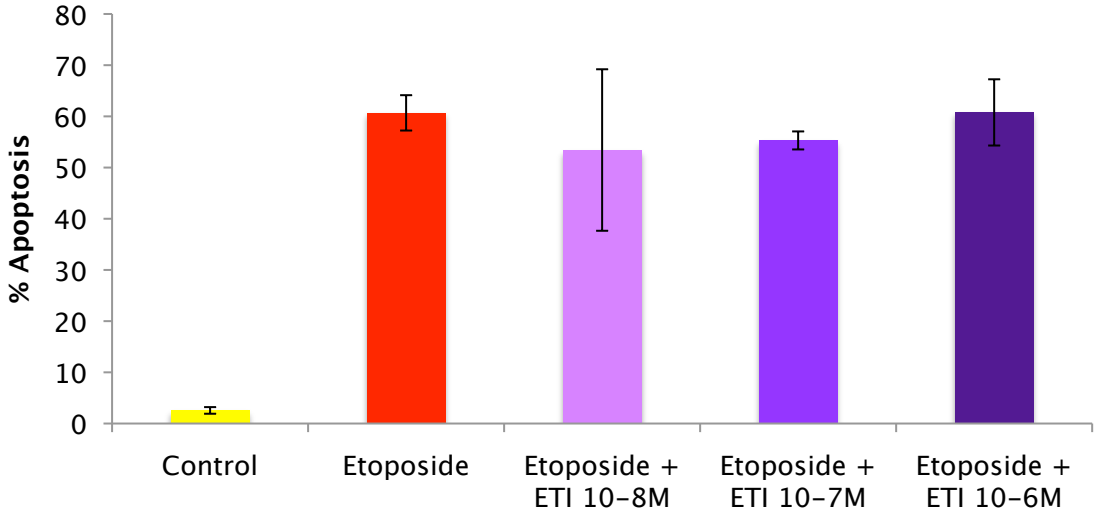

Figure 62 Protection by etidronate of apoptosis induced by etoposide in 2T3 cells.

2T3 cells were pretreated with vehicle or the indicated concentrations of etidronate for 1 h, prior to the addition of 50 μM etoposide for 24 h. Apoptosis was assessed by NT assay in three replicas per condition. Results are expressed as percentage of apoptosis ± SD. There was no significant reduction in apoptosis induced by etoposide treatment with etidronate at any concentration tested in 2T3 cells.

5.2.2 TUNEL staining

In order to confirm the investigation described in 5.2.1 by cell morphology, osteocytic MLO-Y4 cells, grown on coverslips, were subjected to one hour pre-incubation with risedronate (10^{-6} M) and etidronate (10^{-7} M) followed by etoposide (50 μM) treatment for 24 h. TUNEL, cell morphology, and DAPI counter-staining were used to assess the average percentage of apoptotic cells in each condition.

Representative images show that etoposide (50 μM) visibly induced osteocyte apoptosis after 24 h, indicated by the increase in positive TUNEL staining (Figure 63b) compared to the control (Figure 63a). In etidronate (Figure 63c) and particularly in risedronate (Figure 63d) pre-

treatment conditions, the percentages of positive TUNEL-stained cells as well as those exhibiting typical apoptotic morphology were apparently reduced. However differences in the numbers of cells remaining on the coverslips at the end of the procedure meant that differences were not significant (Figure 64).

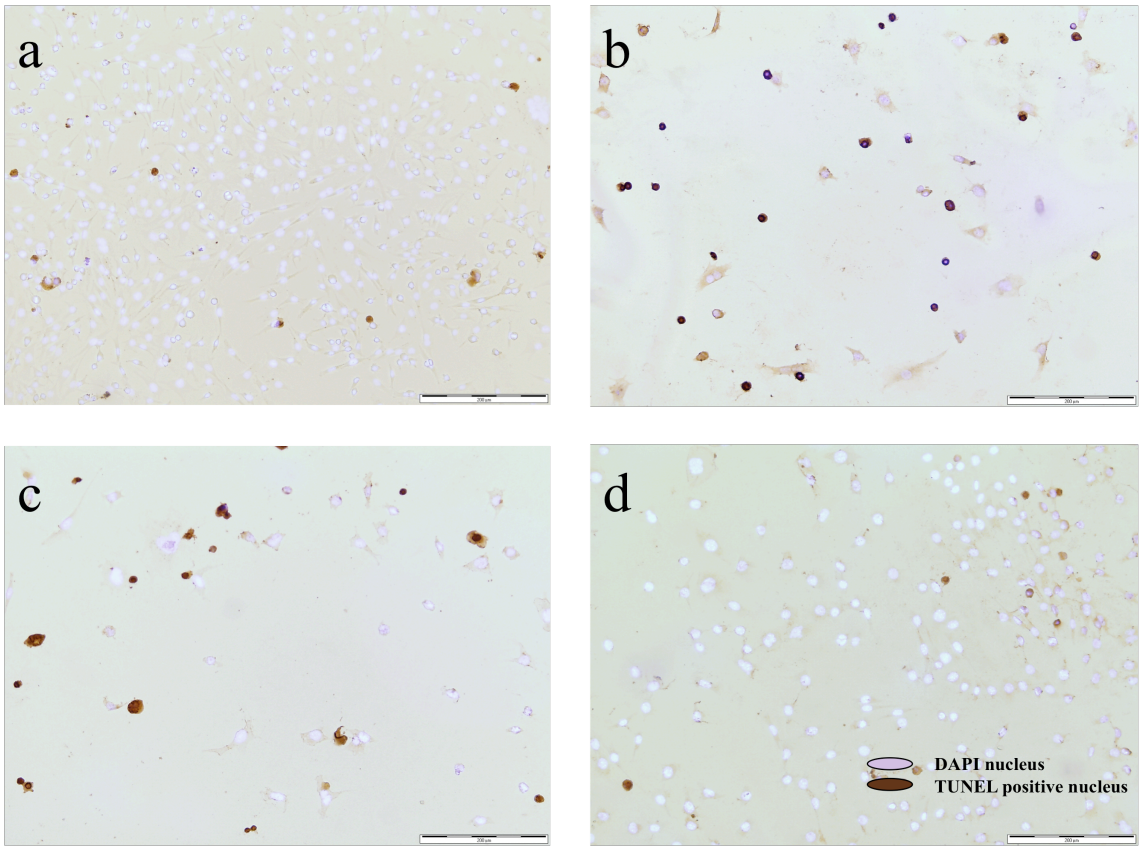

Figure 63 TUNEL/DAPI double staining of MLO-Y4 cells after 24 h treatment.

(a) Control conditions; (b) etoposide (50 µM); (c) etoposide (50 µM) treatment in the presence of etidronate (10^{-7} M); (d) etoposide (50 µM) treatment in the presence of risedronate (10^{-6} M). Representative merged light and fluorescent images at 10x magnification are shown for each condition. The scale bar represents 200 µm.

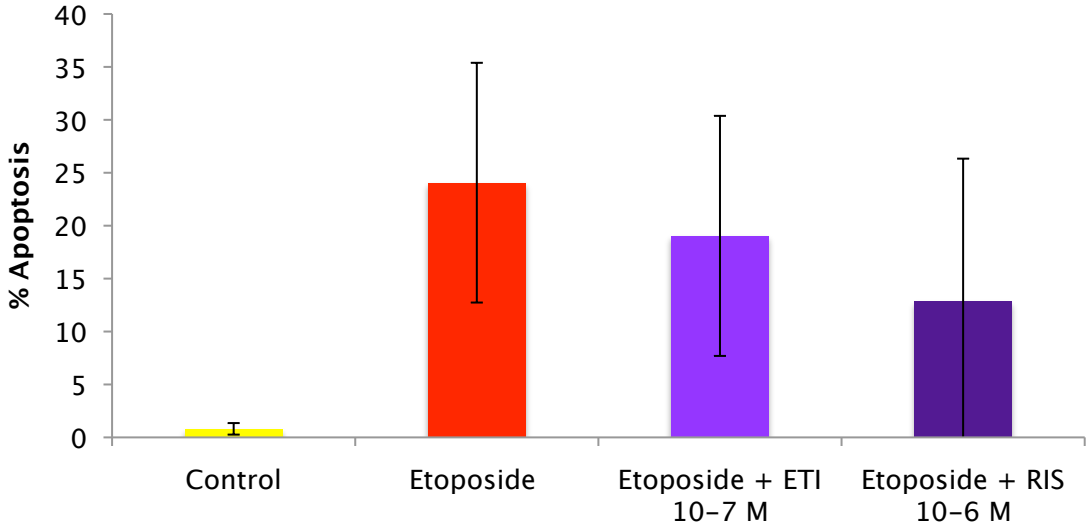

Figure 64 Protection by BPs of apoptosis induced by etoposide in MLO-Y4 cells.

Using cell counts to measure apoptosis, one hour pre-treatment with etidronate (10^{-7} M) and risedronate (10^{-6} M) reduced the apoptosis induced by 24 h etoposide (50 μM) treatment by approximately 20.8% and 46.3% in MLO-Y4 cells. Averages are given as mean ± SD, n=5 per condition.

5.2.3 Western blotting

It has been reported that the mechanism of the anti-apoptotic effect of BPs involves action of ERKs, members of the MAP kinase family that enhance cell survival [154]. To evaluate activation of the ERK pathway, osteocytes and osteoblasts grown on 10 cm^2 plates were treated with 10^{-8} M risedronate for 5, 30 or 60 minutes. A positive control sample of 20% FCS was also included for each time point. Densitometric analysis was performed on the blots. Background was subtracted from each protein band of interest, and values for the phospho-ERK were normalised to total ERK values. Protein expression is reported as a fold change compared to control.

Unlike observed by previous studies that BPs can induce rapid increase in the phosphorylation of ERK in osteocytic MLO-Y4 cells [154], the Western blotting results show that risedronate at a concentration of 10^{-8} M induces no detectable increase in expression of phospho-ERK in MLO-Y4 cells or in 2T3 cells (Figures 65 and 66). In contrast, 20% FCS as a control induced a significant increase in phosphorylation during the time course we studied.

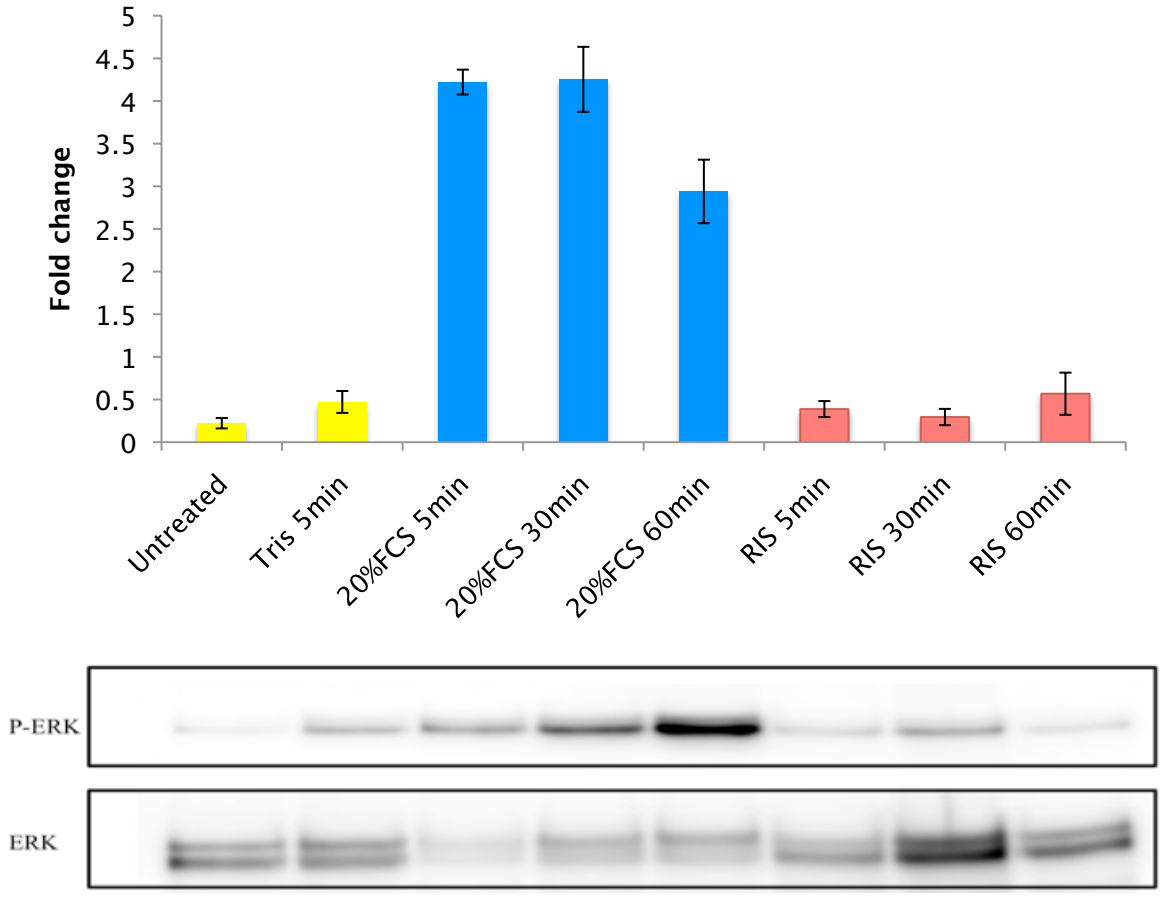

Figure 65 ERK activation in MLO-Y4 cells.

Western blot analysis showed that treatment with risedronate (10^{-8} M) induced no detectable increase in expression of phosphorylation of ERK in MLO-Y4 cells. The blots were probed with antibodies to phospho-ERK. Results were normalised to levels of ERK total protein. Signal quantifications of blots were performed using ImageJ software. 20% FCS was used as a positive control. Results are representative of three independent experiments.

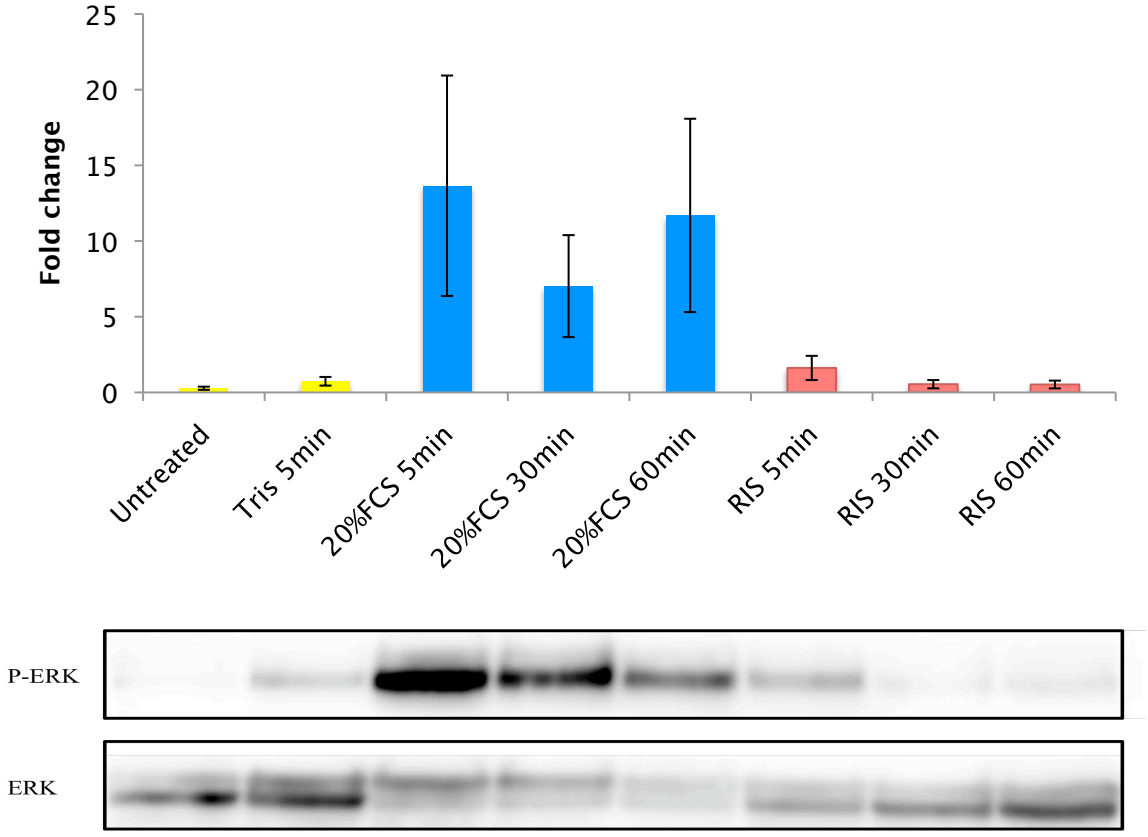

Figure 66 ERK activation in 2T3 cells.

Western blot analysis showed that treatment with risedronate (10^{-8} M) induced no detectable increase in expression of phosphorylation of ERK in 2T3 cells. The blots were probed with antibodies to phospho-ERK. Results were normalised to levels of ERK total protein. Signal quantifications of blots were performed using ImageJ software. 20% FCS was used as a positive control. Results are representative of three independent experiments.

5.3 Discussion

It has been reported recently by Plotkin *et al.* that the anti-apoptotic effects of BPs on osteoblasts and osteocytes are distinct from their anti-resorptive effects on osteoclasts. All 16 BPs they tested were able to demonstrate anti-apoptotic activity in MLO-Y4 cells, with maximal effects at 10^{-8} M which is 3-4 orders of magnitude below that required to induce osteoclast apoptosis [77]. *In vivo* data from Follet *et al.* validated Plotkin's

studies on mice treated with glucocorticoids, showing that BPs can suppress osteocyte apoptosis induced from fatigue loading at doses below those equivalent to doses used for the clinical treatment of osteoporosis [78]. Moreover, studies from Plotkin *et al.* and Kogianni *et al.* both show evidence that amino-olpadronate, a BP lacking anti-resorptive activity, suppresses osteocyte/osteoblast apoptosis [77, 155]. Therefore, it is proposed that BPs act on cells from the osteoblastic and osteoclastic lineages via two different mechanisms [77, 155].

From our *in vitro* study in which osteocyte and osteoblast apoptosis was significantly increased by etoposide, we have shown evidence by using Nick Translation assay that a N-BP risedronate at 10^{-6} M provided protection against osteocytic MLO-Y4 cells apoptosis. This effect is in line with the findings from other groups showing low doses of BPs suppressed osteocyte and osteoblast apoptosis [77, 155]. However, apart from that, no other doses of risedronate and etidronate showed any protective effect on MLO-Y4 cells and 2T3 cells from our study. Furthermore, TUNEL staining was used as a complementary detection method to confirm apoptosis, however, the high SDs of the cell count resulting from the TUNEL staining are largely due to the limitations of the staining techniques used to detect apoptosis. For example, many cells (2-5 x 10^6/test) are required for each condition and during fixation and the subsequent washing procedures, the number of cells lost cannot be

quantified. It is possible to lose the specific cell population that is of interest. In addition, the apoptotic process is transient and TUNEL staining detects nuclear DNA strand breaks that happen at the final stages of apoptosis but not the initial stages of apoptosis, so the incidence of apoptosis might be underestimated. Therefore, it is difficult to interpret the findings from this technique and the use of TUNEL alone to detect the presence of apoptosis is not sufficient. Well-defined and reproducible experimental systems that are cell specific are needed for future work. Only then will we be able to further study the potential protection by BPs on osteocytes and osteoblasts apoptosis.

It has been suggested that BPs attenuate osteocyte apoptosis by phosphorylating ERK, which may be mediated by the opening of connexin 43 hemichannels in the plasma membrane [153, 154]. In our study, risedronate at a concentration of 10^{-8} M has been used to test this hypothesis. However, results from Western blotting studies did not show any significant phosphorylation of ERK in MLO-Y4 and 2T3 cells. This could be due to limitations of the technique such as the requirement of a similar amount of protein loaded onto the gel per sample or the concentration of BPs used. Conditions required to achieve the maximal anti-apoptotic effect need to be optimised. Although protection from apoptosis may involve the rapid phosphorylation of ERK, through the opening of connexin 43 hemichannels, other mechanisms are likely to be

involved. For example, It is possible that not all BPs have the same anti-apoptotic effect through connexin 43 [156]. In addition to the activity through gap junction or hemichannels, connexin 43 can influence cell survival, differentiation, and/or function of bone-forming cells by functioning as a docking platform for signalling molecules [156]. Romanello *et al.* have suggested an alternative mechanism, besides connexin 43 hemichannel opening, to explain the activating effects of BPs on ERKs [157]. It was found that BPs may affect osteoblasts through nucleotide receptors signalling leading to ERKs activation and induce the expression of a heat shock protein, Hsp90 [157]. It is also possible that osteoblast apoptosis occurs through an extrinsic pathway that involves the binding of the Fas Ligand (FasL) to Fas, its cell-surface receptor. Interruption of this pathway appeared to be important in the prevention of apoptosis [155]. Studies by Kogianni *et al.* have shown that glucocorticoids can induce osteocyte apoptosis through increased cell membrane localisation of Fas, while BP treatments can both reduce apoptosis and decrease localisation of Fas in the cell membrane [155]. Finally, the protective effects of BPs on osteocytes and osteoblasts apoptosis may involve other signalling pathways such as SMAD, Akt or a pathway involving integrin-mediated activation of Src kinase.

CHAPTER 6 GENERAL DISCUSSION

BPs are preferentially taken up by the skeleton and decrease osteoclast-mediated bone resorption [73]. The differences in mineral-binding affinities among the clinically used BPs play a critical role in determining their intracellular potencies, with consequent effects on dosing and efficacy. Over the past decade, the ranking of BPs according to their binding affinities towards HAP or bone powder have been studied using a variety of methodologies (Table 6). In spite of the differences in experimental setup, composition of binding surfaces, and readout parameters, the findings from all these studies allow us some general conclusions on this topic. In this thesis, the mineral-binding affinities of nine clinically relevant BPs with different mechanisms of action and different anti-resorptive potencies have been compared by using novel approaches such as HAP FPLC combined with MS and Langmuir adsorption isotherm-based fluorescence competitive binding assays. The results obtained are in general comparable with and add substantially to the previous studies and furthermore have given new insights into this research area.

Table 6 Comparison of the HAP affinity rank orders of BPs generated by different methods at pH 7.4.

BP affinity rank order (High to low)	HAP FPLC (This thesis)	Fluorescence competitive binding assay (This thesis)	NMR-based competitive binding assay [129]	Constant composition kinetic studies of HAP crystal growth [127]
1	PAM	PAM	PAM	ZOL
2	ALN	ALN	ALN	PAM
3	NER	ETI	ZOL	ALN
4	ETI	NER	RIS	IBN
5	ZOL	ZOL	IBN	RIS
6	IBN	RIS		ETI
7	MIN	IBN		CLO
8	RIS	MIN		
9	CLO	CLO		

It is important to note that the structural differences among BPs lead to differences in their physicochemical and pharmacological properties [81, 82]. With regard to the adsorption affinity for bone mineral and biochemical potency on FPPS, BPs used clinically can be ranked in order based on:

• Mineral affinity (based on HAP FPLC study): clodronate < risedronate < minodronate < ibandronate < zoledronate < etidronate < neridronate < alendronate < pamidronate

• FPPS enzyme inhibition: etidronate = clodronate (extremely weak inhibitors) <<< pamidronate < alendronate < ibandronate < risedronate < zoledronate [158, 159]

The differences in mineral-binding affinities among BPs would predict that the skeletal uptake and distribution between trabecular and cortical bone, and also within individual bones to be correspondingly different (Figure 67). BPs with higher affinity will bind avidly to the bone surface once they exit from the circulation, have a low desorption, and less diffusion in bone [70, 81] (Figure 68). On the contrary, lower affinity BPs will undergo weaker uptake, have lower attachment, higher desorption, and distribute more widely through the bone [81, 160]. Access to cortical rather than trabecular sites and to sites which are at a greater distance from vascular channels within bone, e.g., in the osteocytes network, may

be greater for the BPs that have lower mineral-binding affinity [70, 81, 82]. In addition, they may be of relevance in affecting non-resorbing cells. Such low affinity BPs may be useful therapeutically in situations when reduced drug retention is required. These may include paediatric use [161], situations concerning short-term skeletal retention of BPs, and be of value in limiting possibilities of interference with the anabolic response to PTH when combination therapies are required [162], or in treatment of cancers when favourable effects of BPs are due to direct effects on the cancer cells [163].

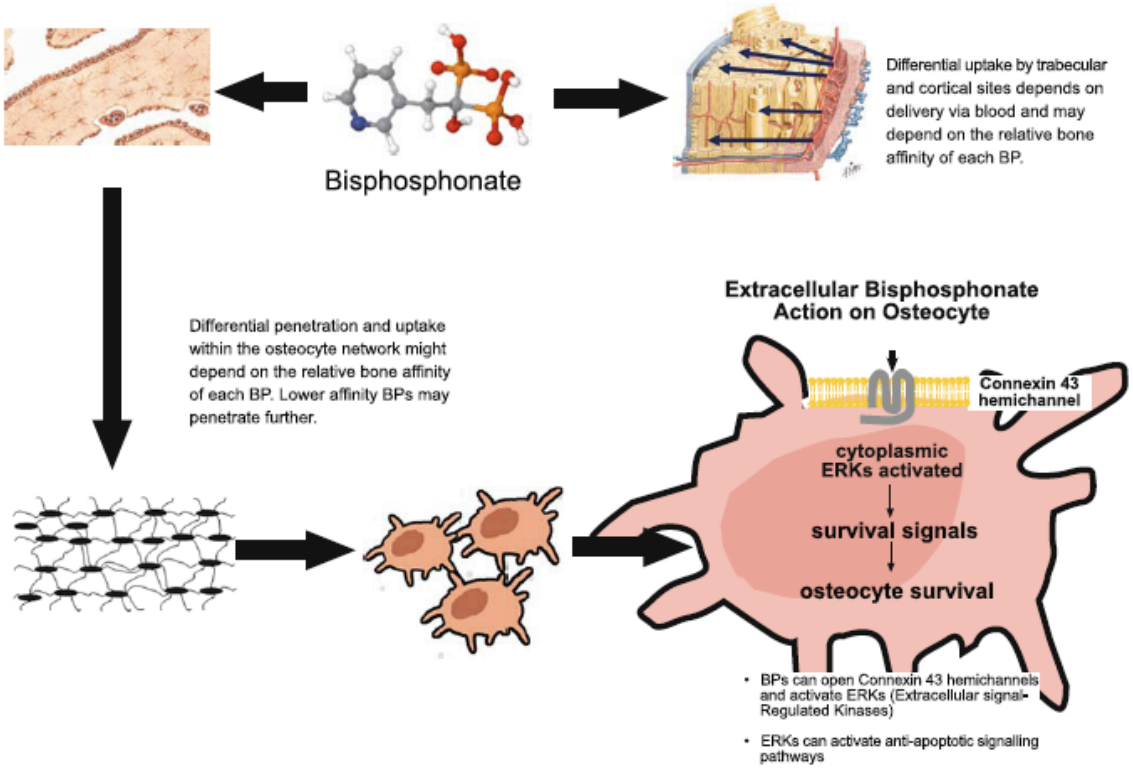

Figure 67 Proposed mechanism of BP uptake and distribution in bone [69].

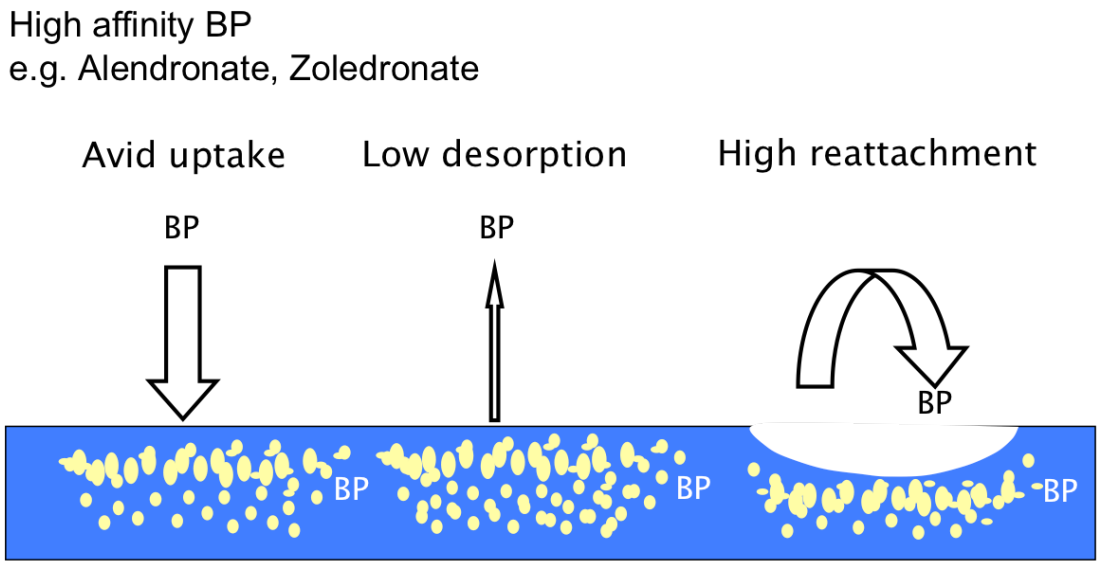

Figure 68 Effect of high binding affinity on recirculation of BP on and off bone surfaces. High affinity BPs may diffuse less well in bone and remain nearer accessible surfaces [127].

It is reassuring that the data from clinical studies have confirmed that there are clinically meaningful differences among the various BPs in terms of relative potency and efficacy, uptake in cortical vs. trabecular bone, types of antifracture effect (vertebral vs. nonvertebral), and the speed of onset and offset of action (Figure 69) [70, 81, 82]. All of the BPs approved for treatment of osteoporosis (i.e., alendronate, risedronate, zoledronate, and ibandronate) are effective against vertebral fractures in RCTs since trabecular bone is accessible to them all, whereas all of these agents except ibandronate have shown to reduce the risk of nonvertebral and hip fractures, which may be more related to cortical bone and effects

varied among the BPs [34, 82]. In addition, high affinity BPs would likely to be associated with greater suppression of bone turnover and longer persistence of effect, such as that seen with alendronate and zoledronate [82]. On the other hand, the FPPS enzyme inhibitory potency of N-BPs correlates well with the pharmacological potency in animals and humans. To a degree, these differences also correlate with speed of fracture protection. As in the examples of zoledronate and risedronate, there reduction effect in vertebral fractures has been observed in less than 12 months, while this has not been observed for alendronate and ibandronate [69]. All those differences observed in clinical use could mostly be attributed to the unique physicochemical and biochemical profile of each BP [81, 82].

Fracture type	Risedronate[1-5]	Alendronate[7-10]	Ibandronate[11]	Zoledronate[12,13]
Vertebral Fracture Efficacy	√	√	√	√
Vertebral at 6 months	√	—	—	—
Nonvertebral Fracture Efficacy	√	√	—*	√
Nonvertebral at 6 months	√	—		—
Hip fracture efficacy	√	√	—	√
Hip at 6 months	√†	—	—	—

√ Data published — No Data published

risedronate:
1.Harris ST *et al*. JAMA 1999; 282:1344-1352
2. Roux C *et al*, CMRO 2004; 4:433-439
3. McClung M *et al*. NEJM 2001; 344:333-340
4. Reginster JY *et al*. Osteoporos Int 2000; 11:83-91
5. Harrington JT et al, CTI 2004; 74:129-135
6. Silverman S *et al*, Osteoporos Int 2007; 18: 25-34
† Observational study

alendronate:
7. Black D *et al*. JCEM 2000; 85:4118-24
8. Black D *et al* Lancet 1996; 348:1535-1541
9. Cummings S *et al* JAMA. 1998;280:2077-2082
10. Pols H *et al* Osteoporos Int 1999; 9:461-468

ibandronate:
11. Chesnut CH *et. al*. JBMR 2004; 19:1241-1249
* non-vertebral fractures: no statistically significant difference in ITT analysis; non-vert efficacy demonstrated in a subgroup with BMD < -3

zoledronate:
12. Black D *et al*, NEJM 2007; 356 (18):1809-1822
13. Black D *et al*, Bone 2009; 44: S241-242

Figure 69 Overall clinical profiles of BPs.

Differences between BPs are noted clinically. Some BPs have failed to demonstrate nonvertebral or hip fracture efficacy in intention-to-treat populations (ibandronate), and only one BP, risedronate, has demonstrated consistent early fracture efficacy (6-months) across all sites (vertebral, nonvertebral and hip).

With regard to the cellular effects of BPs, it has been well characterised that osteoclasts are the major target cells for BPs to execute their anti-resorptive effects. Recent evidence, however, has proposed that some other cells in the bone microenvironment, e.g., osteoblasts and osteocytes, or cells in the marrow space, such as tumour cells that have metastasised to bone and bone marrow monocytes may also be affected by BPs [164]. For example, there are reports on stimulation or suppression of osteoblast activity in a dose-dependent manner by BPs *in vitro*, which raises the possibility that BPs may mediate indirectly some anti-resorptive activity through their action on osteoblasts and that different BPs have distinct effects on osteoblasts [165]. However, it should be noted that due to the uncertainty about the concentrations of BPs that osteoblasts are exposed to *in vivo*, these results should be interpreted carefully. BPs, independent of their anti-resorptive potencies, have also been suggested to prevent apoptosis of murine osteocytic MLO-Y4 cells, whether it was induced by etoposide, TNF-α, or glucocorticoid [28, 77]. These findings suggest that BPs may have positive effects on osteocyte survival and function, and if confirmed in further investigations, these studies may provide new understanding of the action of BPs on bone strength. Finally, numerous studies have suggested that N-BPs have anti-tumour activity, which may be partially attributed to their inhibitory effect on angiogenesis [166]. Interestingly, the structure-activity relationships of N-BPs in affecting tumour cell

adhesion and invasion match their potency for inhibiting FPPS [100, 104]. Similarly, N-BPs have shown to affect endothelial cells in decreasing cell viability [167], inhibiting cell proliferation [166] and modulating cell adhesion and migration [108]. Overall, these potential targets of BPs may help to understand not only their anti-resorptive effects, but also their effects on bone quality, tumours, and other systems [168].

The key to prediction of the clinical efficacy of BPs is their avid binding for bone mineral. However, BPs also have some effects *in vivo* that are not necessarily related to the effects on bone [90, 168]. On one hand, the effects on noncalcified tissues can bring new therapeutic interests to the BPs. For instance, certain lipophilic BPs have proved to be potent inhibitors of squalene synthase and cholesterol biosynthesis in rats, and are effective cholesterol lowering agents in rats and hamsters [169]. In addition, recent studies have demonstrated that the mevalonate pathway is of vital importance to parasite survival. With the fact that the N-BPs are potent inhibitors of FPPS, and their ability to stimulate human γ, δ-T cells [170], N-BPs appear to have potential in treating parasitic protozoan diseases [171]. On the other hand, the extraskeletal activities of BPs can cause clinically important effects. One of the well-recognised side effects of BPs is the acute phase reaction experienced in patients who receive their first intravenous N-BP. Studies have shown that after i.v. administration, uptake of N-BPs by circulating monocytes causes

inhibition of FPPS and accumulation of IPP, which reacts with peripheral blood γ, δ-T cells in a specific way. The activation of γ, δ-T cells subsequently initiates this immunological response (Figure 70) [70, 118, 140]. Such activation is likely to have important effects on osteoporosis, cancer, and microbial infections [168] and can be possibly prevented by statins [118]. In addition, there is a low incidence of oesophageal irritation, associated with acid reflux and improper dosing after oral administration [172]. The discovery that N-BPs act via inhibition of the mevalonate-to-cholesterol pathway raised the possibility that oesophageal irritation by N-BPs is mechanism-based [173].

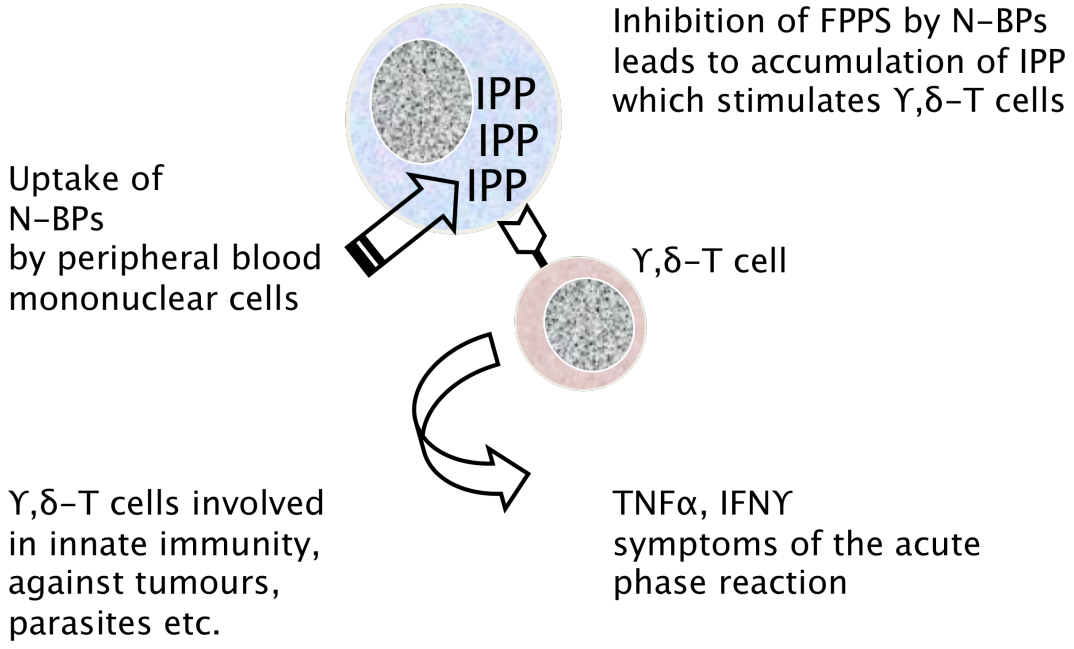

Figure 70 An explanation for the effects of i.v. N-BPs on Υ, δ -T cells [118].

Inhibition of the mevalonate pathway also explains the acute phase response seen in about one third of patients given intravenous N-BP. First, BPs are taken up by blood mononuclear cells, causing inhibition of the mevalonate pathway and accumulation of isoprenoid lipids such as IPP, upstream of FPP synthase. These lipids are somehow released and bind to the Υ, δ -T cell receptor, causing activation and proliferation of Υ, δ -T cells and the subsequent acute phase response.

CHAPTER 7 CONCLUSIONS AND FUTURE PROSPECTS

7.1 Conclusions

The current investigations have established that the bone mineral HAP affinity of current and newly synthesised BPs can be readily determined by using column chromatography with ceramic HAP and FAP. HAP affinity was also measured by Langmuir adsorption isotherms and competitive binding assays, and from these, dissociation constants of BPs were derived. The cell culture studies provide new information on the potential biological activities of BPs on osteocytes and osteoblasts that relates to direct physiological exposure of this class of drug. Given that there is renewed interest in the future development of BPs for novel uses, the investigation of BPs in these chemical and biological processes gives a better understanding of their specific modes of action and, moreover, this is highly relevant to their clinical effects in specific applications.

Overall, effects of modification in chemical structure on mineral-binding affinities, and hence on their biological consequences generated from the physicochemical and cellular aspects of the study reveal that:

1. The P-C-P structure is essential for HAP binding.
2. An OH or NH_2 group at the R1 site usually enhances HAP binding.
3. A nitrogen moiety and its position in the alkyl group or heterocyclic ring in the R2 side chain may also contribute to differences in increased BP binding to HAP.

4. The 3D configuration of a N-BP and molecular orientation of the nitrogen group, its influence on proton dissociation of the phosphonate groups and the degree of nitrogen protonation may all play important roles in mineral-binding affinity (Figures 71, 72).

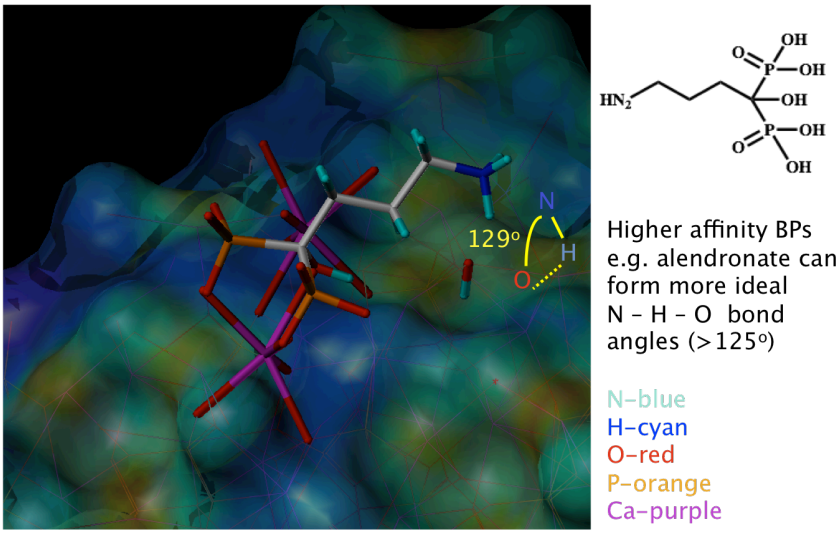

Figure 71 Molecular modelling studies of alendronate on HAP surface [174].

Alendronate forms an idealised N-H-O bond on the bone surface (>125°).

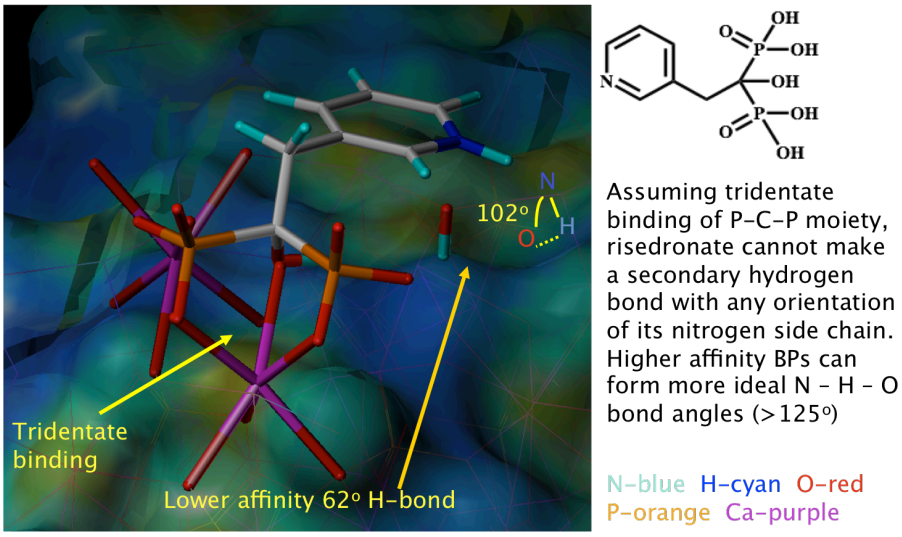

Figure 72 Molecular modelling studies of risedronate on HAP surface [174].

Assuming tridentate binding of P-C-P moiety, risedronate cannot make a secondary hydrogen bond with any orientation of its nitrogen side chain. Higher affinity BPs, e.g. alendronate, can form more ideal N-H-O bond angles (>125°).

5. pH has a profound effect on the ionisation of the phosphonate and R2 functional groups. BPs were eluted more slowly from the columns at lower pH.

6. Modelling studies in progress support the above findings that mineral binding of BPs depends not just on the P-C-P moiety, but also on the R1 OH group and the R2 side chains (Figures 70 and 71), as well as the pH-dependent ionisation of the phosphonate and R2 functional groups.

7. The rank order of BPs based on their binding affinities on bone mineral surfaces obtained from HAP column chromatography appears to be in the following order at pH 7.4: clodronate < risedronate < minodronate < ibandronate < zoledronate < neridronate < etidronate < alendronate < pamidronate.

8. In studies of adsorption isotherms, the capacity for binding of most BPs is found to be in accordance with their mineral-binding affinities.

9. The rank order of BPs based on their dissociation constants determined by competitive binding assays at pH 7.4 is: clodronate < minodronate < ibandronate < risedronate < zoledronate < neridronate < etidronate < alendronate < pamidronate.

10. Differences are seen in the rank order of mineral binding of BPs between various adsorption assays (e.g. kinetic binding affinities by crystal growth assays versus column chromatography) and the clinical significance of these is still under discussion.

11. Low dose of risedronate protects osteocytes from apoptosis induced by etoposide.

12. Prevention of osteocyte and osteoblast apoptosis by BPs may involve the rapid phosphorylation of ERK, but other signalling pathways are likely to be involved.

7.2 Future work

The work presented in this thesis has covered a number of aspects in investigations on the physiological and biological mechanisms of BP action. Based on the data presented, the following avenues can be suggested for future studies.

Study of labelled bisphosphonate compounds

Previous experimental work has evaluated the mineral-binding affinities of BPs and tested their anti-apoptosis effect on osteocytes. However, it remains unclear whether other cells in the bone microenvironment can also take up BPs from the bone surface. It is suggested that the canalicular compartment of osteocytes is bathed in an extracellular fluid that is possible to deliver drug to osteocytes [11]. The presence of BPs in osteocytes and in their canaliculi has been revealed by immunohistochemistry on sections of bone biopsies [140]. Still, it is not known that whether BPs distribute within this network and gain access to

osteocytes differentially according to their distinct mineral-binding affinities and structural properties. To address this topic, FL-BPs or those of lower bone affinity will be useful tools for studying the distribution and cellular uptake of these drugs *in vivo* [40], thus the following experiments to be performed in the future have been designed and experiments using these reagents are already yielding interesting results.

Rats are injected sequentially at appropriate dosages and time intervals with BPs either unlabelled or labelled fluorimetrically and/or with known bone metabolism markers such as calceins, tetracyclines, and fluoresceins to evaluate the relative distributions of the administered BPs on to bone formation and resorption sites. The temporal distribution in different bone compartments is determined by using methods of quantitative analysis, autoradiography and fluorescent detection by microimaging. Density gradient fractionation of newly deposited and older bone mineral deposits can be performed by micropowdering of defatted long bones and subsequent gradient centrifugation followed by quantitative analysis of the resultant fractions. An acid extraction method for BPs from rat bones needs to be developed. In addition, confocal microscopy can be applied for use in detection of the presence of BPs around osteocytes. Information on the relative distributions in bone compartments and presence in osteocytes will provide deeper insights

into how the clinically used BPs differ in terms of their efficacies and mechanisms of action (Figure 73).

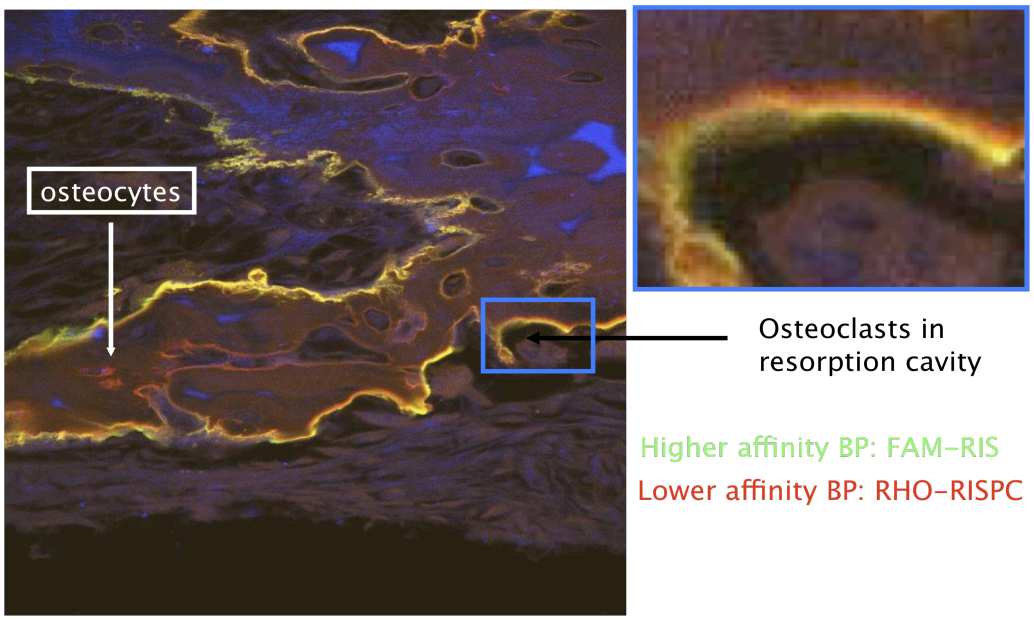

Figure 73 Distributions of fluorescent BPs with different bone affinities in bone compartments.

24 h after injection in rat, at a resorbing surface beneath osteoclasts, the lower affinity compound (Rho-RISPC, red) has diffused further into the mineral than the higher affinity compound (5(6)-FAMRIS, green). Nearer the surface, both lower and higher affinity compounds bind equally, appearing yellow (Dr. Alan Boyde 2009).

Rat BP/FL-BP urine excretion study

Clinical studies suggest that the relative skeletal uptake and retention of BPs *in vivo* does not depend simply on its mineral-binding affinity but also on renal function and prevalent rates of bone turnover. When BPs enter the body, they are rapidly cleared from the blood stream and a portion is taken up by the skeleton. The remainder is eliminated via the kidneys, a process which is largely complete within a few hours. The measurement of BPs in urine is therefore inversely related to skeletal

retention, and can be used to estimate their binding affinities for total bone mineral *in vivo* [11]. However, with regard to the measurement of retained versus excreted BP there are unfortunately very few comparisons between the different BPs. Thus, we have collaborated with colleagues in the United States to conduct *in vivo* experiments on the urinary excretion of BPs with different affinities injected to rats. The measurement of 24-hour skeletal retention of BPs in rats should provide novel findings of clinical relevance related to the HAP binding values obtained from the *in vitro* studies. Preliminary results of the 24-hour urinary excretion of risedronate, ibandronate, zoledronate and alendronate are listed in Table 7. Interestingly, the total BP urinary recoveries (24 h) correlate well with the BP rank order obtained from the *in vitro* studies, i.e., the HAP column chromatography and the competitive binding assays. Therefore, more comprehensive *in vivo* experiments on the urine excretion of BPs with different affinities are planned to extend this work.

Table 7 Urinary recovery (24 h) from the BP 4 mixtures in one (4-in-1) i.v. bolus rat study analysed by LC/MS methods.

Rats simultaneously dosed BPs at 0.1-0.4 mg/kg each.

BP	% BP recovered (urine)	BP/RIS recovered (urine)
Risedronate	43	1.0
Ibandronate	54	1.15
Zoledronate	30	0.69
Alendronate	26	0.63

Study of the potential effects of BPs on endothelial cells

BPs are known to influence mainly the activity of the bone resorbing cells, the osteoclasts. However, potential effects on other cell types present locally in the environment of the skeletal tissues have been reported [48, 154, 175]. Significant differences in bone affinity between the BPs, in terms of binding capacity and desorption rate have been suggested from the physicochemical aspect of my project. This may be an important factor in determining the ability of different BPs to affect non-resorbing cells, especially more relevant to compounds that have lower bone affinity.

There is a growing body of literature suggests that N-BPs such as ibandronate and zoledronic acid have anti-tumour activity, which may be partially attributed to their inhibitory effect on angiogenesis [166]. BPs have been reported to accumulate in human vessels [176], which interior surface is lined by a heterogeneous population of endothelial cells that play a key role in angiogenesis [177]. The impact of N-BPs and non-N-BPs on human umbilical vein endothelial cells (HUVEC) have been investigated in the past, and have shown that N-BPs particularly decrease the cell viability [167], inhibit cell proliferation [166] and modulate cell adhesion and migration [108]. In addition, an anti-angiogenetic effect of BPs is suggested by the fact that BPs could influence the number of circulating endothelial progenitor cells and interfering with endothelial

cell proliferation that contribute to an increase in angiogenesis [178]. However, the anti-angiogenic mechanisms of N-BPs on endothelial cells have not been clearly elucidated. In addition, little information is known about the effects of BPs on endothelial cells derived from different tissue sites. Endothelial cells are very heterogeneous with respect to cellular activities at different tissue sites, future experiments are proposed to look at a wider range of endothelial cells which are available either as cell lines or commercially. Effects on enzyme activity, proliferation and differentiation characteristics of endothelial cell as well as mechanisms of apoptosis and cell death are also suggested as future work. In addition, most research on the biological effects of BPs are performed using free molecules in the solution, hence, the direct effect of HAP-adsorbed BPs on endothelial cells is proposed. A better understanding of the effects of BPs on a cellular level might help to adjust therapeutic regimes in order to maintain clinical success while reducing the side effects. The cell culture and physiological studies proposed will give new information on the sensitivities of different cell types to both free and bound BPs both *in vitro* and *in vivo* that relates to the physiological exposures either directly or following mineral resorption.

APPENDICES

Protocol for quantitating the primary $-NH_2$ side chains in the alkyl-amino BPs using the OPA method

The equilibrium concentration of NH_2-containing BP (e.g., pamidronate) was determined spectrophotometrically by the o-phthaldialdehyde (OPA) method.

1. A 0.04 M sodium borate solution was made by dissolving 1.526 g di-sodium tetraborate ($Na_2B_4O_7.10H_2O$) (BDH Chemicals Ltd, Poole, England) in 100 ml deionised water. This solution was kept in a brown bottle for at least 24 h.
2. A derivatising agent with limit shelf life was prepared by mixing 5.6 ml of the 0.04 M sodium borate solution, 25 mg o-phthaldialdehyde (Phthaldialdehyde, minimum 99% HPLC, Sigma-Aldrich Chemie GmbH, Steinheim, Germany), 625 µl methanol (HPLC grade, Fisher scientific UK limited, Leicestershire, UK) and 30 µl 2-mercaptoethanol (min 98%, Sigma-Aldrich Chemie GmbH, Steinheim, Germany) in a brown bottle 12 h before use.
3. The complete OPA reagent was made by combining 6255 µl anti-precipitating agent 2-propanol (Sigma-Aldrich Chemie GmbH, Steinheim, Germany) to 6255 µl derivatising agent immediately before analysis. The amount of OPA reagent described above was suitable for one 96-well plate analysis.

To perform the fluorescent assay, a calibration curve was constructed by diluting a series of target BP standards ranging from 0 to 800 µM using the same buffer as the Langmuir adsorption isotherm experiment, i.e., 1 mM PBS pH 7.4. Second, 52.5 µl standard or sample was added in each well of a 96-well black plate (Costar®, Corning incorporated, NY), leaving a few empty wells as blank. When all samples were dispersed in the 96-well plate, 70 µl of OPA reagent was added into each well of the plate by using a multichannel pipette as fast as possible. The plate was allowed to incubate for 2-5 minutes followed by 10 sec mixing time and the fluorescence was read on the SPECTRAmax® GEMINI XS Dual-Scanning microplate spectrofluorometer (Molecular Devices Corporation, CA) using an excitation wavelength of 340 nm and an emission wavelength of 455 nm. Fluorescence intensity was read as relative fluorescent unit (RFU) by Softmax® PRO Version 4.0 Software (Molecular Devices Corporation) and analysed by Microsoft Excel.

REFERENCES

1. Gerard J. Tortora, B.D., *Principles of anatomy and physiology*. 2009: John Wiley & Sons, Inc.
2. Russell, R.G., B. Espina, and P. Hulley, *Bone biology and the pathogenesis of osteoporosis.* Curr Opin Rheumatol, 2006. **18 Suppl 1**: p. S3-10.
3. Datta, H., et al., *The cell biology of bone metabolism.* Journal of Clinical Pathology, 2008. **61**(5): p. 577-587.
4. Marks, S.C., Jr. and S.N. Popoff, *Bone cell biology: the regulation of development, structure, and function in the skeleton.* Am J Anat, 1988. **183**(1): p. 1-44.
5. Bartl Reiner, F.B., von Tresckow Emmo, Bartl Christoph *Bisphosphonates in medical practice*. 2007, Berlin Heidelberg New York: Springer-Verlag.
6. Clarke, B., *Normal bone anatomy and physiology.* Clinical journal of the American Society of Nephrology : CJASN, 2008. **3 Suppl 3**: p. S131-9.
7. Triffitt, J.T., *Receptor molecules, co-precipitation and ion exchange processes in the deposition of metal ions in bone*. Metals in bone, ed. N.D. Priest. 1985, Lancaster: MTP press.
8. Fayez F. Safadi, M.F.B., Samir M. Abdelmagid, Mario C. Rico, Rulla A. Aswad, and a.S.N.P. Judith Litvin, *Bone structure, development and bone biology*, in *Bone pathology*, J.S. Khurana, Editor. 2009, Humana Press. p. 1-50.
9. Cummings, B. *Bone structure*. 2004; Available from: http://faculty.irsc.edu/FACULTY/TFischer/AP1/bone%20structure.jpg.
10. Honda, F., et al., *Properties of cattle bone powder-coated composite particles as high-performance and open column liquid chromatographic column packings.* J Chromatogr A, 1998. **813**(1): p. 21-33.
11. Raisz, L.G., *Physiology and pathophysiology of bone remodeling.* Clin Chem, 1999. **45**(8 Pt 2): p. 1353-8.
12. Silver, I.A., R.J. Murrills, and D.J. Etherington, *Microelectrode studies on the acid microenvironment beneath adherent macrophages and osteoclasts.* Exp Cell Res, 1988. **175**(2): p. 266-76.
13. Baron, R., et al., *Cell-mediated extracellular acidification and bone resorption: evidence for a low pH in resorbing lacunae and localization of a 100-kD lysosomal membrane protein at the osteoclast ruffled border.* J Cell Biol, 1985. **101**(6): p. 2210-22.

14. *Bone Health and Osteoporosis: A Report of the Surgeon General*. 2004, U.S. Department of Health and Human Services, Office of the Surgeon General: Rockville, MD.
15. Poole, K.E. and J. Reeve, *Parathyroid hormone – a bone anabolic and catabolic agent.* Curr Opin Pharmacol, 2005. **5**(6): p. 612-7.
16. Bono.C.M, E.T.A., *Overview of osteoporosis: pathophysiology and determinants of bone strength.* Eur Spine J, 2003. **12 (Suppl. 2)**: p. S90-S96.
17. Ducy, P., et al., *Leptin inhibits bone formation through a hypothalamic relay: a central control of bone mass.* Cell, 2000. **100**(2): p. 197-207.
18. *Diagram of bone cells*. Available from: http://www.roche.com/pages/facets/11/ostedefe.htm.
19. Sevgi B. Rodan, L.T.D., *Cathepsin K – A new molecular target for osteoporosis.* IBMS BoneKEy, 2008. **5**: p. 16-24.
20. Bono, C. and T. Einhorn, *Overview of osteoporosis: pathophysiology and determinants of bone strength.* European Spine Journal, 2003. **12**(0): p. S90-S96.
21. Poole, K.E., et al., *Sclerostin is a delayed secreted product of osteocytes that inhibits bone formation.* FASEB J, 2005. **19**(13): p. 1842-4.
22. Bellido, T., et al., *Chronic elevation of parathyroid hormone in mice reduces expression of sclerostin by osteocytes: a novel mechanism for hormonal control of osteoblastogenesis.* Endocrinology, 2005. **146**(11): p. 4577-83.
23. Power, J., et al., *Sclerostin and the regulation of bone formation: Effects in hip osteoarthritis and femoral neck fracture.* J Bone Miner Res. **25**(8): p. 1867-76.
24. Bonewald, L.F., *The amazing osteocyte.* J Bone Miner Res. **26**(2): p. 229-38.
25. Cheng, F. and P. Hulley, *The osteocyte--a novel endocrine regulator of body phosphate homeostasis.* Maturitas. **67**(4): p. 327-38.
26. Bonewald, L.F., *Osteocytes as dynamic multifunctional cells.* Ann N Y Acad Sci, 2007. **1116**: p. 281-90.
27. Feng, J.Q., L. Ye, and S. Schiavi, *Do osteocytes contribute to phosphate homeostasis?* Curr Opin Nephrol Hypertens, 2009. **18**(4): p. 285-91.
28. Plotkin, L., *Bisphosphonates and Estrogens Inhibit Osteocyte Apoptosis via Distinct Molecular Mechanisms Downstream of Extracellular Signal-regulated Kinase Activation.* Journal of Biological Chemistry, 2005. **280**(8): p. 7317-7325.
29. Noble, B.S., et al., *Mechanical loading: biphasic osteocyte survival and targeting of osteoclasts for bone destruction in rat cortical bone.* Am J Physiol Cell Physiol, 2003. **284**(4): p. C934-43.

30. Robling, A.G., A.B. Castillo, and C.H. Turner, *Biomechanical and molecular regulation of bone remodeling.* Annu Rev Biomed Eng, 2006. **8**: p. 455-98.
31. Fitzpatrick, J.S.K.a.L.A., *Osteoporosis and metabolic bone disease*, in *Bone pathology*, J.S. Khurana, Editor. 2009, Humana Press. p. 217-237.
32. Smith Roger, W.P., *Clinical and biochemical disorders of the skeleton*. 2005: Oxford university press.
33. Russell, G., *Bisphosphonates in the Treatment of Metabolic Bone Disease – Future Prospects.* Long-term healthcare, 2006: p. 1-7.
34. Pazianas, M., et al., *Long-term treatment with bisphosphonates and their safety in postmenopausal osteoporosis.* Ther Clin Risk Manag, 2010. **6**: p. 325-43.
35. O'Donnell S, C.A., Wells G.A,Adachi J.D,Reginster J.Y, *Strontium ranelate for preventing and treating postmenopausal osteoporosis (Review).* The Cochrane Library, 2008(2).
36. Ozmen, B., et al., *Influence of the selective oestrogen receptor modulator (raloxifene hydrochloride) on IL-6, TNF-alpha, TGF-beta1 and bone turnover markers in the treatment of postmenopausal osteoporosis.* Eur Cytokine Netw, 2007. **18**(3): p. 148-53.
37. Prestwood, K.M., C.C. Pilbeam, and L.G. Raisz, *Treatment of osteoporosis.* Annu Rev Med, 1995. **46**: p. 249-56.
38. Canalis E, M.G., Giustina A,Bilezikian J.P, *Glucocorticoid-induced osteoporosis: pathophysiology and therapy.* Osteoporosis Int, 2007. **18**: p. 1319-1328.
39. Popp A.W, I.J., Buergi E.M,Buergi U,Lippuner K, *Glucocorticosteroid-induced spinal osteoporosis: scientific update on pathophysiology and treatment.* Eur Spine J, 2006. **15**: p. 1035-1049.
40. Poole, K. and J. Compston, *Osteoporosis and its management.* BMJ, 2006. **333**(7581): p. 1251-1256.
41. Owens, G., R. Jackson, and E.M. Lewiecki, *An integrated approach: bisphosphonate management for the treatment of osteoporosis.* Am J Manag Care, 2007. **13 Suppl 11**: p. S290-308; quiz S309-12.
42. Follin, S.L. and L.B. Hansen, *Current approaches to the prevention and treatment of postmenopausal osteoporosis.* Am J Health Syst Pharm, 2003. **60**(9): p. 883-901; quiz 903-4.
43. *Management of osteoporosis, a national clinical guideline*. 2003, Scottish intercollegiate guidelines network.
44. Hodsman, A., *Parathyroid Hormone and Teriparatide for the Treatment of Osteoporosis: A Review of the Evidence and Suggested Guidelines for Its Use.* Endocrine Reviews, 2005. **26**(5): p. 688-703.
45. Deeks, E.D. and S. Dhillon, *Spotlight on strontium ranelate: in postmenopausal osteoporosis.* Drugs Aging. **27**(9): p. 771-3.

46. Delmas, P.D., *Treatment of postmenopausal osteoporosis.* Lancet, 2002. **359**(9322): p. 2018-26.
47. Reid, I.R., *Bisphosphonates.* Skeletal Radiol, 2007. **36**(8): p. 711-4.
48. Green, J.R., *Bisphosphonates: preclinical review.* Oncologist, 2004. **9 Suppl 4**: p. 3-13.
49. Martin, T. and K. Ng, *New Agents for the Treatment of Osteoporosis.* International Bone and Mineral Society Knowledge Environment, 2007. **4**(11): p. 287-298.
50. Shoback, D., *Update in Osteoporosis and Metabolic Bone Disorders.* Journal of Clinical Endocrinology & Metabolism, 2006. **92**(3): p. 747-753.
51. Cranney, A., et al., *Parathyroid hormone for the treatment of osteoporosis: a systematic review.* CMAJ, 2006. **175**(1): p. 52-9.
52. Roodman, G.D., *Insights into the pathogenesis of Paget's disease.* Annals of the New York Academy of Sciences, 2010. **1192**(1): p. 176-80.
53. Roodman, G.D. and J.J. Windle, *Paget disease of bone.* J Clin Invest, 2005. **115**(2): p. 200-8.
54. Reid, I.R. and D.J. Hosking, *Bisphosphonates in Paget's disease.* Bone, 2010.
55. Hocking, L.J., et al., *Genomewide search in familial Paget disease of bone shows evidence of genetic heterogeneity with candidate loci on chromosomes 2q36, 10p13, and 5q35.* Am J Hum Genet, 2001. **69**(5): p. 1055-61.
56. Lucas, G.J., A. Daroszewska, and S.H. Ralston, *Contribution of genetic factors to the pathogenesis of Paget's disease of bone and related disorders.* J Bone Miner Res, 2006. **21 Suppl 2**: p. P31-7.
57. Ralston, S.H., *Pathogenesis of Paget's disease of bone.* Bone, 2008. **43**(5): p. 819-25.
58. Siris, E., et al., *Medical Management of Paget?s Disease of Bone: Indications for Treatment and Review of Current Therapies.* Journal of Bone and Mineral Research, 2006. **21**(Supplement 2): p. P94-P98.
59. Siris, E.S., *Paget's disease of bone.* J Bone Miner Res, 1998. **13**(7): p. 1061-5.
60. Francis, M.D. and D.J. Valent, *Historical perspectives on the clinical development of bisphosphonates in the treatment of bone diseases.* Journal of musculoskeletal & neuronal interactions, 2007. **7**(1): p. 2-8.
61. Papapoulos, S.E., *Bisphosphonate actions: physical chemistry revisited.* Bone, 2006. **38**(5): p. 613-6.
62. Fleisch, H., Russell, R. G. G., Francis, M. D., *Diphosphonates inhibit hydroxyapatite dissolution in vitro and bone resorption in tissue culture and in vivo.* Science, 1969. **165**: p. 1262-1264.

63. Francis, M.D., Russell, R. G. G., Fleisch, H., *Diphosphonates inhibit formation of calcium phosphate crystals in vitro and pathological calcification in vivo.* Science, 1969. **165**: p. 1264-1266.
64. Russell, R.G. and H. Fleisch, *Pyrophosphate and diphosphonates in skeletal metabolism. Physiological, clinical and therapeutic aspects.* Clin Orthop Relat Res, 1975(108): p. 241-63.
65. *Chemical structures of bisphosphonate and pyrophosphate* 2009; Available from: http://en.wikipedia.org/wiki/File:BisphosStruct.svg.
66. Russell, G., *Determinants of structure-function relationships among bisphosphonates.* Bone, 2007. **40**: p. S21-S25.
67. van Beek, E.R., et al., *Binding and antiresorptive properties of heterocycle-containing bisphosphonate analogs: structure-activity relationships.* Bone, 1998. **23**(5): p. 437-42.
68. van Beek, E., et al., *Structural requirements for bisphosphonate actions in vitro.* J Bone Miner Res, 1994. **9**(12): p. 1875-82.
69. Russell, R., et al., *Mechanisms of action of bisphosphonates: similarities and differences and their potential influence on clinical efficacy.* Osteoporos Int, 2008. **19**(6): p. 733-759.
70. Russell, R., et al., *Bisphosphonates: An Update on Mechanisms of Action and How These Relate to Clinical Efficacy.* Annals of the New York Academy of Sciences, 2007. **1117**(1): p. 209-257.
71. Russell, R., *Bisphosphonates: Mode of Action and Pharmacology.* PEDIATRICS, 2007. **119**(Supplement): p. S150-S162.
72. Flanagan, A.M. and T.J. Chambers, *Dichloromethylenebisphosphonate (Cl2MBP) inhibits bone resorption through injury to osteoclasts that resorb Cl2MBP-coated bone.* Bone Miner, 1989. **6**(1): p. 33-43.
73. Papapoulos, S.E., *Bisphosphonates: how do they work?* Best Pract Res Clin Endocrinol Metab, 2008. **22**(5): p. 831-47.
74. Luckman, S.P., et al., *Nitrogen-containing bisphosphonates inhibit the mevalonate pathway and prevent post-translational prenylation of GTP-binding proteins, including Ras.* J Bone Miner Res, 1998. **13**(4): p. 581-9.
75. van Beek, E., et al., *Farnesyl pyrophosphate synthase is the molecular target of nitrogen-containing bisphosphonates.* Biochem Biophys Res Commun, 1999. **264**(1): p. 108-11.
76. Monkkonen, H., et al., *A new endogenous ATP analog (apppI) inhibits the mitochondrial adenine nucleotide translocase (ANT) and is responsible for the apoptosis induced by nitrogen-containing bisphosphonates.* Br J Pharmacol, 2006. **147**(4): p. 437-45.
77. Plotkin, L.I., S.C. Manolagas, and T. Bellido, *Dissociation of the pro-apoptotic effects of bisphosphonates on osteoclasts from their anti-apoptotic effects on osteoblasts/osteocytes with novel analogs.* Bone, 2006. **39**(3): p. 443-52.

78. Follet, H., et al., *Risedronate and alendronate suppress osteocyte apoptosis following cyclic fatigue loading.* Bone, 2007. **40**(4): p. 1172-7.
79. Shinoda, H., et al., *Structure-activity relationships of various bisphosphonates.* Calcif Tissue Int, 1983. **35**(1): p. 87-99.
80. Schenk, R., et al., *Quantitative morphometric evaluation of the inhibitory activity of new aminobisphosphonates on bone resorption in the rat.* Calcif Tissue Int, 1986. **38**(6): p. 342-9.
81. Watts, N.B. and D.L. Diab, *Long-term use of bisphosphonates in osteoporosis.* J Clin Endocrinol Metab, 2010. **95**(4): p. 1555-65.
82. Simon, J.A., *Are All Bisphosphonates the Same? Potential Reasons for Clinical Differences: A Perspective.* Journal of women's health (2002), 2010.
83. Green, J.R., K. Muller, and K.A. Jaeggi, *Preclinical pharmacology of CGP 42'446, a new, potent, heterocyclic bisphosphonate compound.* J Bone Miner Res, 1994. **9**(5): p. 745-51.
84. Russell, R.G. and M.J. Rogers, *Bisphosphonates: from the laboratory to the clinic and back again.* Bone, 1999. **25**(1): p. 97-106.
85. Kennel, K.A. and M.T. Drake, *Adverse effects of bisphosphonates: implications for osteoporosis management.* Mayo Clin Proc, 2009. **84**(7): p. 632-7; quiz 638.
86. Chapurlat, R.D. and P.D. Delmas, *Drug insight: Bisphosphonates for postmenopausal osteoporosis.* Nature clinical practice Endocrinology & metabolism, 2006. **2**(4): p. 211-9; quiz following 238.
87. Lin, J.H., *Bisphosphonates: a review of their pharmacokinetic properties.* Bone, 1996. **18**(2): p. 75-85.
88. Reid, I., *Bisphosphonates.* Skeletal Radiol, 2007. **36**(8): p. 711-714.
89. Jones, A.G., M.D. Francis, and M.A. Davis, *Bone scanning: radionuclidic reaction mechanisms.* Semin Nucl Med, 1976. **6**(1): p. 3-18.
90. Fleisch, H., *Bisphosphonates: mechanisms of action.* Endocr Rev, 1998. **19**(1): p. 80-100.
91. Knight, R.J., et al., *Bisphosphonate-related osteonecrosis of the jaw: tip of the iceberg.* J Craniofac Surg, 2010. **21**(1): p. 25-32.
92. Oizumi, T., et al., *Necrotic actions of nitrogen-containing bisphosphonates and their inhibition by clodronate, a non-nitrogen-containing bisphosphonate in mice: potential for utilization of clodronate as a combination drug with a nitrogen-containing bisphosphonate.* Basic Clin Pharmacol Toxicol, 2009. **104**(5): p. 384-92.
93. Seton, M., et al., *Paget's disease of bone: The skeletal distribution, complications and quality of life as perceived by patients.* Bone, 2010.

94. Reid, I.R., et al., *Comparison of a single infusion of zoledronic acid with risedronate for Paget's disease.* N Engl J Med, 2005. **353**(9): p. 898-908.
95. Barni, S., *Bisphosphonates and metastatic bone disease.* Annals of Oncology, 2006. **17**(Supplement 2): p. ii91-ii95.
96. Jagdev, S., et al., *The bisphosphonate, zoledronic acid, induces apoptosis of breast cancer cells: evidence for synergy with paclitaxel.* Br J Cancer, 2001. **84**(8): p. 1126-1134.
97. Lipton, A., *Toward New Horizons: The Future of Bisphosphonate Therapy.* The Oncologist, 2004. **9**(suppl_4): p. 38-47.
98. Coleman, R., *Bisphosphonates: Clinical Experience.* The Oncologist, 2004. **9**(suppl_4): p. 14-27.
99. van der Pluijm, G., et al., *Bisphosphonates inhibit the adhesion of breast cancer cells to bone matrices in vitro.* J Clin Invest, 1996. **98**(3): p. 698-705.
100. Boissier, S., et al., *Bisphosphonates inhibit prostate and breast carcinoma cell adhesion to unmineralized and mineralized bone extracellular matrices.* Cancer Res, 1997. **57**(18): p. 3890-4.
101. Coxon, J.P., et al., *Zoledronic acid induces apoptosis and inhibits adhesion to mineralized matrix in prostate cancer cells via inhibition of protein prenylation.* BJU Int, 2004. **94**(1): p. 164-70.
102. van der Pluijm, G., et al., *Interference with the microenvironmental support impairs the de novo formation of bone metastases in vivo.* Cancer Res, 2005. **65**(17): p. 7682-90.
103. Tanimori, Y., et al., *Nitrogen-containing bisphosphonate, YM529/ONO-5920, inhibits tumor metastasis in mouse melanoma through suppression of the Rho/ROCK pathway.* Clin Exp Metastasis, 2010. **27**(7): p. 529-38.
104. Boissier, S., et al., *Bisphosphonates inhibit breast and prostate carcinoma cell invasion, an early event in the formation of bone metastases.* Cancer Res, 2000. **60**(11): p. 2949-54.
105. Lee, M.V., et al., *Bisphosphonate treatment inhibits the growth of prostate cancer cells.* Cancer Res, 2001. **61**(6): p. 2602-8.
106. Dasy, *Bisphosphonate induces apoptosis and inhibits pro-osteoclastic gene expression in prostate cancer cells.* 2006: p. 1-8.
107. Yamada, J., et al., *Anti-angiogenic property of zoledronic acid by inhibition of endothelial progenitor cell differentiation.* J Surg Res, 2009. **151**(1): p. 115-20.
108. Hashimoto, K., et al., *Alendronate suppresses tumor angiogenesis by inhibiting Rho activation of endothelial cells.* Biochem Biophys Res Commun, 2007. **354**(2): p. 478-84.
109. Neville-Webbe, H.L. and R. Coleman, *Bisphosphonates and RANK ligand inhibitors for the treatment and prevention of metastatic bone disease.* European journal of cancer (Oxford, England : 1990), 2010.

110. Clyburn, R.D., et al., *Increased anti-tumour effects of doxorubicin and zoledronic acid in prostate cancer cells in vitro: supporting the benefits of combination therapy.* Cancer Chemother Pharmacol, 2010. **65**(5): p. 969-78.
111. Coleman, R., et al., *The effects of adding zoledronic acid to neoadjuvant chemotherapy on tumour response: exploratory evidence for direct anti-tumour activity in breast cancer.* Br J Cancer, 2010. **102**(7): p. 1099-105.
112. Diel, I.J., R. Bergner, and K.A. Grotz, *Adverse effects of bisphosphonates: current issues.* J Support Oncol, 2007. **5**(10): p. 475-82.
113. Robinson, N.A. and J.F. Yeo, *Bisphosphonates--a word of caution.* Ann Acad Med Singapore, 2004. **33**(4 Suppl): p. 48-9.
114. Marshall, J.K., *The gastrointestinal tolerability and safety of oral bisphosphonates.* Expert Opin Drug Saf, 2002. **1**(1): p. 71-8.
115. Pecherstorfer, M., et al., *Effect of first treatment with aminobisphosphonates pamidronate and ibandronate on circulating lymphocyte subpopulations.* J Bone Miner Res, 2000. **15**(1): p. 147-54.
116. Thiebaud, D., et al., *An in vitro and in vivo study of cytokines in the acute-phase response associated with bisphosphonates.* Calcif Tissue Int, 1997. **61**(5): p. 386-92.
117. Adami, S., et al., *The acute-phase response after bisphosphonate administration.* Calcif Tissue Int, 1987. **41**(6): p. 326-31.
118. Thompson, K. and M.J. Rogers, *Statins prevent bisphosphonate-induced gamma,delta-T-cell proliferation and activation in vitro.* J Bone Miner Res, 2004. **19**(2): p. 278-88.
119. Miller, P.D., *Is there a role for bisphosphonates in chronic kidney disease?* Semin Dial, 2007. **20**(3): p. 186-90.
120. Marx, R.E., *Pamidronate (Aredia) and zoledronate (Zometa) induced avascular necrosis of the jaws: a growing epidemic.* J Oral Maxillofac Surg, 2003. **61**(9): p. 1115-7.
121. Woo, S.B., J.W. Hellstein, and J.R. Kalmar, *Narrative [corrected] review: bisphosphonates and osteonecrosis of the jaws.* Ann Intern Med, 2006. **144**(10): p. 753-61.
122. Sellmeyer, D.E., *Atypical fractures as a potential complication of long-term bisphosphonate therapy.* JAMA. **304**(13): p. 1480-4.
123. Black, D.M., et al., *Once-yearly zoledronic acid for treatment of postmenopausal osteoporosis.* N Engl J Med, 2007. **356**(18): p. 1809-22.
124. Wysowski, D.K., *Reports of esophageal cancer with oral bisphosphonate use.* N Engl J Med, 2009. **360**(1): p. 89-90.
125. Ryan, P., I. Saleh, and L.F. Stassen, *Osteonecrosis of the jaw: a rare and devastating side effect of bisphosphonates.* Postgrad Med J, 2009. **85**(1010): p. 674-7.

126. Negoescu, A., et al., *Importance of DNA fragmentation in apoptosis with regard to TUNEL specificity.* Biomed Pharmacother, 1998. **52**(6): p. 252-8.
127. Nancollas, G.H., et al., *Novel insights into actions of bisphosphonates on bone: differences in interactions with hydroxyapatite.* Bone, 2006. **38**(5): p. 617-27.
128. Henneman, Z., et al., *Bisphosphonate binding affinity as assessed by inhibition of carbonated apatite dissolutionin vitro.* J. Biomed. Mater. Res., 2008. **85A**(4): p. 993-1000.
129. Jahnke, W. and C. Henry, *An in vitro assay to measure targeted drug delivery to bone mineral.* ChemMedChem, 2010. **5**(5): p. 770-6.
130. Lawson, M.A., et al., *Differences between bisphosphonates in binding affinities for hydroxyapatite.* J Biomed Mater Res Part B Appl Biomater, 2010. **92**(1): p. 149-55.
131. Leu, C.T., et al., *Relative binding affinities of bisphosphonates for human bone and relationship to antiresorptive efficacy.* Bone, 2006. **38**(5): p. 628-36.
132. Moreno, E.C., M. Kresak, and D.I. Hay, *Adsorption of molecules of biological interest onto hydroxyapatite.* Calcif Tissue Int, 1984. **36**(1): p. 48-59.
133. Bankston, T.E., L. Dattolo, and G. Carta, *pH Transients in hydroxyapatite chromatography columns-experimental evidence and phenomenological modeling.* J Chromatogr A, 2010. **1217**(14): p. 2123-31.
134. Kawasaki, T., S. Takahashi, and K. Ikeda, *Hydroxyapatite high-performance liquid chromatography: column performance for proteins.* Eur J Biochem, 1985. **152**(2): p. 361-71.
135. Schubert, S. and R. Freitag, *Comparison of ceramic hydroxy- and fluoroapatite versus Protein A/G-based resins in the isolation of a recombinant human antibody from cell culture supernatant.* J Chromatogr A, 2007. **1142**(1): p. 106-13.
136. Bio-Rad Laboratories, I., *CHT™ Ceramic Hydroxyapatite Instruction Manual*.
137. Bio-Rad Laboratories, I., *Macro-Prep® Chromatography Supports Ceramic Hydroxyapaptite*.
138. Ebetino, F.H., Francis, M. D., Rogers, M. J., *Mechanisms of action of etidronate and other bisphosphonates.* Rev Contemp Pharmacother, 1998. **9**: p. 233-243.
139. Schroder, E., T. Jonsson, and L. Poole, *Hydroxyapatite chromatography: altering the phosphate-dependent elution profile of protein as a function of pH.* Anal Biochem, 2003. **313**(1): p. 176-8.
140. Roelofs, A.J., et al., *Fluorescent risedronate analogues reveal bisphosphonate uptake by bone marrow monocytes and*

localization around osteocytes in vivo. J Bone Miner Res. **25**(3): p. 606-16.
141. Kashemirov, B.A., et al., *Fluorescently labeled risedronate and related analogues: "magic linker" synthesis.* Bioconjug Chem, 2008. **19**(12): p. 2308-10.
142. Van Beek, E., et al., *Dissociation of binding and antiresorptive properties of hydroxybisphosphonates by substitution of the hydroxyl with an amino group.* J Bone Miner Res, 1996. **11**(10): p. 1492-7.
143. Vitha, T., et al., *Complexes of DOTA-bisphosphonate conjugates: probes for determination of adsorption capacity and affinity constants of hydroxyapatite.* Langmuir, 2008. **24**(5): p. 1952-8.
144. Mukherjee, S., Y. Song, and E. Oldfield, *NMR investigations of the static and dynamic structures of bisphosphonates on human bone: a molecular model.* J Am Chem Soc, 2008. **130**(4): p. 1264-73.
145. Kubala, M., J. Plasek, and E. Amler, *Fluorescence competition assay for the assessment of ATP binding to an isolated domain of Na+, K(+)-ATPase.* Physiol Res, 2004. **53**(1): p. 109-13.
146. Cairns, D., *Essentials of Pharmaceutical Chemistry*. Third edition ed. 2008: Pharmaceutical Press.
147. Watson, D.G., *Pharmaceutical Analysis*. 1999: Harcourt Publishers Limited.
148. Bouropoulos, N. and J. Moradian-Oldak, *Analysis of Hydroxyapatite Surface Coverage by Amelogenin Nanospheres Following the Langmuir Model for Protein Adsorption.* Calcif Tissue Int, 2003. **72**(5): p. 599-603.
149. Josse, S., et al., *Novel biomaterials for bisphosphonate delivery.* Biomaterials, 2005. **26**(14): p. 2073-80.
150. Mukherjee, S., et al., *Thermodynamics of bisphosphonates binding to human bone: a two-site model.* J Am Chem Soc, 2009. **131**(24): p. 8374-5.
151. Plotkin, L., et al., *Connexin 43 Is Required for the Anti-Apoptotic Effect of Bisphosphonates on Osteocytes and Osteoblasts In Vivo.* Journal of Bone and Mineral Research, 2008. **23**(11): p. 1712-1721.
152. Plotkin, L., *Mechanical stimulation prevents osteocyte apoptosis: requirement of integrins, Src kinases, and ERKs.* AJP: Cell Physiology, 2005. **289**(3): p. C633-C643.
153. Plotkin, L. and T. Bellido, *Bisphosphonate-Induced, Hemichannel-Mediated, Anti-Apoptosis Through the Src/ERK Pathway: A Gap Junction-Independent Action of Connexin43.* Cell Comm. & Adhesion, 2001. **8**(4): p. 377-382.
154. Plotkin, L.I., et al., *Prevention of osteocyte and osteoblast apoptosis by bisphosphonates and calcitonin.* J Clin Invest, 1999. **104**(10): p. 1363-74.

155. Kogianni, G., et al., *Fas/CD95 is associated with glucocorticoid-induced osteocyte apoptosis.* Life Sci, 2004. **75**(24): p. 2879-95.
156. Civitelli, R., *Connexin43 modulation of osteoblast/osteocyte apoptosis: a potential therapeutic target?* J Bone Miner Res, 2008. **23**(11): p. 1709-11.
157. Romanello, M., et al., *Bisphosphonates activate nucleotide receptors signaling and induce the expression of Hsp90 in osteoblast-like cell lines.* Bone, 2006. **39**(4): p. 739-53.
158. Dunford, J.E., et al., *Structure-activity relationships for inhibition of farnesyl diphosphate synthase in vitro and inhibition of bone resorption in vivo by nitrogen-containing bisphosphonates.* J Pharmacol Exp Ther, 2001. **296**(2): p. 235-42.
159. Dunford, J.E., et al., *Structure-activity relationships among the nitrogen containing bisphosphonates in clinical use and other analogues: time-dependent inhibition of human farnesyl pyrophosphate synthase.* J Med Chem, 2008. **51**(7): p. 2187-95.
160. Francis, M.D., Benedict, J. J., Davis, T. L., *Diphosphonates in vitro adsorption and desorption studies hydroxyapatite and diffusion in bone.* Caniggia A (ed) Etidronate, Proceedings from the 1st International Symposium on Diphosphonate in Therapy. Instituto Gentili, Pisa, 1980: p. 33-50.
161. Srivastava, T. and U. Alon, *The role of bisphosphonates in diseases of childhood.* European Journal of Pediatrics, 2003. **162**(11): p. 735-751.
162. Black, D.M., et al., *The effects of parathyroid hormone and alendronate alone or in combination in postmenopausal osteoporosis.* N Engl J Med, 2003. **349**(13): p. 1207-15.
163. Fournier, P., et al., *Lowering Bone Mineral Affinity of Bisphosphonates as a Therapeutic Strategy to Optimize Skeletal Tumor Growth Inhibition In vivo.* Cancer Research, 2008. **68**(21): p. 8945-8953.
164. Coxon, F.P., et al., *Visualizing mineral binding and uptake of bisphosphonate by osteoclasts and non-resorbing cells.* Bone, 2008. **42**(5): p. 848-60.
165. Idris, A., et al., *Aminobisphosphonates Cause Osteoblast Apoptosis and Inhibit Bone Nodule Formation In Vitro.* Calcified Tissue International, 2008. **82**(3): p. 191-201.
166. Wood, J., et al., *Novel antiangiogenic effects of the bisphosphonate compound zoledronic acid.* J Pharmacol Exp Ther, 2002. **302**(3): p. 1055-61.
167. Walter, C., et al., *Influence of bisphosphonates on endothelial cells, fibroblasts, and osteogenic cells.* Clinical oral investigations, 2009.
168. Bukowski, J.F., C.C. Dascher, and H. Das, *Alternative bisphosphonate targets and mechanisms of action.* Biochem Biophys Res Commun, 2005. **328**(3): p. 746-50.

169. Ciosek, C.P., Jr., et al., *Lipophilic 1,1-bisphosphonates are potent squalene synthase inhibitors and orally active cholesterol lowering agents in vivo.* J Biol Chem, 1993. **268**(33): p. 24832-7.
170. Kunzmann, V., E. Bauer, and M. Wilhelm, *Gamma/delta T-cell stimulation by pamidronate.* N Engl J Med, 1999. **340**(9): p. 737-8.
171. Srivastava, A., et al., *Structural analysis of farnesyl pyrophosphate synthase from parasitic protozoa, a potential chemotherapeutic target.* Infect Disord Drug Targets, 2008. **8**(1): p. 16-30.
172. de Groen, P.C., et al., *Esophagitis associated with the use of alendronate.* N Engl J Med, 1996. **335**(14): p. 1016-21.
173. Reszka, A.A., J. Halasy-Nagy, and G.A. Rodan, *Nitrogen-bisphosphonates block retinoblastoma phosphorylation and cell growth by inhibiting the cholesterol biosynthetic pathway in a keratinocyte model for esophageal irritation.* Mol Pharmacol, 2001. **59**(2): p. 193-202.
174. F. H. Ebetino, P.E., B. Barnett, G. H. Nancollas, *Differentiation of hydroxyapatite affinity of bisphosphonate analogs for mechanism of action studies.* ASBMR abstract, 2004.
175. Iwata, K., et al., *Bisphosphonates suppress periosteal osteoblast activity independently of resorption in rat femur and tibia.* Bone, 2006. **39**(5): p. 1053-8.
176. Ylitalo, R., et al., *Accumulation of bisphosphonates in human artery and their effects on human and rat arterial function in vitro.* Pharmacol Toxicol, 1998. **83**(3): p. 125-31.
177. Ribatti, D., Nico, B., Vacca, A., Roncali, L., Dammacco, F., *Endothelial cell heterogeneity and organ specificity.* Journal of hematotherapy & stem cell research, 2002. **11**: p. 81-90.
178. Allegra, A., et al., *Patients with bisphosphonates-associated osteonecrosis of the jaw have reduced circulating endothelial cells.* Hematological oncology, 2007. **25**(4): p. 164-9.